Øyvind Nistad Stamnes

Nonlinear Estimation with Applications to Drilling

Thesis for the degree of Philosophiae Doctor

Trondheim, April 2011

Norwegian University of Science and Technology
Faculty of Information Technology, Mathematics and Electrical Engineering,
Department of Engineering Cybernetics

NTNU
Norwegian University of
Science and Technology

ISBN 978-82-471-2645-5 (printed version)

ISBN 978-82-471-2647-9 (electronic version)

ISSN 1503-8181

ITK report 2011-5-W

Thesis at NTNU:2011:60

Printed by Skipnes Kommunikasjon as, Trondheim

To
Amarpreet

Summary

This thesis addresses the topic of nonlinear estimation and its applications. Particular emphasis is given to downhole pressure estimation for Managed Pressure Drilling (MPD), but due to the mathematical similarities of the two problems, velocity estimation for mechanical systems is also considered. The thesis consists of the following three parts:

Part I of this thesis addresses the problem of pressure estimation for MPD systems. Over the last decade MPD has emerged as a tool for drilling offshore wells with tight pressure margins. Several technologies for MPD have been developed and this thesis focuses on the so called constant bottomhole pressure variation. This version of MPD aims at keeping the pressure at one location in the annulus section of a well constant by applying back-pressure through the use of a choke manifold at the rig. As the pressure profile in the well is not measured, a key element of any control system (manual or automatic) is some sort of estimation scheme for the pressure in the well. To aid in control design for MPD systems, and to solve the pressure estimation problem, a fit for purpose low order model has been developed. Using data from offshore wells, and dedicated experiments onshore, it is demonstrated that the model captures the dominant pressure dynamics. It is also demonstrated that a newly developed adaptive observer, combined with a recursive least squares parameter identification scheme, is able to predict the downhole pressure in the presence of significant parametric uncertainties.

Part II of this thesis addresses the problem of adaptive observer design for a class of nonlinear systems including the drilling model. To estimate unmeasured states, in dynamical systems with parametric uncertainties, one can use adaptive observers. Furthermore, if the system is sufficiently (persistently) excited, adaptive observers can be used to identify uncertain parameters. The current state of the art in adaptive observer design does not cover the class of systems to which the drilling model belongs. Motivated by this, a method for adaptive observer design for this class of systems is developed. The method guarantees stability and convergence of the state estimate without requiring persistent excitation. Another weakness with the current

state of the art is that existing Lyapunov based adaptive laws have poor parameter identification properties, and can be very hard to tune, when estimating more than one parameter. This motivated the developement of an adaptive observer design that uses multiple delayed observers to improve the convergence rate of the estimation scheme, at the cost of an increased computational burden. In particular, explicit lower bounds on the convergence rate of the state and parameter estimation error are given, and, if the original non-adaptive observer has tunable convergence rate, the redesigned adaptive observer will have tunable convergence rate as well.

Part III of this thesis addresses the topic of observer-based output feedback control of general Euler-Lagrange systems. The design of a globally stabilizing output (position) feedback tracking controller for general Euler-Lagrange systems has been an active field of research for at least two decades. Still, it was not until recently that a globally convergent velocity observer was developed. In part III of this thesis a significant obstacle in the development of a *constructive* observer design is removed yielding a constructive speed observer design with global performance guarantees. In addition, a separation principle is proven, guaranteeing global stability and convergence when the observer is used in conjunction with certain types of certainty equivalence controllers. To the best of the authors knowledge this represents the first *observer-based* output feedback tracking control solution that guarantees a global region of attraction for general Euler-Lagrange systems.

Preface

This thesis is submitted to the Norwegian University of Science and Technology (NTNU) for partial fulfillment of the requirements for the degree of philosophiae doctor. The research presented here has been carried out from January 2008 to February 2011, for the most part at the Department of Engineering Cybernetics, NTNU, Trondheim, under the guidance of Professor Ole Morten Aamo. I have spent some time away from NTNU during my studies, in particular I have worked closely with my co-advisor Dr. Glenn-Ole Kaasa both at Statoil's Research Centre in Porsgrunn and at Ullrigg, a land based drilling rig for running experiments and tests, operated by the International Research Institute of Stavanger. During the first half of 2010 I was also privileged to visit Professor João P. Hespanha's research group at the University of California Santa Barbara.

Acknowledgements

First and foremost, I would like to express my deep gratitude to Professor Ole Morten Aamo for all the support and motivation you have given me. I appreciate the friendship we have developed and the genuine interest and participation you have shown in my research. I am also deeply grateful to Dr. Glenn-Ole Kassa at Statoil for your interest, guidance and practical insight. With the help of my two advisors I feel that I have been able to perform theoretically sound research on practical problems. I would also like to thank Statoil for funding my work and Professor João P. Hespanha for the chance to visit his research group at the University of California Santa Barbara.

During my studies I have collaborated with amongst others Dr. Jing Zhou, Professor Lars Imsland, Dr. John-Morten Godhavn, Dr. Gerhard H. Nygaard and Dr. Alexey Pavlov, I would like to thank you all for many fruitful and constructive discussions. My stay at the department would not have been as great without the good social atmosphere amongst the PhD students, and the excellent support of the administrative and technical staff, thank you.

Finally I would like to thank my parents, Wenche and Kjell, for teaching me the value of education, my brother and good friend, Håkon, for reminding me of what the important things in life are, and my wonderful wife, Amarpreet, for the endless support and encouragement you have given me through both the ups and the downs during these past three years.

Øyvind Nistad Stamnes
Trondheim, April 2011

Contents

Abbreviations

BHA	Bottomhole Assembly
EL	Euler-Lagrange
IADC	International Association of Drilling Contractors
IEEE	Institute of Electrical and Electronics Engineers
IFAC	International Federation of Automatic Control
LMI	Linear Matrix Inequality
MD	Measured Depth
MPD	Managed Pressure Drilling
NTNU	Norwegian University of Science and Technology
PD	Proportional Derivative
PE	Persistently Exciting
PI	Proportional Integral
PVT	Pressure-Volume-Temperature
PWD	(Downhole) Pressure While Drilling
ROP	Rate of Penetration
SPE	Society of Petroleum Engineers
SPR	Strictly Positive Real
TVD	True Vertical Depth
U(G)ES	Uniformly (Globally) Exponentially Stable
U(G)AS	Uniformly (Globally) Asymptotically Stable

Chapter 1

Introduction

This thesis is concerned with state and parameter estimation and its applications with particular emphasis on downhole pressure estimation for drilling operations. We will mostly work with continuous time systems in the form of ordinary differential equations of the form

$$\dot{y} = f_1(t, y, z) \tag{1.1a}$$

$$\dot{z} = f_2(t, y, z) \tag{1.1b}$$

where $t \in \mathbb{R}^+$ represents time, $y \in \mathbb{R}^m$ is measured and $z \in \mathbb{R}^m$ is unmeasured. For estimation any control input $u(t)$ is considered a known time-varying signal that can be included in f_1 and f_2 through the dependence on time. In the following sections we will first present an introduction to managed pressure drilling, briefly motivate the need for automatic control, state and parameter estimation and review the current state of the art. Then we will give an introduction to state and parameter estimation and the current state of the art. We will end this chapter by with an outline of the thesis, where the main contributions are highlighted, and a list of publications.

1.1 Managed Pressure Drilling

To meet the increasing demand for oil and gas there is a need to find new reserves and to extract these. Most of the larger fields that are accessible with conventional drilling technology have been drilled. Consequently the remaining fields typically contain less oil and gas, and are harder to drill (located in less accessible formations). It is therefore a strong demand for drilling technologies that can drill where conventional drilling cannot be used, while still being cost and time efficient.

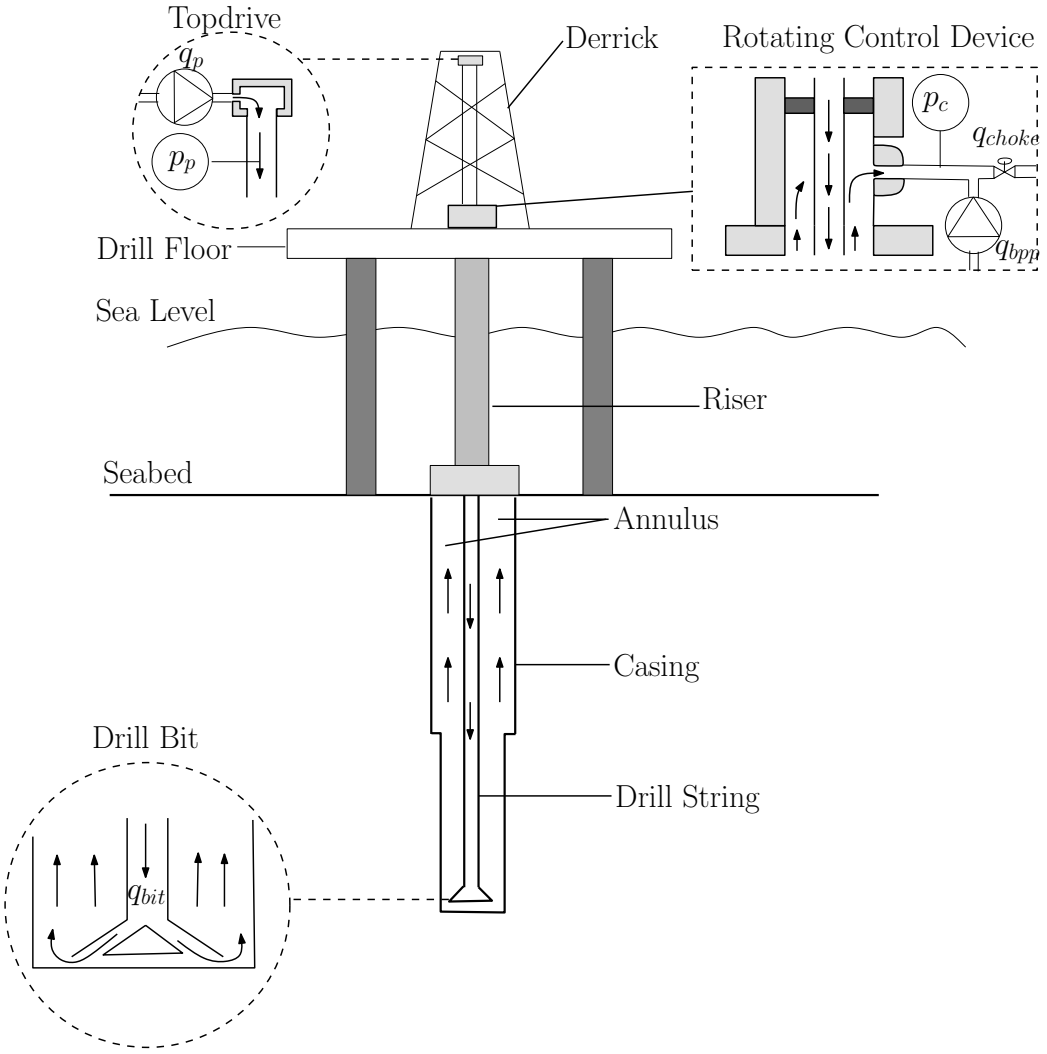

Figure 1.1: Offshore drilling from a jacket platform. Drill mud flows from the main pump through the drill string, drill bit and out through the choke. The mud transports cuttings out of the wellbore and helps to maintain the desired pressure in the borehole.

1.1.1 Introduction to Drilling

As an introduction to drilling consider the drill rig set-up illustrated in Fig. 1.1. The figure illustrates a jacket platform performing offshore managed pressure drilling. At the top of the derrick the drill string is attached to the top drive, which is a motor that turns the drill string. The drill string can move up and down inside the derrick as the top drive is attached to a hook that can be lowered or raised. As the drilling progresses the top of the drill string sinks towards the drill floor. After approximately $27m$ a new stand of drill pipe is connected to the top and drilling resumes. This procedure is referred to as a pipe connection. For a typical rate of penetration of $15\frac{m}{hr}$ a pipe connection is performed roughly every two hours.

During drilling, downhole cuttings need to be transported out of the bore hole. This is done by using a drilling fluid (mud) circulation system. On board the rig, tanks filled with drilling fluid feed the main mud pump which pumps the drilling fluid through the top drive and into the drill string. The fluid then flows down through the bit and up through the annulus carrying the cuttings along before the fluid exits through a choke. After exiting, the fluid is recycled and returned to the mud tanks. The example illustrated in Fig. 1.1 has a rotating control device which seals off the annulus from the outside, a choke that controls the flow rate of drilling fluid out from the annulus and an additional back pressure pump that ensures a minimum flow rate through the choke. The rotating control device and the choke thus pressurizes the annulus so that pressure can be increased or decreased by manipulating the choke. In conventional drilling there is no rotating control device, choke and back pressure pump thus reducing the possibilities to influence the pressure in the annulus.

A drilling fluid needs sufficiently high viscosity to carry the cuttings to the surface, and sufficiently high density to balance the downhole pressure conditions. Drilling fluids can be water based, oil based or even pneumatic (contain or consist of gas). The design of drilling fluids is its own technical discipline that we will not describe futher in this work. For more details see e.g. Jr., Millheim, Chenevert, and Jr. (1991).

The main reason for pressure control is to maintain the annulus pressure profile within its margins, i.e. above the pore pressure of the reservoir or the collapse pressure of the bore hole, and below the fracturing pressure of the bore hole. If the pressure in the annulus falls below the pore pressure, fluids (e.g. gas) can flow from the formation into the annulus, which is called a kick. If a kick is not detected and dealt with properly it can lead to an uncontrolled surface blowout with large financial losses, environmental damage and possible loss of lives. If the pressure in the annulus falls below the collapse pressure, the well can collapse onto the drill string which in turn gets stuck. In the worst case scenario the pipe must be severed

and parts of the well drilled over again. If the pressure in the annulus exceeds the fracturing pressure, drilling fluid can be lost to the formation which can damage the permeability of the reservoir, and if severe losses occur, the annulus pressure might fall below the pore pressure (due to loss of hydrostatic height) inducing a kick. A typical pressure versus depth graph for an offshore well is shown in Fig. 1.2. The figure shows that when the drill bit has reached depth B we cannot drill further, because the pressure in the well (dashed line) is very close to the pore/collapse pressure (red line). To solve this issue one would like to increase the density of the drilling fluid, therby increasing the pressure in the well. However, as the figure shows, the pressure in the well at depth A is very close to the fracture pressure (blue line) thus we cannot increase the pressure in the well without fracturing the well at depth A. The result is that we cannot continue drilling without setting casing (steel cylinders) into the well. A 9 5/8" casing is set down to depth B, isolating the well from the formation, enabling us to increase the mud weight without fracturing the well. The full line shows the pressure in the well when the well has been drilled into the reservoir, note that it is above pore/collapse pressure in the reservoir and below the fracturing pressure at depth B.

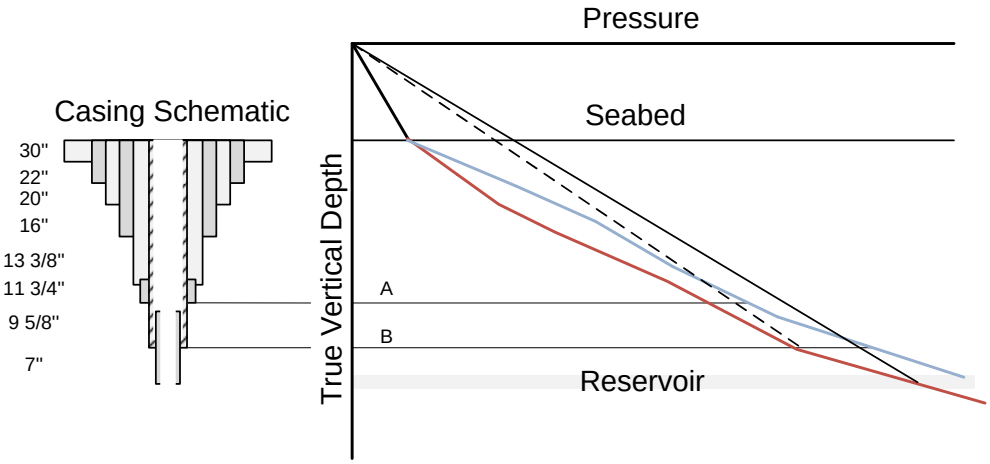

Figure 1.2: A pressure vs. depth graph of a typical offshore well. The red line represents the maximum of the pore and collapse pressures while the blue line represents the fracture pressure. A typical casing set-up is shown on the left, starting with a 30" conductor casing and ending with a 7" liner into the reservoir. The dashed line shows the pressure in the annulus with the mud weight used when drilling from depth A to depth B and the full line shows the pressure in the annulus when drilling with a higher density mud from depth B into the reservoir.

The pressure in the annulus is mainly affected by the hydrostatic weight and the

pressure due to friction losses (Brill and Mukherjee, 1999; Rehm, Schubert, Haghshenas, Paknejad, and Hughes, 2008). In addition, if the annulus is closed off, the pressure at the top of the annulus induced by choking will significantly affect the pressure in the well. There are several operational procedures that affect the pressure in the annulus. Pipe connection affects the pressure as the main pump must be disconnected to attach a new section of drill pipe, which leads to zero flow and loss of pressure due to friction. Moving the drill string all the way in/out of the well (tripping) changes the volume in the annulus and creates a piston effect around the bottom hole assembly (BHA). Tripping out pipe causes reduced pressure in the annulus, and tripping in pipe creates a surge in the pressure. Similar effects can be experienced due to wave-induced motion (heave) when drilling from a floating drilling rig. There are several other operations, such as drill string rotation and rate of penetration (ROP), that also affect the downhole pressure.

1.1.2 Pressure Control

As described in the previous section there is a demand for accurate control of the annulus pressure. As a response to these demands a fairly new (for offshore drilling) technology for pressure control has emerged (Hannegan, 2006). It is named Managed Pressure Drilling (MPD) and is defined by the International Association of Drilling Contractors (IADC), Underbalanced Operations Committee as (Malloy, Stone, George H. Medley, Hannegan, Coker, Reitsma, Santos, Kinder, Eck-Olsen, McCaskill, May, Services, Smith, and Sonneman, 2009):
Definition 1.1. "Managed Pressure Drilling is an adaptive drilling process used to precisely control the annular pressure profile throughout the wellbore. The objectives are to ascertain the down hole pressure environment limits and to manage the annular hydraulic pressure profile accordingly. The intention of MPD is to avoid continuous influx of formation fluids to the surface. Any influx incidental to the operation will be safely contained using an appropriate process."

Over the last 10 years much research has been devoted to the field offshore managed pressure drilling and there have been several successful applications both on the Norwegian continental shelf (Eck-Olsen, Pettersen, Ronneberg, Bjørkevoll, and Rommetveit, 2005; Bjørkevoll, Molde, Rommetveit, and Syltøy, 2008b; Bjørkevoll, Hovland, Aas, and Vollen, 2010; Godhavn, 2010; Godhavn and Knudsen, 2010) and in the rest of the world (Chustz, Smith, and Dell, 2008; Fredericks, Reitsma, Runggai, Hudson, Zaeper, Backhaus, and Hernandez, 2008; Calderoni and Girola, 2009). Hannegan (2006) divides existing MPD technologies into several categories, all of which have their pros and cons. In this thesis we consider the so called constant bottomhole pressure variation which uses an additional seal, choke manifold and

possibly a back pressure pump to pressurize the annulus as shown in Fig. 1.1. When using the term managed pressure drilling we usually refer to the constant bottomhole version.

A typical automatic MPD system is illustrated in Fig. 1.3. The control objective is to keep the pressure p_{dh} at a critical location in the well, typically corresponding to the bit or the casing shoe, constant. As most of the measurements are taken top side (at the rig), and only a low bandwidth delayed measurement of the pressure close to the bit is available, it is common to use a hydraulic model to calculate the reference trajectory for the pressure controller.

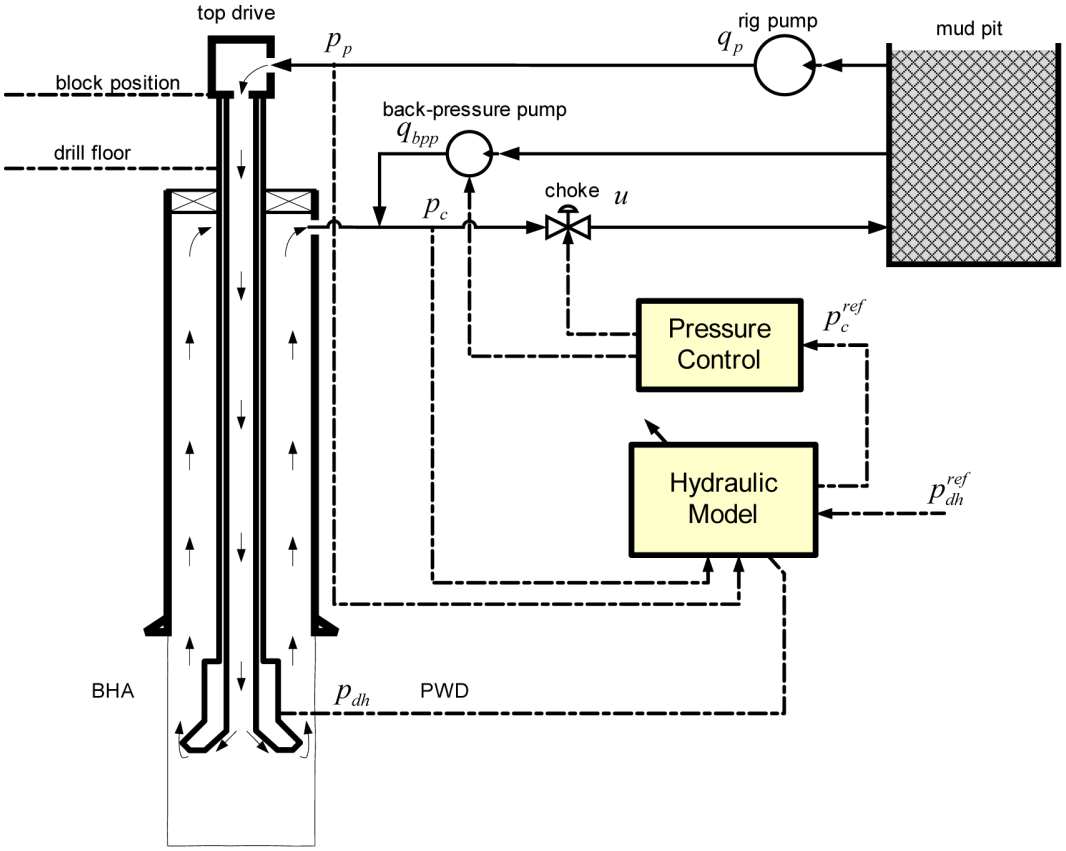

Figure 1.3: Simplified schematic of an automatic MPD system Kaasa et al. (2011a). The hydraulic model uses available measurements to calculate a reference trajectory p_c^{ref} so that the downhole pressure, p_{dh}, is kept close to its desired value p_{dh}^{ref}.

Given a desired choke pressure reference one can choose to operate the choke either manually or automatically. Manual control is easier to implement but the performance depends on individual attention, interpretation and skill, and so it typically

has less accuracy, slower response times and less repeatability. Automatic control has the potential to improve these performance issues at the cost of higher initial implementation costs. Automatic control also enables the driller to focus on more high level tasks, such as drilling the well as fast as possible within safety limitations, instead of low level tasks such as controlling a choke or a pump. Thus, for high performance MPD, it is necessary to use automatic control (Godhavn, 2010).

1.1.3 Pressure Estimation

As pointed out in the previous section an essential part of an automated MPD control system is the hydraulic model. As choke pressure control can be made very accurate by choosing appropriate hardware and designing high performance control loops, the accuracy of the hydraulic model is in most cases the limiting factor for the achievable accuracy of the entire control system. This has triggered a lot of research into developing advanced hydraulic models in order to capture all aspects of the drilling hydraulics, see e.g. (Lage, 2000; Lage, Fjelde, and Time, 2003; Petersen, Bjørkevoll, and Rommetveit, 2008a; Petersen, Rommetveit, Bjørkevoll, and Frøyen, 2008b). These models are based on distributed parameter models of multiphase flow and are able to reproduce a wide range of drilling-specific events such as, pipe connections, cementing, gelling and multi-fluid scenarios to an impressingly high degree of detail (Bjørkevoll, Rommetveit, Aas, Gjeraldstveit, and Merlo, 2003; Bjørkevoll, Molde, and Fjeldberg, 2008a). Real-time versions of the models have also been developed and used with success (Eck-Olsen et al., 2005; Bjørkevoll et al., 2008a,b).

There are some issues related to using advanced hydraulic models. Due to the high level of accuracy they contain both fast (e.g. pressure wave traveling through the system) and slow dynamics (e.g. temperature effects). This implies that the implemented differential equations are inherently stiff and numerically difficult to simulate. Advanced models also contain dynamics that are faster than the bandwidth of the controller. As the model is used to calculate a reference trajectory for the choke pressure, these fast dynamics are injected into the controller, which is undesireable as the controller cannot compensate for them. Furthermore the amount of data needed to set up advanced models can be quite large. As this data is typically entered by a user it increases the chance for errors. And finally, many of the parameters needed to take full advantage of the achievable accuracy of an advanced model are hard to specify and will change during operations. It is therefore crucial that some sort of calibration or parameter adaptation is performed online. In practice calibration of advanced hydraulic models is performed manually by an expert (Bjørkevoll et al., 2010) although there has been attempts at applying Unscented

Kalman Filters (Lohne, Gravdal, Dvergsnes, Nygaard, and Vefring, 2008; Gravdal, Lorentzen, Fjelde, and Vefring, 2010) to tune the models online. As an automated MPD system is safety-critical[1] robustness under all circumstances of both hardware and the implemented algorithms is crucial. The above issue illustrates that verifying the robustness of an advanced hydraulic model under all circumstances is a very difficult task.

Contrary to using an advanced hydraulic model it is possible to derive fit for purpose low order models that capture the dominant phenomenon relevant for pressure control and estimation. In the work Nygaard and Nævdal (2006) a low order model for underbalanced drilling[2] is derived. The later work by Nygaard, Imsland, and Johannessen (2007a) and Nygaard, Johannessen, Gravdal, and Iversen (2007b) focuses on control and estimation based on the low order model. More recently Godhavn (2010), shows how a simplified model of the choke pressure dynamics can be used to derive a, possibly nonlinear, proportional-integral (PI) controller.

1.2 State and Parameter Estimation

This section contains an introduction to state and parameter estimation. For increased readability we have chosen to use fairly standard notation from the control community (see e.g. (Khalil, 2002)), without being very explicit with the mathematical definitions. Typically upper case letters refer to matrices while lower case letters refer to vectors.

A common problem facing the control engineer is lack of measurements that are needed for control purposes, or that the signals are measured but the measurement quality is low due to noise, delays or slow sampling rates. In these cases, signals needed for control purposes can be estimated by using a dynamical system that is adjusted based on the available measurements. In the deterministic setting such a dynamical system is typically called an observer as in the seminal work done by Luenberger (1964), while in the stochastic setting it is called filter or an estimator as in the seminal work done by Kalman (1960); Kalman and Bucy (1961). This thesis focuses on the deterministic case so we will not review extensions of Kalmans work to nonlinear systems such as the popular Extended Kalman Filter (Brown and Hwang, 1997; Reif, Sonnemann, and Unbehauen, 1998; Besançon, 2007), and the more recently developed Unscented Kalman Filter (Julier, Uhlmann, and Durrant-Whyte,

[1] E.g. a failure can lead to an induced kick, which has the potential of leading to a blowout with large financial losses, large environmental damages and possible loss of human lives.

[2] During underbalanced drilling the well pressure is kept below the pore pressure so that the well is actually producing while drilling.

2000; Julier and Uhlmann, 1997). There are several definitions of observers in the literature (Luenberger, 1964; Gauthier, Hammouri, and Othman, 1992; Marino and Tomei, 1996; Besançon, 2007; Karagiannis, Carnevale, and Astolfi, 2008). Loosely speaking they all consider an observer to be a dynamical system

$$\dot{\xi} = w_1(\xi, u, y, t) \tag{1.2}$$
$$\hat{x} = w_2(\xi, u, y, t) \tag{1.3}$$

such that:

- $\hat{x}(0) = x(0) \Rightarrow \hat{x}(t) = x(t), \quad \forall t \geq 0,$
- $\lim_{t\to\infty} \|\hat{x}(t) - x(t)\| = 0,$

where $x(t) = [y(t), z(t)]^T$ is the solution to (1.1). The functions w_1 and w_2 represent the design freedom given to the control engineer. In some cases it might be desirable to only estimate the unknown elements of the state vector (e.g. z in (1.1)), thus reducing the computational complexity of the estimation algorithms. Such observers are called reduced order observers. In the next subsections we will give an introduction to state and parameter estimation for continuous time systems and review the existing state of the art.

1.2.1 Linear Systems

Non-Adaptive Observers

Consider linear systems of the form

$$\dot{x} = Ax + Bu \tag{1.4}$$
$$y = Cx, \tag{1.5}$$

where x is the state, u is the measured input and y represents the measurements. A full order observer can be designed by appending an output injection term to the right hand side of (1.4) giving

$$\dot{\xi} = A\xi + Bu + L(y - C\xi), \tag{1.6}$$

with $\hat{x} = \xi$. Denote the state estimation error as $e = x - \hat{x}$. Subtracting (1.6) from (1.4) we get

$$\dot{e} = (A - LC)e. \tag{1.7}$$

The linear system (1.7) has an exponentially stable equilibrium at the origin if all the eigenvalues of the matrix $A-LC$ are in the left half plane ($A-LC$ is then called Hurwitz). If the pair (A, C) is observable (or at least detectable) then there exists L so that $A - LC$ is Hurwitz (Luenberger, 1964; Chen, 1999). In the more general case where the matrices A, B and C are time-varying and the system is uniformly completely observable, one can use the so called Kalman-Bucy filter (Kalman and Bucy, 1961; Brown and Hwang, 1997; Besançon, 2007), which is a time-varying version of (1.6) where the gain L depends on the solution of a Riccati differential equation.

Adaptive Observers

If there are uncertain parameters in the linear system (1.4), then one can use parameter adaptation to ensure that the state estimate converges to the true state. The simplest case of parameter uncertainty is probably when the unknown parameter vector θ enters the system multiplied by a measured function, that is

$$\dot{x} = Ax + Bu + \phi(t)\theta \tag{1.8}$$
$$y = Cx. \tag{1.9}$$

In this case we can simply create an extended state vector $z = [x, \theta]$ so that we get

$$\dot{z} = \begin{bmatrix} A & \phi(t) \\ 0 & 0 \end{bmatrix} z + Bu \tag{1.10}$$

for which we can design a Kalman-Bucy filter provided the system is uniformly completely observable. However, as pointed out in Zhang (2005), it is hard to verify the uniform complete observability of the extended system, and application of the Kalman-Bucy filter requires the solution of a Riccati equation of the same order as the extended system. Zhang (2002) provides an observer with less complexity that only requires uniform complete observability of the time-varying part of (1.8), and does not require the solution to a Riccati equation (in the case where A, B and C are constant matrices). For the case where the unknown parameter vector enters the system multiplied by the state vector and the input in the form

$$\dot{x} = \hat{A}x + \theta_b u \tag{1.11}$$
$$y = Cx \tag{1.12}$$

with u and y scalar and

$$A = \begin{bmatrix} & 1 & 0 & 0 \\ \theta_a & 0 & \ddots & 0 \\ & 0 & 0 & 1 \\ & 0 & 0 & 0 \end{bmatrix} \quad C = [1,\ 0, \ldots,\ 0], \tag{1.13}$$

one can design so-called adaptive Luenberger observers (Ioannou and Sun, 1996). These observers build on the earlier results by Luders and Narendra (1973) with important extensions developed by Kreisselmeier (1977). The adaptive Luenberger observer consists of a Luenberger type observer combined with different types of parameter adaptation laws such as SPR[3]-Lyapunov based, gradient based and least-squares methods (Ioannou and Sun, 1996). To illustrate these ideas we consider a linear mass-spring-damper example of the form

$$\dot{x}_1 = x_2 \tag{1.14a}$$
$$\dot{x}_2 = -kx_1 - bx_2 + u \tag{1.14b}$$

where $y = x_1$ is measured, $k > 0$ is the unknown spring constant and $b > 0$ is the unknown damping coefficient. Due to the bx_2 term this system is not in the form (1.8) nor in the form (1.11)–(1.13). However, as the system is observable it can be transformed into the observable canonical form (1.11)–(1.13) by defining a new state vector $\bar{x}_1 = x_1$ and $\bar{x}_2 = bx_1 + x_2$. Straight-forward differentiation leads to

$$\dot{\bar{x}} = \begin{bmatrix} -b & 1 \\ -k & 0 \end{bmatrix} \bar{x} + \begin{bmatrix} 0 \\ 1 \end{bmatrix} u \tag{1.15}$$

which is in the form (1.11)–(1.13) with $\theta_a = [-b, -k]^T$ and θ_b known. Following the approach in Ioannou and Sun (1996) an adaptive observer for $\bar{x}$ is

$$\dot{\hat{\bar{x}}} = \begin{bmatrix} \hat{\theta}_{a1} & 1 \\ \hat{\theta}_{a2} & 0 \end{bmatrix} \bar{x} + \begin{bmatrix} 0 \\ 1 \end{bmatrix} u + K(t)(y - C\hat{x}) \tag{1.16}$$

with $K(t) = K^* - \hat{\theta}$ where $K^* = [k_1^*, k_2^*]^T$ is chosen so that $\begin{bmatrix} -k_1^* & 1 \\ -k_2^* & 0 \end{bmatrix}$ is Hurwitz. The adaptive law that generates $\hat{\theta}$ is a design choice. We will now illustrate how to design this adaptive law. Note that (1.14) can be written as

$$\ddot{y} + \theta_{a1}\dot{y} + \theta_{a2}y = u. \tag{1.17}$$

[3]Strictly Positive Real

Transforming this system into the Laplace domain, letting s denote the complex variable, and pre-multiplying with a second order low-pass filter gives

$$\frac{s^2}{(\tau s+1)^2}y + \theta_{a1}\frac{s}{(\tau s+1)^2}y + \theta_{a2}\frac{1}{(\tau s+1)^2}y = \frac{1}{(\tau s+1)^2}u. \tag{1.18}$$

Letting $z(t) = \frac{1}{(\tau s+1)^2}u - \frac{s^2}{(\tau s+1)^2}y$ and $\phi(t) = \begin{bmatrix} \frac{s}{(\tau s+1)^2}y \\ \frac{1}{(\tau s+1)^2}y \end{bmatrix}$ it is clear that we can write (1.18) as

$$z(t) = \theta_a^T \phi(t). \tag{1.19}$$

Eq. (1.19) represents a linear parameterization of the unknown parameter vector and a vast selection of parameter identification algorithms are available. Before continuing with the selection of an identification algorithm we will briefly look at the concept of persistent excitation.

At a given time instant t_1 Eq. (1.19) represents one equation with two unknowns. If we take two time instances t_1 and $t_2 > t_1$ we get two equations with two unknowns in the form

$$z(t_1) = \phi^T(t_1)\theta_a \tag{1.20}$$
$$z(t_2) = \phi^T(t_2)\theta_a. \tag{1.21}$$

This set of equations has a unique solution only if the equations are linearly independent, i.e. if the matrix

$$\Phi(t_1, t_2) = \begin{bmatrix} \phi^T(t_1) \\ \phi^T(t_2) \end{bmatrix} \tag{1.22}$$

has full rank. The solution can then be found by inverting $\Phi(t_1, t_2)$. On the other hand, if $\phi(t_1) = \phi(t_2)$ then the rows of (1.22) are linearly dependent, consequently Φ is not invertible and we cannot identify θ_a. Clearly $\phi(t)$ must satisfy some condition to guarantee invertibility (or observability) with respect to the unknown parameter vector. This condition is called persistency of excitation (PE) and is crucial for parameter identification. For continuous time linear systems the condition is stated as (see e.g. Ioannou and Sun (1996)):

$$\alpha_1 I \geq \frac{1}{T_0}\int_t^{t+T_0} \phi(\tau)\phi^T(\tau)d\tau \geq \alpha_0 I, \quad \forall t \geq 0. \tag{1.23}$$

We will not go into a deep discussion around eq. (1.23) but point out that it guarantees that the moving average of $\phi(t)\phi^T(t)$ has full rank $\forall t \geq 0$. Roughly speaking,

for linear single input single output systems (1.23) is satisfied if u contains at least $\frac{p}{2}$ number of distinct frequencies where p is the number of unknown parameters (Ioannou and Sun, 1996).

Returning to the example we select the gradient algorithm with normalization from Ioannou and Sun (1996). The adaptive law minimizes the cost function

$$J\left(\hat{\theta}_a\right) = \frac{\left(z(t) - \hat{\theta}_a^T \phi(t)\right)^2}{2m^2}, \tag{1.24}$$

where $m(t)$ is a normalization factor (e.g. $m(t) = 1 + \phi^T(t)\phi(t)$). Using a steepest descent method one can argue that

$$\dot{\hat{\theta}}_a = -\Gamma \nabla J\left(\hat{\theta}\right) \tag{1.25}$$

$$= \Gamma \frac{\phi(t)(z(t) - \hat{\theta}^T \phi(t))}{m^2(t)}, \tag{1.26}$$

where $\nabla J\left(\hat{\theta}\right)$ denotes the gradient of $J\left(\hat{\theta}\right)$, is a good search direction. Ioannou and Sun (1996) proves the stability of (1.26) in conjuction with the adaptive Luenberger observer (1.16) and guarantees that :

- All signals are uniformly bounded.
- The output observation error $y - \hat{y}$ converges to zero as $t \longrightarrow \infty$.
- If the system is sufficiently excited (PE) by an external input $u(t)$ both the parameter estimation error $\theta - \hat{\theta}$ and the state estimation error $\bar{x} - \hat{x}$ converge to zero.

Note that to get an estimate of the true state $x_2 = \bar{x}_2 - \theta_{a1} x_1$ we must identify θ_{a1}. This can only be guaranteed if the input u is such that the system is sufficiently excited.

1.2.2 Nonlinear Systems

Non-Adaptive Observers

Observers for nonlinear systems has been an active field of study for several decades. High-gain observers (Thau, 1973; Tornambe, 1989; Gauthier et al., 1992; Khalil, 1999; Grip, 2010) can be used for uniformly observable systems where the nonlinearities satisfy a Lipschitz condition. These observers rely on sufficiently high-gain

output injection to dominate the nonlinear terms in the observer error dynamics. The class of systems for which high-gain observers can be designed has shown to contain many practical systems making high-gain observers a popular choice, however, as one might expect the use of high-gain injection from measurements can make these observers sensitive to measurement noise (Bullinger and Allgöwer, 1997).

If one looks at smaller classes of systems one can find observers that do not rely on high-gain injection terms. We will now look at some of these design methods. For the case when the system consists of linear dynamics combined with measured nonlinearities e.g.

$$\dot{x} = Ax + \phi(y) \tag{1.27a}$$
$$y = Cx \tag{1.27b}$$

one can design an observer of the form

$$\dot{\xi} = A\xi + \phi(y) + L(y - C\xi). \tag{1.28}$$

As the nonlinearity is replicated in the observer, the error dynamics become

$$\dot{e} = (A - LC)e \tag{1.29}$$

which is the same as in the linear case (1.7), making the observer design problem solvable with linear systems theory. A natural extension of this idea is to characterize the class of nonlinear systems which are transformable (by a diffeomorphism) into the form (1.27). This idea was first pursued by Krener and Isidori (1983) where the authors give necessary and sufficient conditions for the existence of such a transformation. It turns out that the conditions derived by Krener and Isidori (1983) are extremely restrictive, in particular due to the requirement of a linear output map. This requirement was relaxed by Kazantzis and Kravaris (1998), where the authors extended Luenbergers original ideas (Luenberger, 1964) to nonlinear systems. Kazantzis and Kravaris (1998) derive conditions for the existence of a local nonlinear transformation that transforms the original system into a linear system, driven by a nonlinear measured term, and having a nonlinear output map. Extensions to this class of systems have been developed in (Krener and Xiao, 2002, 2004; Andrieu and Praly, 2006; Kravaris, Sotiropoulos, Georgiou, Kazantzis, Xiao, and Krener, 2007).

If the system is of the form

$$\dot{x} = Ax + \phi(y) + G\gamma(Hx) \tag{1.30}$$
$$y = Cx \tag{1.31}$$

where $\gamma(Hx)$ is an r-dimensional vector of monotonic nonlinearities, that is γ satisfies

$$(a-b)[\gamma_i(a)-\gamma_i(b)] \geq 0, \tag{1.32}$$

where γ_i is the ith element of γ, one can use the circle criterion to design an observer (Arcak and Kokotović, 2001). The results by Arcak and Kokotović (2001) require the solution of a linear matrix inequality (LMI) to find the output injection gains used in the observer. Fan and Arcak (2003) extend these results to systems perturbed by multivariable nonlinearities.

Karagiannis et al. (2008) reduce the observer design problem for nonlinear systems into finding certain mappings so that a chosen manifold, corresponding to the estimation error being equal to zero, is rendered attractive and invariant. The concept is illustrated in Fig. 1.4. The mapping $\phi_{y,t}(x)$, parameterized by y and t, and the mapping $\beta(y,\xi,t)$ represent the design freedom for the control engineer. $\phi_{y,t}(x)$ must be left-invertible so that a state estimate can be generated as $\hat{x} = \phi^L_{y,t}(\beta(y,\xi,t))$, where $\phi^L_{y,t}$ denotes the left-inverse. Note that $p \geq n$ so that the observer can be of a higher order than the state it estimates. Although the approach in (Karagiannis et al., 2008) has been successfully applied to several practical examples, finding the mappings $\phi_{y,t}$ and β so that the error manifold is rendered attractive and invariant is in general extremely difficult.

Adaptive Observers

As was pointed out in Section 1.2.1, for linear systems it is possible to separate the adaptive observer design into two parts, namely the Luenberger observer design and the parameter estimator design. For nonlinear systems it might not be possible to parameterize the plant so that one can separate the observer design into these two subproblems. If this is the case, then one can instead attempt a Lyapunov based design. This method is best illustrated by an example. Consider the system

$$\dot{x}_1 = x_2 + \theta^T \phi(t) \tag{1.33a}$$

$$\dot{x}_2 = -b_1 x_2 - b_2 |x_2| x_2 + u, \tag{1.33b}$$

where b_1 and b_2 are the known, positive coefficients and θ is a vector of unknown constant parameters. For θ a scalar and $\phi = 1$, (1.33) could be a simplified model (in the surge direction) of a ship maneuvering on the surface of the ocean, where x_2 is the velocity of the ship with respect to the water around the ship, b_1 and b_2 are known hydrodynamic damping coefficients, θ is an unknown current (assumed to be slowly changing) and x_1 is the global position of the ship. Of course, for it to be

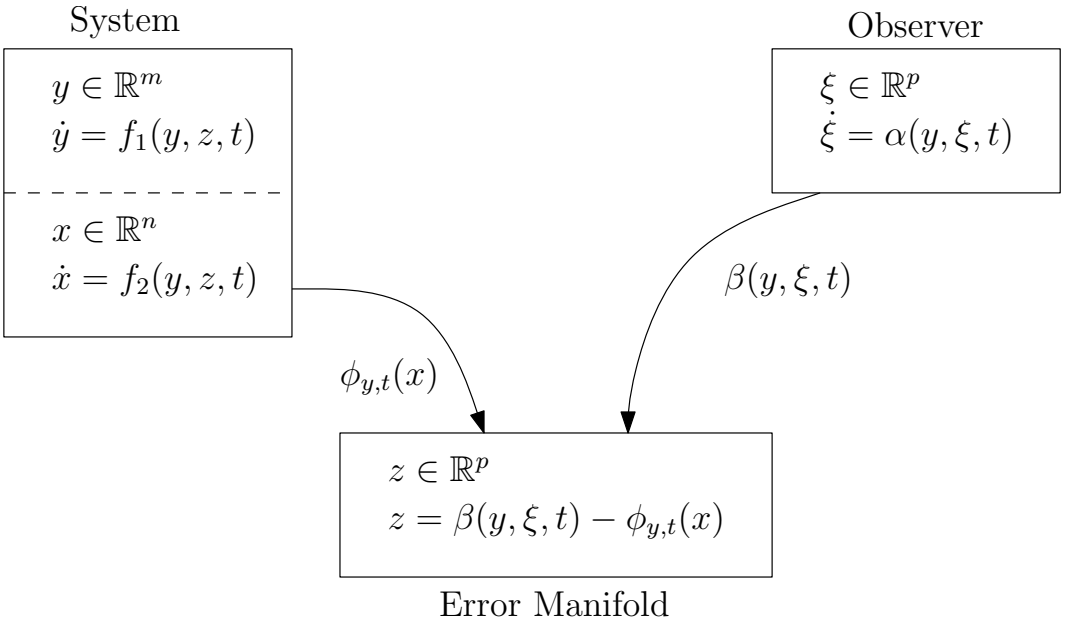

Figure 1.4: Illustration of the reduced order observer design in Karagiannis et al. (2008).

a proper model we would need to add at least two more directions, sway and yaw (Fossen, 2002), but the model is only intended to be an illustration of a Lyapunov-based design. Let us assume that we measure the position, x_1, and want to estimate the unmeasured velocity, x_2. System (1.33) can be written as

$$\dot{x} = Ax + B_1(u - b_2|x_2|x_2) + B_2\theta^T\phi(t) \tag{1.34}$$

$$y = x_1 \tag{1.35}$$

where

$$A = \begin{bmatrix} 0 & 1 \\ 0 & -b_1 \end{bmatrix}, \quad B_1 = \begin{bmatrix} 0 \\ 1 \end{bmatrix}, \quad B_2 = \begin{bmatrix} 1 \\ 0 \end{bmatrix}. \tag{1.36}$$

For illustration purposes, we propose a very simple observer

$$\dot{\xi} = A\xi + B_1(u - b_2|\xi_2|\xi_2)) + B_2\theta^T\phi(t) + L(y - C\xi) \tag{1.37}$$

with $\xi = \hat{x}$ and the observer gain $L = [l_1, l_2]^T$. Denoting the state observation error as $e = x - \xi$, and the parameter estimation error $\tilde{\theta} = \theta - \hat{\theta}$, we find the dynamics

$$\dot{e} = (A - LC)e - B_1b_2(|x_2|x_2 - |\xi_2|\xi_2) + B_2\tilde{\theta}^T\phi(t). \tag{1.38}$$

To prove the stability properties of the proposed observer we consider the positive definite function

$$V_1(e) = \frac{1}{2}e_1^2 + \frac{1}{2}e_2^2 \tag{1.39}$$

$$\tag{1.40}$$

with time-derivative

$$\dot{V}_1 \leq -l_1 e_1^2 + (1 - l_2)e_1 e_2 - b_1 e_2^2 + \tilde{\theta}^T \phi(t) e_1, \tag{1.41}$$

where $-b_2(|x_2|x_2 - |\xi_2|\xi_2)e_2 \leq 0$ has been used. Selecting $l_1 = l_2 = 1$ gives $\dot{V}_1 \leq -e_1^2 - b_1 e_2^2 + \tilde{\theta}^T \phi(t) e_1$. We see that if θ was known ($\tilde{\theta} = 0$), then we would have $\dot{V}_1 \leq -cV_1$ for some positive c, and exponential stability of the origin of (1.38) would follow using standard results found in e.g. Khalil (2002). To deal with the parameter perturbation term, it is common to add a quadratic parameter error term to V_1 according to

$$V_2 = V_1 + \frac{1}{2}\tilde{\theta}^T \Gamma^{-1} \tilde{\theta} \tag{1.42}$$

with $\Gamma = \Gamma^T > 0$. Differentiating V_2 with respect to time using (1.41) gives

$$\dot{V}_2 \leq -e_1^2 - b_1 e_2^2 + \tilde{\theta}^T \phi(t) e_1 + \tilde{\theta}^T \Gamma^{-1} \dot{\tilde{\theta}}. \tag{1.43}$$

Since θ is a constant $\dot{\tilde{\theta}} = -\dot{\hat{\theta}}$ so we choose

$$\dot{\hat{\theta}} = \Gamma \phi(t) e_1, \tag{1.44}$$

which gives

$$\dot{V}_2 \leq -e_1^2 - b_1 e_2^2. \tag{1.45}$$

Since $\dot{V}_2$ is only negative semi-definite we can only conclude that the equilibrium point $(e, \tilde{\theta}) = 0$ is stable. Further use of Barbălat's lemma allows us to conclude that $\lim_{t\to\infty} e(t) = 0$ and $\lim_{t\to\infty} \tilde{\theta}^T \phi(t) = 0$ (Krstić, Kanellakopoulos, and Kokotović, 1995). As a consequence of the specific choice of a Lyapunov function (1.42), and the fact that the unknown parameter vector enters only one integration away from the output, the adaptive law (1.44) is driven by the state estimation error e_1, which just happens to be a known signal. It is not hard to imagine that if θ entered the system two (or more) integrations away from the output, or we had chosen a more general Lyapunov function (e.g. containing the term $e^T P e$ for some $P = P^T > 0$), then the adaptive law would have been driven by a combination of e_1 and e_2. As e_2

is not measured this would be a major obstacle to implementing the adaptive law. To ensure that the adaptive law is driven by measured state estimation errors it is common to assume that the system is (or at least can be transformed into one that is) Strictly-Positive-Real (SPR) with the unknown parameter term as input and the measurements as output (Bastin and Gevers, 1988; Marino and Tomei, 1996; Cho and Rajamani, 1997; Besançon, 2000a; Zhang, 2005). In the example above we were only able to conclude that $\lim_{t\to\infty} \tilde{\theta}^T \phi(t) = 0$. Note that this does not imply that $\lim_{t\to\infty} \tilde{\theta} = 0$! Consider for instance the case where we have two unknown parameters and $\phi = [1, 2]^T$. In the limit as t approaches infinity we have

$$\tilde{\theta}^T \phi(t) = \tilde{\theta}_1 + 2\tilde{\theta}_2 = 0 \tag{1.46}$$

which clearly does not imply that $\lim_{t\to\infty} \tilde{\theta} = 0$. On the other hand, consider the case where $\phi(t) = [\sin(t), \cos(t)]$. In this case we have (in the limit as t approaches infinity)

$$\tilde{\theta}^T \phi(t) = \sin(t)\tilde{\theta}_1 + \cos(t)\tilde{\theta}_2 = 0 \tag{1.47}$$

which for each time t does not imply that $\tilde{\theta} = 0$, but since (1.47) holds over time it implies $\lim_{t\to\infty} \tilde{\theta} = 0$. As in Section 1.2.1 one needs to assume that $\phi(t)$ is persistently exciting (satisfies condition (1.23)) to ensure that $\lim_{t\to\infty} \tilde{\theta} = 0$.

To guarantee that the system satisfies some given performance criterion, one might be interested in providing lower bounds on the convergence rates of both the state and parameter estimation error. Many adaptive observers that use Lyapunov based adaptive laws end up with a common structure to the error system. For instance the systems considered in (Marino and Tomei, 1992; Cho and Rajamani, 1997; Marino, Santosuosso, and Tomei, 2001; Zhang, 2002, 2005) can eventually (after proving boundedness of all the signals) be described by the linear time-varying system

$$\begin{bmatrix} \dot{e} \\ \dot{\tilde{\theta}} \end{bmatrix} = \begin{bmatrix} A(t) & B(t) \\ -C(t) & 0 \end{bmatrix} \begin{bmatrix} e \\ \tilde{\theta} \end{bmatrix}. \tag{1.48}$$

This class of systems has been studied in (Fossen, Loría, and Teel, 2001; Loría, 2004). Loría (2004) provides explicit expressions for the convergence rate provided $B(t)$ satisfies the PE condition (1.23). One might think that these bounds would be useful for tuning adaptive observers to achieve good performance, but unfortunately they are not, because the expressions defining the lower bound on the convergence rate are very complex.

Robustness of Adaptive Observers

It is well known that adaptive laws may generate unbounded estimates in the presence of bounded disturbances (Ioannou and Sun, 1996; Marino et al., 2001). In practice there will always be such disturbances so it is crucial that the adaptive laws are made robust towards such disturbances. If the system is sufficiently excited so that PE conditions such as (1.23) are satisfied, it is usually possible to show that the origin of the error dynamics is Uniformly Exponentially Stable (UES) or Uniformly Asymptoticaly Stable (UAS), ensuring robustness towards small bounded disturbances. For linear systems such proofs can be found in e.g. Narendra and Annaswamy (1989) or Ioannou and Sun (1996), while for nonlinear systems one typically uses Matrosov's theorem (see e.g. (Marino and Tomei, 1996)), or extensions of it (Panteley, Loría, and Teel, 2001; Loría, Panteley, Popović, and Teel, 2005). In addition to the robustness guaranteed by PE one can implement additional safe-guards such as parameter projection, leakage, deadzones and normalization (Ioannou and Sun, 1996). In this thesis we only consider the robustness inherent with UES or UAS of the error system, but in a practical application we recommend additional precautions such as parameter projection.

1.3 Outline and Contribution

This thesis is divided into three main parts each consisting of a separate selection of papers. The first part is aimed at the drilling community with more emphasis on applications and less emphasis on matematical technicalities. The second and third part is aimed at the control community with emphasis on mathematical rigour and provable performance guarantees.

Part I is motivated by the increased focus on automation in the drilling industry, in particular when it comes to Managed Pressure Drilling. The main contributions in Part I are:

1. The development of a novel simplified hydraulic model for drilling that is well suited for control and observer design compared to existing models.
2. The application of algorithms for calibration of the model using measurements available in real-time. In particular, the novel adaptive observer with improved parameter identification properties, derived in Chapter 4, is shown to sucessfully estimate correction factors for friction and annulus density.
3. Verification that the model captures the dominating hydraulics of the well and so it can be used for control design and downhole pressure estimation.

The chapter is based on the two articles (Kaasa et al., 2011a) and (Kaasa, Stamnes, Imsland, and Aamo, 2011b).

Part II is motivated by the lack of adaptive observer design methods for a class of nonlinear systems including the drilling model presented in Part I, and the weak parameter identification properties of Lyapunov based adaptive laws such as (1.44). The main contributions in Part II are:

1. A novel methodology that permits adaptive observers to be designed for a class of systems including the drilling model. The result extends the existing class of systems for which adaptive observers with global stability properties can be designed. In particular, it allows terms containing both uncertainty and nonlinearity in the unmeasured states to appear in the dynamics of the unmeasured states, and still achieves convergence of the state estimate without requiring persistent excitation.

2. The development of a novel adaptive observer that uses multiple delayed observers to improve the convergence rate of the estimation scheme. In particular an explicit lower bound on the convergence rate is given, and, if the original non-adaptive observer has tunable convergence rate, the redesigned adaptive observer will have tunable convergence rate as well.

Part II consists of the two articles (Stamnes, Aamo, and Kaasa, 2011a) and (Stamnes, Aamo, and Kaasa, 2010a) which generalize and build on the results presented in (Stamnes, Zhou, Kaasa, and Aamo, 2008; Stamnes, Zhou, Aamo, and Kaasa, 2009; Stamnes, Aamo, and Kaasa, 2010b).

Part III is motivated by the lack of a constructive procedure to design observers and certainty equivalence controllers with global stability guarantees for general Euler-Lagrange systems without velocity or acceleration measurements. Another motivating factor is that the observer design problem for Euler-Lagrange systems has several similarities with the observer design problem based on the drilling model. The main contributions in Part III are:

1. The developent of two constructive designs of observers for general Euler-Lagrange systems guaranteeing uniform global asymptotic stability and semi-global exponential stability. In particular, the designs remove a significant obstacle to a constructive observer design, present in the recent work by Astolfi, Ortega, and Venkatraman (2010).

2. The derivation of a separation principle that guarantees uniform stability and convergence when the observer is used in a certainty equivalence output feedback control scheme with certain types of tracking controllers. The result includes popular controllers such as the PD+ controller proposed in Paden and

Panja (1988) and the controller proposed by Slotine and Li (Slotine and Li, 1987).

Part III consists of the two articles Stamnes, Aamo, and Kaasa (2011c) and Stamnes, Aamo, and Kaasa (2011b).

1.4 Publications

The following is a list of publications that forms the basis for the rest of this thesis:

- **Ø. N. Stamnes**, J. Zhou, G.-O. Kaasa and O. M. Aamo, Adaptive Observer Design for the Bottomhole Pressure of a Managed Pressure Drilling System, *IEEE Conference on Decision and Control*, 2008.
- **Ø. N. Stamnes**, J. Zhou, O. M. Aamo and G.-O. Kaasa, Adaptive Observer Design for Nonlinear Systems with Parameteric Uncertainties in Unmeasured State Dynamics, *IEEE Conference on Decision and Control*, 2009.
- **Ø. N. Stamnes**, O. M. Aamo and G.-O. Kaasa, Redesigned Adaptive Observers with Tunable Convergence Rate, *IFAC Symposium on Nonlinear Control Systems*, 2010.
- **Ø. N. Stamnes**, O. M. Aamo and G.-O. Kaasa, Adaptive Redesign of Nonlinear Observers, *IEEE Transactions on Automatic Control*, 2011, (accepted).
- **Ø. N. Stamnes**, O. M. Aamo and G.-O. Kaasa, Redesign of Adaptive Observers for Improved Parameter Identification in Nonlinear Systems, *Automatica*, 2011.
- **Ø. N. Stamnes**, O. M. Aamo and G.-O. Kaasa, A Constructive Speed Observer Design for General Euler-Lagrange Systems, *Automatica*, 2011, (accepted).
- **Ø. N. Stamnes**, O. M. Aamo and G.-O. Kaasa, Global Output Feedback Tracking Control of Euler-Lagrange Systems, *IFAC World Congress*, 2011 (accepted).
- **Ø. N. Stamnes**, G.-O. Kaasa and O. M. Aamo, Adaptive Estimation of Downhole Pressure for Managed Pressure Drilling Operations, *IEEE Multi-Conference on Systems and Control*, 2011, (submitted).
- G.-O. Kaasa, **Ø. N. Stamnes**, L. Imsland and O. M. Aamo, Intelligent Estimation of Downhole Pressure Using a Simple Hydraulic Model, *IADC/SPE*

Managed Pressure Drilling and Underbalanced Operations Conference and Exhibition, 2011.

- G.-O. Kaasa, **Ø. N. Stamnes**, L. Imsland and O. M. Aamo, Simplified Hydraulic Model used for Intelligent Estimation of Downhole Pressure for an MPD Control System , *SPE Drilling & Completion*, 2011, (submitted).

In the last two articles my contributions have been: a) the development and application of algorithms for state and parameter estimation (with emphasis on friction and density estimation); b) participation in developing and validating the hydraulic model, including setting up and performing experiments at Ullrigg (a full scale drilling rig in Stavanger); c) general discussions and work on the written presentation.

The following is a list of additional contributions made during my PhD studies. These publications are not included in this thesis.

- J. Zhou, **Ø. N. Stamnes**, O. M. Aamo and G.-O. Kaasa, Observer-based control of a managed pressure drilling system. *Chinese Control and Decision Conference*, 2008.
- J. Zhou, **Ø. N. Stamnes**, O. M. Aamo and G.-O. Kaasa, Adaptive output feedback control of a managed pressure drilling system, *IEEE Conference on Decision and Control*, 2008
- J. Zhou, **Ø. N. Stamnes**, O. M. Aamo and G.-O. Kaasa, Pressure Regulation with Kick Attenuation in a Managed Pressure Drilling System, *IEEE Conference on Decision and Control*, 2009.
- J. Zhou, **Ø. N. Stamnes**, O. M. Aamo and G.-O. Kaasa, Switched Control for Pressure Regulation and Kick Attenuation in a Managed Pressure Drilling System, *IEEE Transactions on Control Systems Technology*, 2011.

My contributions in the four foregoing articles consists of setting up simulations, proof-reading, general discussion on the developed methods and some work on the written presentation.

Part I

PART 1: Estimation for Managed Pressure Drilling

Chapter 2

Intelligent Estimation of Downhole Pressure Using a Simple Hydraulic Model

Abstract: *An essential part of an automated MPD control system is the hydraulic model, which in many cases is the limiting factor for achievable accuracy of the system. A lot of effort has therefore been put into developing advanced hydraulic models that capture all aspects of the drilling fluid hydraulics. However, a main drawback is the resulting complexity of these models, which require expert knowledge to set up and calibrate, making it a high-end solution.*

In practice, much of the complexity does not contribute to improve the overall accuracy of the pressure estimate, simply because conditions in the well changes during MPD operations, and there are not enough measurements to keep all of the parameters in an advanced model calibrated.

We will demonstrate that a simplified hydraulic model based on basic fluid dynamics is able to capture the dominating hydraulics of an MPD system. Furthermore, we will demonstrate that by applying algorithms for online parameter estimation, similar to those used in advanced control systems in the automotive and aerospace industry, the model can be calibrated automatically using existing measurements to achieve a level of accuracy comparable to that of an advanced hydraulic model. The results are demonstrated using field data from MPD operations in the North Sea, as well as dedicated experiments carried out in a full-scale drilling rig in Stavanger.

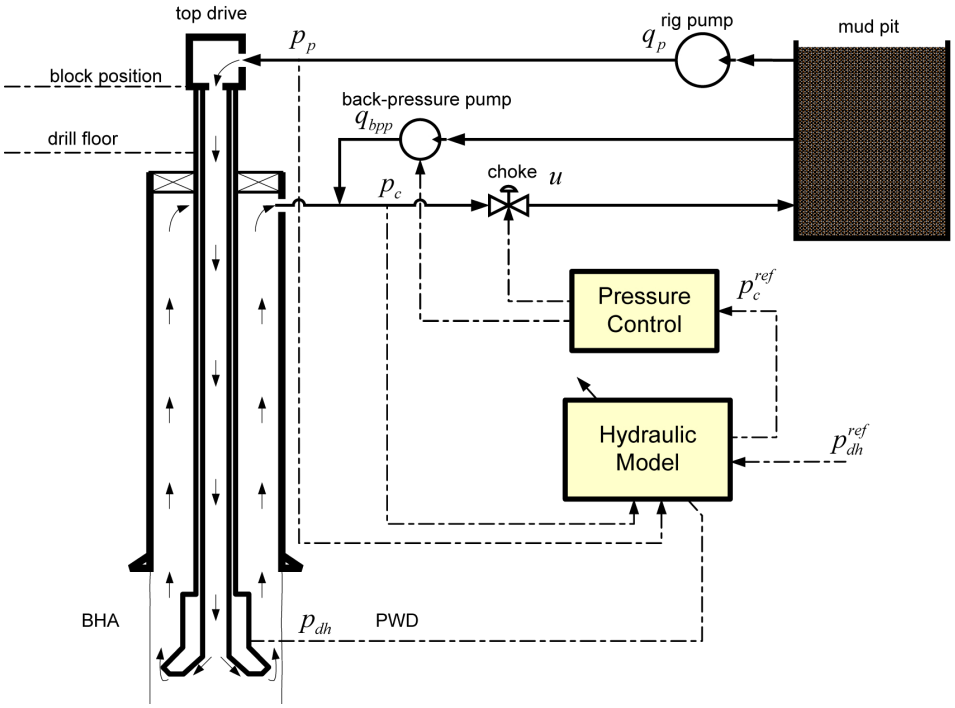

Figure 2.1: Simplified schematic of an automated MPD system.

2.1 Introduction

The main objective of MPD is accurate control of the annular downhole pressure during drilling operations. The basic principle of MPD is to apply back-pressure to control the downhole pressure and compensate for annular pressure fluctuations. In a standard MPD setup, a rotating control device seals the top of the annulus, and the flow of mud from the well is controlled by a choke manifold to apply a desired back-pressure. A back-flow pump is usually installed to boost the flow through the choke, enabling control of the back-pressure also in the case of low flow from the mud pumps. A description of the standard setup of an automated MPD system can be found in e.g. (van Riet, Reitsma, and Vandecraen, 2003). In an automated MPD system, the automation of the choke manifold is performed by a control system usually consisting of two main parts: A hydraulic model that estimates the downhole pressure in real-time and outputs a desired choke pressure according to a desired downhole pressure set-point, and a feedback control algorithm which automates the choke manifold to maintain the desired choke pressure. A simplified schematic diagram of this configuration is shown in Fig. 2.1.

In many cases, the hydraulic model is the limiting factor for achievable accuracy of

the MPD system. A lot of effort has therefore been put into developing advanced hydraulic models in order to capture all aspects of the drilling hydraulics (Rommetveit and Vefring, 1991; Petersen, Rommetveit, and Tarr, 1998; Hansen, Rommetveit, Sterri, Aas, and Merlo, 1999; Lage, Nakagawa, Time, Vefring, and Rommetveit, 1999; Lage and Time, 2000; Bjørkevoll, Anfinsen, Merlo, Eriksen, and Olsen, 2000; Petersen, Bjørkevoll, and Lekvam, 2001; Bjørkevoll et al., 2003; Bjørkevoll, Rommetveit, Rønneberg, and Larsen, 2006; Petersen et al., 2008b). These models are able to reproduce a wide range of drilling-specific effects to an impressingly high degree of detail. Real-time versions of these models have also been used in MPD operations–both offline and online (Eck-Olsen et al., 2005; Bjørkevoll et al., 2008b, 2010).

For any simulation model, however, the overall accuracy is limited by the least accurate term. Typically, several parameters are both uncertain and slowly changing, such as the friction coefficients along the well, the amount of gas dissolved in the mud, or external boundary conditions like the unmeasured reservoir temperature, etc. Calibration is thus a vital part of any real-time hydraulic model in order to predict the downhole pressure with high accuracy. In practice, the calibration of a hydraulic model must be based on available topside measurements, and measurements at the drill bit, such as pressure while drilling (PWD) data. These data contain insufficient information to properly calibrate all of the physical parameters of an advanced hydraulic model. Hence, as the conditions downhole in the well are typically inhomogeneous and uncertain due to changes during MPD operation, without additional distributed measurements along the well available for calibration, many of the sophisticated details of an advanced model do not contribute to improve the overall accuracy of the downhole pressure.

2.1.1 Motivation

There are several points that motivate the use of simpler hydraulic models in an MPD control system. The below main points are described in the following paragraphs:

- Bandwidth of the control systems
- Robustness of the implemented algorithm
- Online calibration of the hydraulic model.

A control system is only able to compensate for changes which are slower than a particular frequency range, referred to as the bandwidth of the closed-loop control system. Typically, the achievable bandwidth of an MPD system is determined

by the dynamic response of the choke actuator, and the sampling frequency of the control system. The system is inherently incapable of compensating changes with frequencies higher than this limit. Consequently, a control system behaves like a low-pass filter in the sense that it is not able to compensate high-frequency dynamics. Furthermore, if the bandwidth of the control system is pushed closer to the physical limit in an attempt to compensate for high-frequency changes, the stability margins of the system are reduced, making the system less robust to disturbances. Therefore, it is undesireable that the output of the hydraulic model contains high-frequency dynamics, simply because the control system is not able to compensate fast changes.

A primary concern in a failure-critical[1] control system such as MPD is the complexity and robustness of the implemented algorithm. An advanced hydraulic model is defined in terms of partial differential equations which are inherently stiff, that is, consisting of both slow and fast dynamics which makes the model computationally demanding, and challenging to run robustly in real-time.

There are also very few results readily available for online parameter estimation (calibration) for systems described by partial differential equations that enable automatic calibration in a robust manner. The combination of high complexity and a large number of uncertain physical parameters in advanced hydraulic models, makes it hard to develop an online parameter estimation scheme that can robustly handle all possible situations. Consequently, calibration of advanced models used for MPD operations are typically done manually by an expert (Bjørkevoll et al., 2010). Despite its challenges, there are several examples of online methods for parameter estimation applied for calibration of advanced hydraulic models. See. e.g. (Gravdal, Lohne, Nygaard, Vefring, and Time, 2008; Lohne et al., 2008; Gravdal et al., 2010) for applications of the Unscented Kalman Filter (UKF), and (Nybø, Bjørkevoll, Rommetveit, Skalle, and Herbert, 2008) for an application of adaptive neural networks. A common drawback of these methods is that the robustness of the estimation algorithms are not thoroughly analysed.
Remark 2.1. In the automotive and the aerospace industry, uncertainty with respect to robustness of software algorithms in failure-critical control systems are strictly prohibited by safety regulations. See e.g. (ISO 26262; IEC 61508; DO-178B). These are industries that are at the forefront when it comes to safety of control systems, and they have learned this lesson the hard way.

[1] By failure-critical we mean that a failure may have a critical impact on the safety of the operation and high economical consequences. A typical worst-case scenario would be a wellbore collapse or fracture, leading to a well control situation and loss of the entire well.

2.1.2 Contribution

From a control point of view, the objective is to have as simple and transparent hydraulic model as possible, that is, to remove unnecessary complexity without sacrificing accuracy in the frequency range of interest. In this paper, we will demonstrate that a fit-for-purpose model based on basic fluid dynamics combined with an accurate steady-state friction characteristics, is able to capture the dominating dynamics of the downhole pressure during drilling operations. This work also includes a revised version of the main results from Kaasa (2007), describing the derivation of a simplified hydraulic model in detail.

Furthermore, we demonstrate how this simplified model enables robust calibration, based on accessible real-time measurements, using advanced algorithms for online parameter estimation. The results are demonstrated using field data, and dedicated experiments obtained at a full-scale drilling rig in Stavanger.

The remainder of the paper is organized into two main parts: First, we describe the derivation of a simplified fit-for-purpose hydraulic model, discussing the dominating dynamics of the MPD hydraulics, and show why certain sophisticated dynamics are not important with respect to an accurate downhole pressure estimate. Second, we illustrate how online algorithms can be used to calibrate the model using both topside and pressure while drilling (PWD) measurements, and discuss the importance of robustness and stability of these algorithms.

2.2 Fit-for-purpose modeling

The objective of the hydraulic model is to estimate the downhole pressure and provide a choke pressure set-point to the MPD control system in real-time. As discussed above, to ensure robustness of the resulting control system, the model should not be more complex than required by the control system. Since dynamics are in essence what complicates a model, the main challenge is to remove unnecessary dynamics such that the model includes only the dominating dynamics of the system. For maximum accuracy, the model should in addition be optimized for utilizing existing measurements for online calibration. Typically, the main simplifications applied to obtain a fit-for-purpose model are to:

- Neglect dynamics which is much faster than the bandwidth of the control system. The hydraulic model should not contain high-frequency dynamics which the control system is not able to compensate.

- Neglect slow dynamics. Slowly changing properties of a model can usually be handled much more efficiently by feedback from measurements, than to include these effects in the model as dynamics.
- Lump together parameters which are not possible to distinguish or calibrate independently from existing measurements.

In the following, we will first outline the derivation of the simplified hydraulic model and describe the main simplifications and differences compared to an advanced model, then we go into details on some of the important aspects of the modeling with respect to accuracy of the downhole pressure.
Remark 2.2. Note that we do not consider multi-fluid operations, gelling and temperature dynamics in this work. These are topics that can be pursued with a similar apporach of simplified modelling, and which are the object of current research.

2.2.1 Outline of model derivation

The starting point for the derivation of an hydraulic model is the assumption that the drilling fluid (mud) can be treated as a viscous fluid, which means that the flow is completely described by the following fundamental equations (Merritt, 1967)[2]:

- *Fluid viscosity:* The viscosity is a function of pressure and temperature.
- *Equation of state*: The density is a function of pressure and temperature.
- *Conservation of mass:* The mass balance.
- *Conservation of momentum:* The force balance, or Newton's second law of motion.
- *Conservation of energy:* The energy balance, or the first law of thermodynamics.

First of all, the following basic assumptions are applied:

A1 We assume that the flow can be treated as one-dimensional along the main flow path (through the drillstring and annulus), i.e. time-averaging the fluctuations due to turbulence. For reference, see e.g. White (1994), p. 304.

A2 We assume the flow is radially homogeneous, i.e. averaging properties over the cross section of the flow.

[2]The derivation presented here is mainly based on Merritt (1967), supplemented by details from White (1994).

A3 We assume incompressible flow, that is, we neglect the time-variance of the density in the momentum equation[3].

A4 We assume the time-variance of the viscosity is negligible in the momentum equation.

Applying these simplifying assumptions, we end up with formulations for the momentum, continuity and energy equation which are the basis for most models. We will further clarify the implications of the above simplifications, and additional simplifications in detail in the following paragraphs.

2.2.2 Fluid viscosity

The main effect of the viscosity is related to frictional losses in the flow, and will be discussed in relation to the momentum equation in subsequent sections. The viscosity of a liquid decreases markedly as temperature increases and increases somewhat with pressure. It may in general be written as

$$\mu = \mu\left(p, T\right). \tag{2.1}$$

Maglione, Gallino, Robotti, Romagnoli, and Rommetveit (1996) provide a comprehensive overview of existing literature on viscosity of drilling fluids.

Typically, the dependence on pressure is negligible, and the dependence on temperature can be described by an equation of the form

$$\mu = \mu_0 e^{-\lambda(T-T_0)} \tag{2.2}$$

where μ is absolute viscosity at temperature T, μ_0 is viscosity at reference temperature T_0, and λ is a constant which depends on the fluid.

2.2.3 Equation of state

The equation of state may in general be written as

$$\rho = \rho\left(p, T\right). \tag{2.3}$$

In contrast to the ideal gas law which is derived from the kinetic theory of gases, the equation of state cannot be mathematically derived from physical principles. In

[3]Density effects in the flow do not become significant before the flow velocity approaches the speed of sound. In particular, the flow is generally termed incompressible for Mach number less than 0.3 (White, 1994).

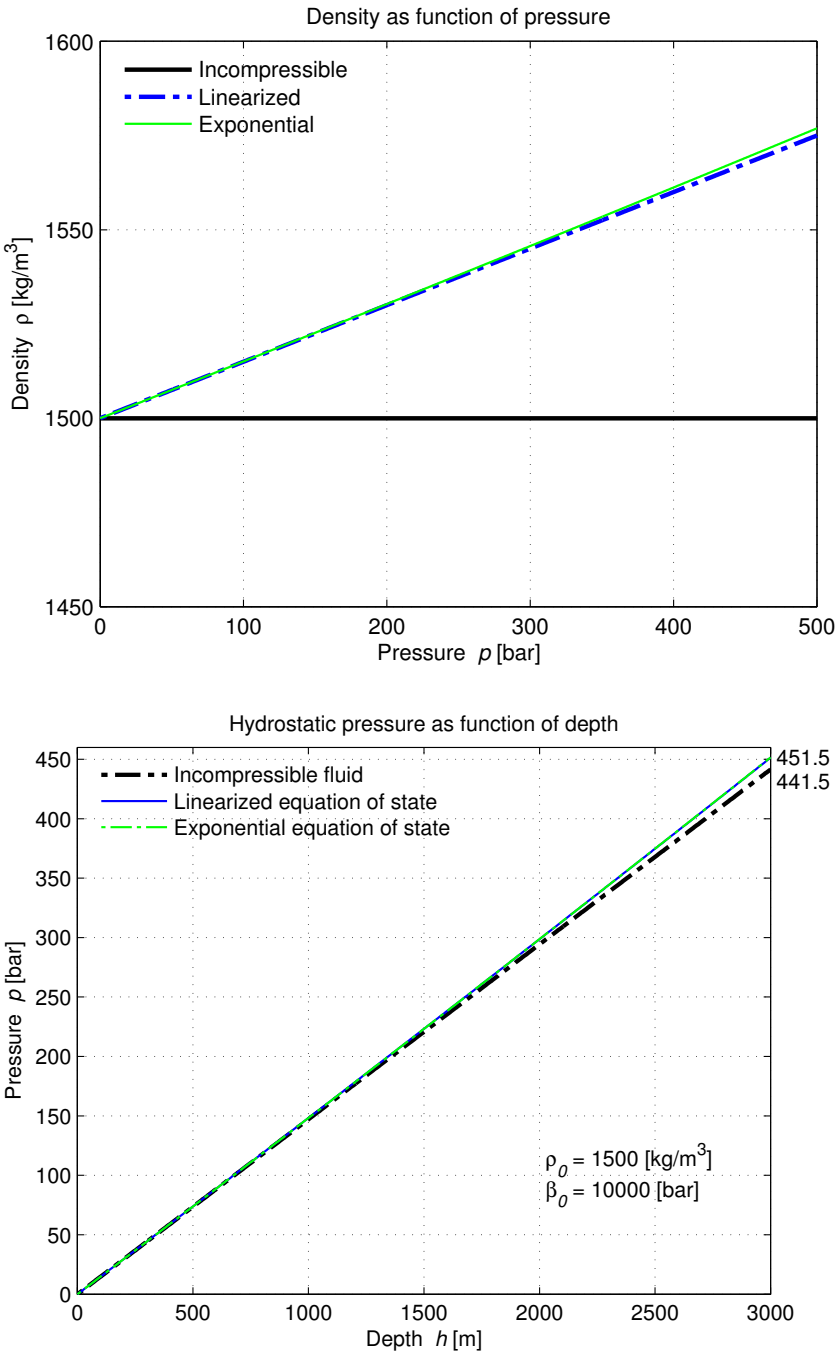

Figure 2.2: Illustrating the differences between equations of state for a liquid. Top: Density as function of pressure; Bottom: Hydrostatic pressure as a function of depth.

general, measured PVT data may be used to obtain an empirical map of pressure and temperature dependencies which can be interpolated, see e.g. Isambourg, Anfinsen, and Marken (1996).

Since the changes in density as a function of pressure and temperature are small for a liquid, it is common to use the linearized equation of state

$$\rho = \rho_0 + \frac{\rho_0}{\beta}(p - p_0) - \rho_0 \alpha (T - T_0) \tag{2.4}$$

where

$$\beta = \rho_0 \left(\frac{\partial p}{\partial \rho} \right)_{(p_0, T_0)} \tag{2.5}$$

$$\alpha = -\frac{1}{\rho_0} \left(\frac{\partial p}{\partial T} \right)_{(p_0, T_0)}. \tag{2.6}$$

Here ρ_0, p_0 and T_0 define the reference point for the linearization, while β is called the isothermal *bulk modulus* of the liquid, and α is the *cubical expansion* coefficient of the liquid. In general, the accuracy of the linearized equation of state reduces with increasing pressure and temperature ranges, but can be said to be accurate for most drilling fluids for pressure ranges $0 - 500$ bar, and temperature ranges $0 - 200\ ^\circ\mathrm{C}$. This can be verified by experimental PVT data e.g. in Isambourg et al. (1996). The resulting error by assuming constant density may be considerable. This is illustrated in Fig. 2.2 for the case of a liquid with bulk modulus $\beta_0 = 10000$ bar and atmospheric density $\rho_0 = 1500 \frac{kg}{m^3}$. In this case, the resulting difference in pressure at a depth of 3000 m amounts to 10 bar. The figure also includes plots of an exponential equation of state for highly compressible fluids (which is not shown here).

The bulk modulus β relates to the stiffness of the fluid, and is the reciprocal of the *compressibility* of the liquid, $c = \frac{1}{\beta}$. The bulk modulus is the most important property in determining the dynamics of the hydraulic system as it characterizes the dominating pressure transients in the system. The pressure transients of a well are in the range of seconds to minutes, which is in the range of a typical MPD controllers bandwidth. The temperature dynamics on the other hand, are much slower, and have transients in the range of minutes to hours.

In the following, we derive a simplified dynamic model for the pressure transients in the system based on the following differential form of (2.4)

$$d\rho = \frac{\rho_0}{\beta} dp \tag{2.7}$$

where we neglect dependence on the temperature. Even though significant temperature gradients may exist, the thermal expansion coefficient α for liquids is usually small, thus density changes due to temperature changes are in many cases negligible with respect to transient effects. Furthermore, since transient temperature effects are relatively slow compared to the pressure transients of the system, such effects are usually more effectively handled by online calibration based on feedback from measurements.

Remark 2.3. As demonstrated by Isambourg et al. (1996) in laboratory tests with a number of drilling fluids, density changes can be significant when temperature ranges are high. In particular for High-Pressure High-Temperature wells, relatively large transient temperature gradients can occur e.g. during start-up of circulation, as discussed in Bjørkevoll et al. (2000). To capture these transient effects, the simplified model must be developed based on the full linearized equation of state, that is, using the following differential form of eq. (2.4)

$$d\rho = \frac{\rho_0}{\beta} d\rho - \rho_0 \alpha dT. \tag{2.8}$$

2.2.4 Conservation of mass

For a control volume V with average density ρ, conservation of mass gives

$$\frac{d}{dt}(\rho V) = \rho_{in} q_{in} - \rho_{out} q_{out} \tag{2.9}$$

where $w_{in} = \rho_{in} q_{in}$ and $w_{out} = \rho_{out} q_{out}$ are the mass flow rates in and out of the control volume, respectively. To obtain a more convenient form, we can rewrite (2.9) using (2.7) to get pressure as the main variable according to

$$\rho_0 \frac{V}{\beta} \frac{dp}{dt} = -\rho \frac{dV}{dt} + \rho_{in} q_{in} - \rho_{out} q_{out} \tag{2.10}$$

where ρ_0 is the linearization point for the equation of state (2.4), p is the average pressure in the control volume, and q_{in} and q_{out} are the volumetric flow rates, with inlet density ρ_{in} and outlet density ρ_{out}. Equation (2.10) can be used to approximate the dominating dynamics of the hydraulic system.

2.2.5 Conservation of momentum

The main effect of assumption A1 is that the differential equation of momentum for incompressible flow reduces from three to one dimensions, which is much simpler,

but still relatively accurate with respect to averaged flow variables (White, 1994). The resulting partial differential equation can be written as

$$\rho \frac{\partial v}{\partial t} = -\frac{\partial p}{\partial x} - \frac{\partial \tau}{\partial x} + \rho g \cos \phi \tag{2.11}$$

where x is the spatial coordinate along the flow path, v the velocity of the flow, τ is the viscous friction pressure, and ϕ is the angle of the flow path. Equation (2.11) is similar to the one used in advanced hydraulic models. See e.g. Petersen et al. (2008b). Denoting A as the cross sectional area we can rewrite (2.11) with flow rate $q = vA$ as the main variable according to

$$\frac{\rho}{A} \frac{\partial q}{\partial t} = -\frac{\partial p}{\partial x} - \frac{\partial \tau}{\partial x} + \rho g \cos \phi. \tag{2.12}$$

The friction τ is typically a lumped friction term depending on the velocity of the flow, that accounts for all frictional losses due to viscous dissipation, turbulence, swirl flow, and non-ideal flow conditions caused by restrictions, section changes, bends, etc. often referred to as *minor losses* (Merritt, 1967). This means that the loss of accuracy due to the assumption of one dimensional flow (A1) can be recovered to a large extent. In general, the friction term τ can be modelled as a function

$$\tau = \tau \left(v, \mu, t \right) \tag{2.13}$$

based on any realistic viscosity model in the form (2.1), and in addition, any time-varying variables such as frictional dynamics or external inputs. Examples of frictional dynamics can be a dynamic gelling model, and an example of external input can be dependence on the drillpipe rotational velocity (RPM) to account for the effect of swirl flow. In this way, the steady-state accuracy of the model, and possibly the accuracy during transients, can be significantly improved.

In the same manner, the steady-state accuracy of the model can be further improved by a more realistic model of the density

$$\rho = \rho \left(p, T, t \right). \tag{2.14}$$

Remark 2.4. Note that (2.13) and (2.14) violate the basic assumptions of constant viscosity (A4) and constant density (A3) applied in the derivation of the momentum equation (2.11). However, the resulting errors in dynamic behavior of the model is usually more than justified by the improved steady-state accuracy obtained.

Pressure transients propagate as pressure waves in the fluid, which travel with the speed of sound, a. The speed of sound is a characteristic determined by the density and compressibility of the fluid according to

$$a = \sqrt{\frac{\beta_e}{\rho}} \tag{2.15}$$

where β_e is the effective bulk modulus, including fluid and mechanical compliance. Typically, for hydraulic fluids the speed of sound is about 1000 m/s. This means that the propagation time for a 1000 meter long pipe is about 1 second. For a distributed parameter model this results in very fast dynamics for the propagation of pressure transients. These high-frequency dynamics are typically much faster than the bandwidth of the MPD control system, and can thus be neglected in the hydraulic model[4]. Like for the pressure dynamics, we derive a simple model for the average flow dynamics in the following paragraph.

Assuming the fluid accelerates homogeneously as a stiff mass, eq. (2.12) can be integrated along the flow path to obtain a simple equation for the average flow rate dynamics according to

$$M(l_1, l_2)\frac{dq}{dt} = p_1 - p_2 - F(l_1, l_2, q, \mu) + G(l_1, l_2, \rho) \tag{2.16}$$

$$M(l_1, l_2) = \int_{l_1}^{l_2} \frac{\rho(x)}{A(x)} dx \tag{2.17}$$

$$F(l_1, l_2, q, \mu) = \int_{l_1}^{l_2} \frac{\partial \tau\left(\frac{q}{A(x)}, \mu\right)}{\partial x} dx \tag{2.18}$$

$$G(l_1, l_2, \rho) = \int_{l_1}^{l_2} \rho(x)\, g \cos\phi(x)\, dx. \tag{2.19}$$

Here, q is the average flow rate of the fluid in the control volume between the spatial coordinate $x = l_1$ and $x = l_2$ of the flow path, p_1 is the pressure at $x = l_1$, and p_2 is the pressure at $x = l_2$. Furthermore, the parameter $M(l_1, l_2)$ is the integrated density per cross-section over the flow path, $F(l_1, l_2, q, \mu)$ is the integrated friction along the flow path, and $G(l_1, l_2, \rho)$ is the total gravity affecting the fluid. Equations (2.16)–(2.19) can be used to approximate the flow dynamics of the hydraulic system.

2.2.6 Conservation of energy

The developement of a simplifed model for the transient temperature effects is outside the scope of this paper, hence, the energy equation will not be discussed here.

[4]Note that the pressure propagation in the flow results in a characteristic inverse transient response in the pressure that should be taken into account when tuning the feedback gain of the closed-loop control system. In control terminology, this characteristic is termed non-minimum phase dynamics, or unstable zero dynamics.

2.2.7 Simplified hydraulic model

As simple hydraulic model of a well can be obtained using (2.10) and (2.16)–(2.19), derived in the previous section, combined with an accurate steady-state characteristic of the downhole pressure, p_{dh}. To further simplify the presentation here, we assume

$$\rho = \rho_0 = \rho_{in} = \rho_{out}. \tag{2.20}$$

First, consider the flow in the drillstring from mud pump to the bit as our first control volume, and let the mud pump pressure p_p be described by (2.10) according to

$$\frac{V_d}{\beta_d}\dot{p}_p = q_p - q \tag{2.21}$$

where V_d is the volume of the drillstring, β_d is the effective bulk modulus, q_p is the pump flow rate and q is the flow rate through the bit, respectively. Notice that the densities have cancelled out due to (2.20), and that the volume of the drillstring is constant for each stand drilled, such that the time derivative $\dot{V}_d$ is zero.

Similarly, we consider the flow in the annulus from the bit, and up the well through the choke. Let the upstream choke pressure be described by (2.10) according to

$$\frac{V_a}{\beta_a}\dot{p}_c = -\dot{V}_a + q + q_{bpp} - q_c \tag{2.22}$$

where V_a is the volume of the annulus, β_a is the effective bulk modulus, q_{bpp} is the flow rate through the back pressure pump, and q_c is the flow rate through the choke. Note also that this model accounts for changes in the annulus volume through the time derivative of V_a. Consequently, the model can describe the averaged surge and swab effects caused by a moving drillstring. Finally, we assume that the flow through the bit is approximately equal to the average flow from the mud pump ($x = 0$) to the choke ($x = L$), and let it be described by (2.16)–(2.19) according to

$$M\dot{q} = p_p - p_c - F(q) + G(\rho) \tag{2.23}$$

where the spatial coordinate is defined as $x = 0$ at the pump pressure p_p and L is the total length of the well from mud pump to choke such that $x = L$ becomes the spatial coordinate for the choke pressure, p_c. Furthermore, the parameter $M = M(0, L)$ is a constant obtained from (2.17), $F(q) = F(0, L, q, \mu)$ is the steady-state frictional pressure drop along the entire flow path according to (2.18), and $G(\rho) = G(0, L, \rho)$ is the steady-state hydrostatic term affecting the flow, given by (2.19).

The accuracy of the parameter M is not crucial since it relates to the fast dynamics of the flow rate q, which in most cases can be neglected, hence, it can be taken as an approximate value. In the simplified flow rate dynamics (2.23) it may be reasonable to approximate the total hydrostatic term by

$$G(\rho) = -\Delta\rho g h_{TVD} \tag{2.24}$$

where h_{TVD} is the true vertical depth of the well, and $\Delta\rho$ is a constant representing the integrated density difference between the drillstring and the annulus. This density difference $\Delta\rho = \rho_a - \rho_d$, is typically a small, uncertain parameter related to the amount of cuttings in the annulus, which is particularly well suited for online calibration based on topside pump and choke pressures, p_p and p_c, respectively.

In the simplified model, we assume that the pressure along the entire flow path is given by the steady-state pressure characteristics of the flow. Thus, the downhole pressure p_{dh} at any location l in the well is given by the steady-state solution of (2.16)–(2.19), referenced either to the pump pressure p_p, or to the choke pressure p_c.

The downhole pressure profile is described by the choke pressure p_c, via the annulus according to

$$p_{dh}(l) = p_c + F_a(l, q) - G_a(l, \rho) \tag{2.25}$$

where $F_a(l, q) = F(l, L, q, \mu)$ is the frictional pressure drop, and $G_a(l, \rho) = G(l, L, \rho)$ is the hydrostatic pressure term for the flow from the downhole location l to the choke obtained from (2.18) and (2.19), respectively. The hydrostatic pressure term G_a is here negative relative to the direction of the flow up the annulus as defined in (2.19).

Alternatively, the downhole pressure is described by the standpipe pressure p_p, via the drillstring according to

$$p_{dh}(l) = p_p - F_d(l, q) - G_d(l, \rho) \tag{2.26}$$

with the frictional presssure drop $F_d(l, q) = F(0, l, q, \mu)$, and hydrostatic pressure term $G_d(l, \rho) = G(0, l, \rho)$. Note that in (2.25), the frictional pressure drop F_a and hydrostatic pressure G_a are obtained by integrating along the flow path from the downhole pressure p_{dh} at $x = l$, up the annulus to the choke pressure p_c at $x = L$. Equation (2.26) on the other hand, is obtained by integrating from the pump pressure p_p at $x = 0$, and down the drillstring to the downhole pressure p_{dh} (at $x = l$). Consequently, the downhole pressure can be given either by the flow in the annulus of the well by using (2.25), or alternatively by the flow in the drillstring by using (2.26).

To summarize, the complete simple hydraulic model consists of the dynamics (2.21)–(2.23), augmented by a relation for the steady-state downhole pressure, given either via the annulus flow (2.25), or via the drillstring flow (2.26). It is worth noting that (2.25) and (2.26) are generic mathematical descriptions of the fundamental relation between pressure, frictional pressure drop, and hydrostatic pressure, which should be well known to any drilling engineer. To make this clear, consider the downhole pressure given by (2.25) written more compactly as

$$p_{dh} = p_c + F_a(q) + \rho_a g h_{TVD} \tag{2.27}$$

where $F_a(q)$ is the frictional pressure drop as a function of flow rate q, and the last term is the hydrostatic pressure.

Remark 2.5. Notice that the right-hand side of (2.16) which defines the friction term $F(l_1, l_2, q, \mu)$, and the hydrostatic term $G(l_1, l_2, \rho)$ of the simplified model is identical to the steady-state solution of the full differential equation of momentum given by (2.12) which is the basis for advanced hydraulic models. Consequently, the simplified model can incorporate any advanced steady-state relations for the downhole pressure into (2.25) or (2.26), thus achieving the same level of accuracy in steady-state as an advanced hydraulic model.

Remark 2.6. In many drilling operations there is a float (check) valve close to the bit. The valve prevents flow from the annulus and up the drillstring. This valve can easily be incorporated in the model by replacing (2.23) with

$$M\dot{q} = \begin{cases} p_p - p_c - F(q) + G(\rho) & q > 0 \\ \max(0, p_p - p_c - F(q) + G(\rho)) & q = 0 \end{cases}. \tag{2.28}$$

When the float valve is closed (2.26) is no longer valid so (2.25) must be used to model the downhole pressure.

2.2.8 Effective bulk modulus

As pointed out in the derivation of the simple hydraulic model above, the bulk modulus β is the most imporant property in determining the transient response of the hydraulic system, as it is a measure of the stiffness of the fluid. An important aspect of a hydraulic system is that the bulk modulus decreases sharply with small amounts of entrained gas, and/or mechanical compliance. Hence, in all wells the effective bulk modulus is significantly lower than the bulk modulus that is measured in the laboratory. An example is from the Kvitebjørn field in the North Sea, where the bulk modulus of a particularly stiff Cesium formate drilling fluid was measured in the laboratory to $\beta_{Cs} \approx 50000$ bar, while the resulting effective bulk modulus measured in the well was $\beta_e \approx 15000$ bar.

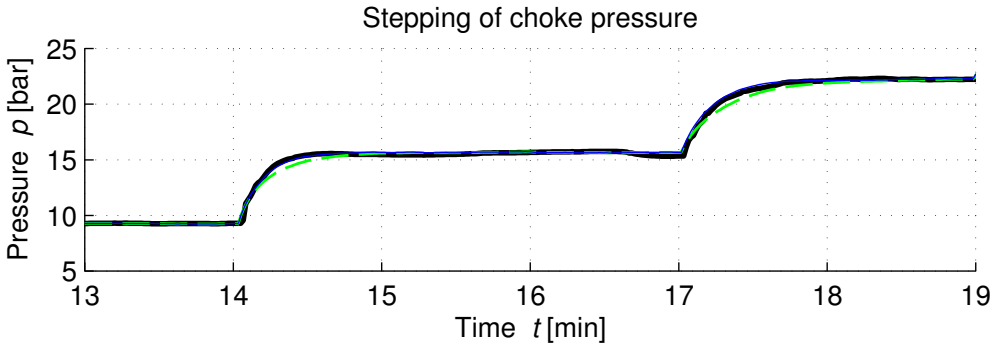

Figure 2.3: Measured (black) and simulated choke pressure based on estimated (blue) and fixed (green) bulk modulus.

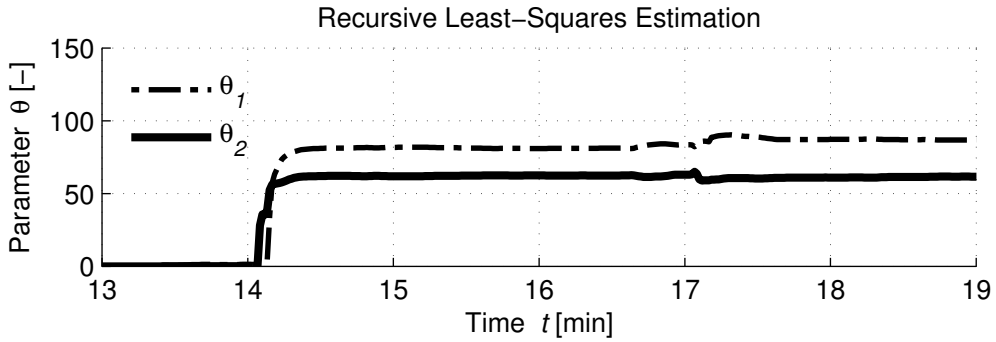

Figure 2.4: Online estimation of the bulk modulus in annulus and drillstring based on topside pressure measurements.

Fig. 2.3 illustrates how the transient response of the simulated choke pressure of the simple hydraulic model compares to experiments performed on a well in the North Sea. The experiment illustrates the typical response to steps in the choke opening while circulating at 2000 l/min. The figure shows both an open-loop simulation with a fixed β_a, and the case when β_a is continuously estimated online using a recursive least squares algorithm. The corresponding parameter convergence is plotted in Fig. 2.4.

2.3 Online Model Calibration

In this section we illustrate how both topside and downhole pressure-while-drilling (PWD) measurements can be used to calibrate parameters of the simple hydraulic

model online. We also make some remarks regarding the severity of non-robust algorithms in failure-critical systems.

The algorithms used for online model calibration in this section, are primarily based on the results found in (Stamnes et al., 2008, 2010a; Ioannou and Sun, 1996; Ljung, 1999). For references on similar research, see e.g. (Grip, Johansen, Imsland, and Kaasa, 2010).

2.3.1 Estimating the effective bulk modulus from topside pressure measurements

A good model of the pressure transients of the hydraulics requires a good estimate of the effective bulk modulus. Since the degree of mechanical compliance of casing/pipe/hoses etc. is uncertain, and it is impossible to accurately predict the amount of gas pockets, bubbles, or "breathing" of the well, any estimate of the effective bulk modulus must be based on measurements from the actual well to have any chance of being accurate.

Using the simplified hydraulic model it is possible to estimate the effective bulk modulus effectively from the measured standpipe and choke pressures online, provided there is enough excitation in the pressures. Based on the field data plotted in Fig. 2.3 and 2.4, we demonstrate that a recursive least-squares method can be applied to obtain an accurate estimate of both the bulk modulus for the drillstring and the annulus, with a single step in the choke pressure.

2.3.2 Estimating friction characteristics and density difference

As both the friction characteristics F and the density in the annulus ρ_a are uncertain there is a need to tune these parameters online. During drilling the sensors located at the rig (top side) usually provide good accuracy at high sampling rates (1 Hz or faster), while the available measurements from the downhole sensors have much lower sampling rate ($\frac{1}{20}$Hz or slower) and suffer from uncertain delays (several seconds or more). Furthermore, the downhole measurements are transmitted by creating pressure pulses in the mud and consequently only available at high flow rates[5]. We will first illustrate how we can tune these parameters online using only topside measurements, and afterwards illustrate how additional parameters can be

[5]Note that measurements of the average, maximum and minimum downhole pressure during zero flow can be transmitted as the first data points after full flow is resumed. These data can be used to further calibrate the model.

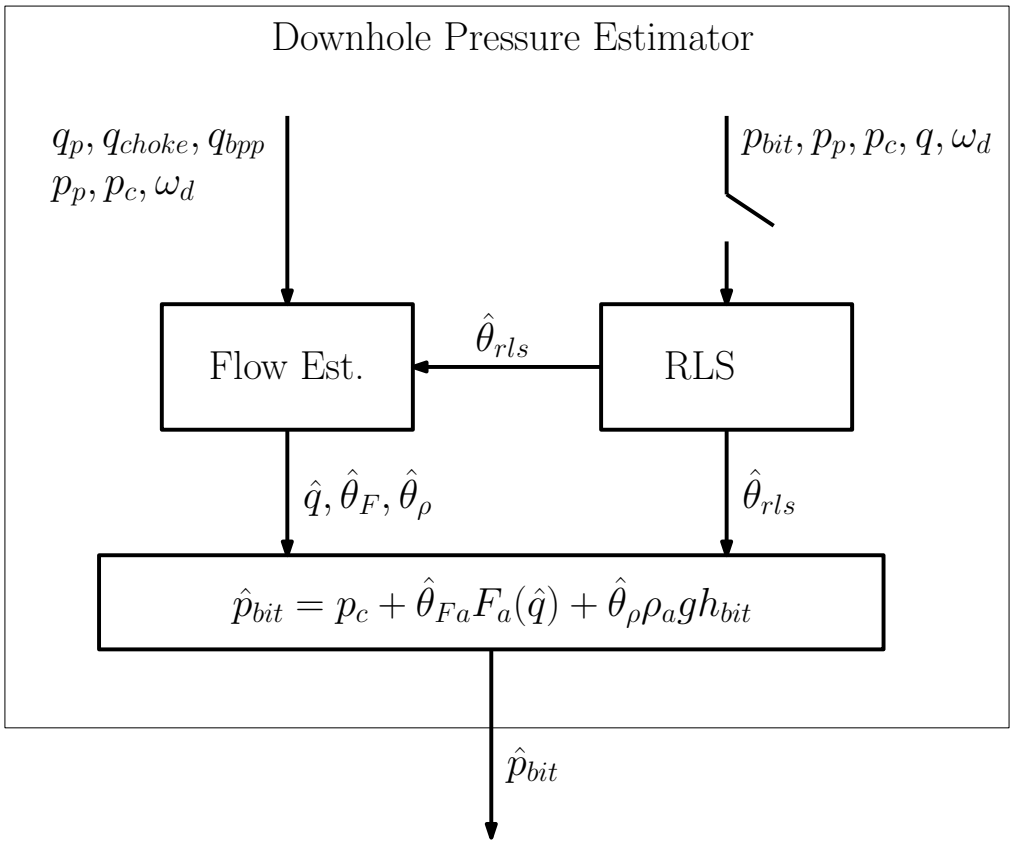

Figure 2.5: Overview of estimation algorithm.

estimated when using both topside and downhole measurements. For simplicity we only consider the pressure at the bit $p_{bit} = p_{dh}(l_{bit})$ and not the entire pressure profile $p_{dh}(l)$. An overview of the complete algorithm is shown in Fig. 2.5. In the case where only topside measurements are available an adaptive observer is used to estimate the unmeasured flow rate and two parameters. If downhole measurements are available a recursive least squares algorithm is used to identifiy additional parameters.

Estimation using topside measurements

To allow for uncertainties in the friction characteristics and the density in the annulus we parameterize (2.23) and (2.24) according to

$$M\dot{q} = p_p - p_c - \theta_F F(q) - (\theta_\rho - 1)\rho g h_{TVD}, \tag{2.29}$$

where θ_F is a tuning parameter for the total friction loss, ρ is the density of the drilling mud and θ_ρ is a tuning parameter for the uncertain density in the annulus (i.e. $\rho_a = \theta_\rho \rho$). Note that in steady-state ($\dot{q} = 0$) we have one equation with two unknowns so that any estimation scheme will require variation in the flow rate q to determine the two uncertain parameters. Using data gathered from pre-drilling tests from an offshore well in the Norwegian North Sea we test the algorithm. The data from the well consists of a pipe connection scenario which has been duplicated to generate enough data to test the algorithm. A second order polynomial was fitted to a different data set to find the steady state friction characteristic $F(q) = F_a(q) + F_d(q)$ which is given in (2.32). For this friction characteristic the "true" values for θ_F and θ_ρ are both equal to one. For robustness and fast tunable parameter identification we apply the algorithm developed in Stamnes et al. (2010a). Details on the algorithm can be found in Appendix 2.5.1 while key parameters for the well are summarized in Table 2.1. We ran the algorithm with three sets of gains namely low, medium and high adaptation gains. The estimation algorithm was started at $t \approx 7.5$min, with initial conditions $\hat{\theta}_F = 1.5$ and $\hat{\theta}_\rho = 1.1$ corresponding to a 50% error in the total friction loss and a 10% error in the density in the annulus. Fig. 2.6 shows the downhole pressure, its estimates, the topside pressures, the pump flow rate and the estimated bit flow rate. From Fig. 2.6a we see that the downhole pressure is accurately estimated after initial transients. We can also see that the red line, corresponding to the low adaptive gain, converges slower than the black dash-dotted line which corresponds to a high adaptive gain. The parameter estimates are shown in Fig. 2.7 where we can see that they all converge to the "true" value with faster convergence rates for higher adaptation gain.

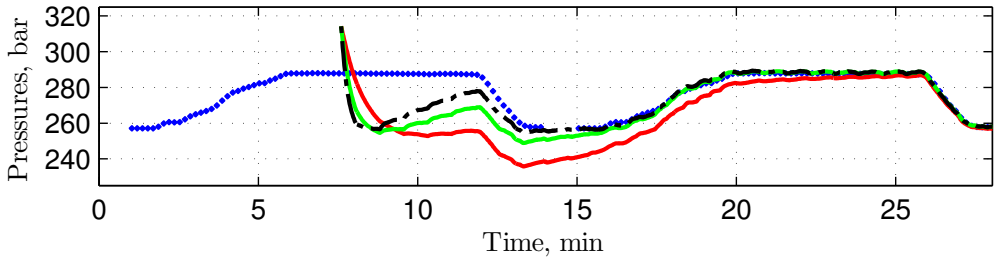

(a) Downhole pressures. Blue crosses corresponds to the logged downhole pressure, red, green and black lines corresponds to low, medium and high adaptation gain respectively.

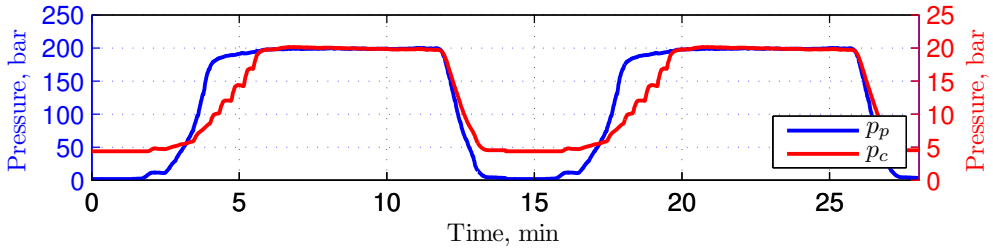

(b) Topside pressures.

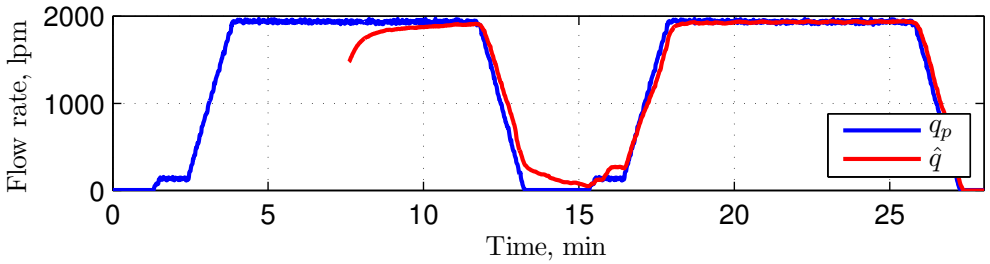

(c) Pump flow rate and estimate of unmeasured flow rate.

Figure 2.6: Estimation based on top-side measurements.

Parameter	**Value**	**Description**
h_{dh}	$1632m$	True vertical depth of bit
ρ	$1580\frac{kg}{m^3}$	Density of mud
$\beta_d = \beta_a$	$20000bar$	Effective bulk modulus
V_d	$15.5m^3$	Volume of mud in drill string
V_a	$75.4m^3$	Volume of mud in annulus
M	$4100\frac{10^5 kg}{m^4}$	Integrated density per cross section

Table 2.1: Well parameters used to estimate parameters using top-side measurements only.

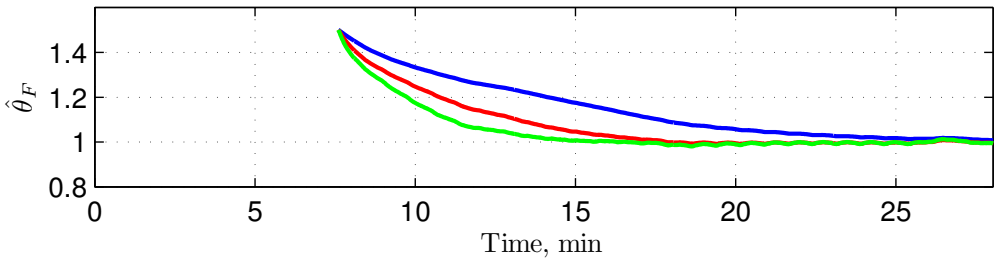

(a) Estimates of θ_F.

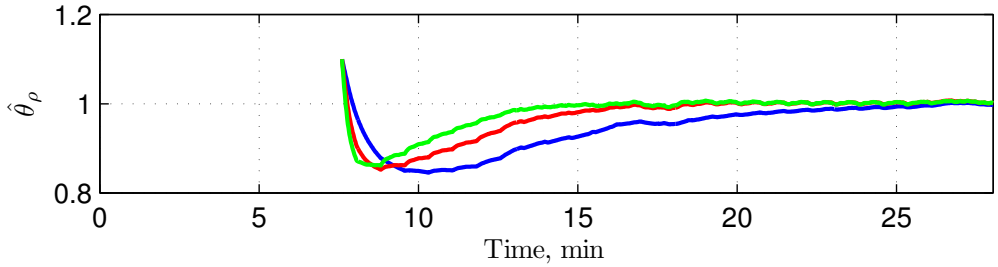

(b) Estimates of θ_ρ

Figure 2.7: Parameter estimates based on top-side measurements. Blue, red and green lines corresponds to low, medium and high adaptive gains respectively.

Estimation using downhole measurements

When downhole measurements are available they can be used to tune additional parameters in the model. As pointed out in Section 2.3.2 the downhole pressure measurement is only available at high flow rates, with low sampling rate and uncertain delays. This limits the number of additional parameters that can be estimated using the measurement to one. The low frequency measurement of the downhole pressure is used to tune the friction in the drillstring based on the relationship (2.26) according to

$$p_{dh}(l) = p_p - \theta_{Fd} F_d(q) + \rho_d g h_{TVD}, \tag{2.30}$$

where θ_{Fd} is estimated using a recursive least squares scheme included in Appendix 2.5.2. We also change the parametrization in (2.29) to

$$M\dot{q} = p_p - p_c - \theta_{Fa} F_a(q) - \theta_{Fd} F_d(q) - (\theta_\rho - 1)\rho g h_{TVD} \tag{2.31}$$

so that the RLS scheme is responsible for updating the friction loss in the drillstring, while the adaptive observer updates the friction loss and density in the annulus. This parameterization allows for separate uncertainties in both the drillstring and the annulus friction in contrast to the scheme without downhole measurements for

which $\theta_{Fa} = \theta_{Fd} = \theta_F$. As the parameterization was changed from the previous section we retuned the observer and the gains for both the observer and the RLS algorithm are given Appendix 2.5.1. Since the downhole pressure measurement is only available at full flow rates the convergence rate of this scheme is slower than the previous scheme and so it was neccessary to replicate the pipe connection data three times to achieve convergence. The algorithm was started at $t \approx 7.5$min with initial conditions $\hat{\theta}_{Fa} = \hat{\theta}_{Fd} = 1.5$ and $\hat{\theta}_{\rho} = 1.1$ corresponding to a 50% error in both drillstring and annulus friction and a 10% error in annulus density. Fig. 2.8 compares the results for two different forgetting factors in the RLS scheme. From Fig. 2.8a we see that the estimates converge to the true downhole pressure in both cases. Fig. 2.8b–2.8d shows that the estimated friction factor in the drillstring and the estimated density factor in the annulus both converge quickly to the "true" value one, while the estimate of the friction factor in the annulus converges slower to a value slightly less than one. One possible explanation for this behaviour is that $\hat{\theta}_{Fa}$ is sensitive to errors in $\hat{\theta}_{Fd}$ as the total friction pressure in the drillstring is much higher than in the annulus. A small error in $\hat{\theta}_{Fd}$ will therefore give a large error in $\hat{\theta}_{Fa}$.

2.3.3 Robustness of adaptive algorithms

When calibrating a model online, transparency with respect to the relation between measurements, the model, and its parameters are crucial in order to ensure that the resulting adaptive solution is robust. It is essential that the parameter estimation problem has a unique solution, that is, it must be possible to uniquely identify the selected parameters from the given model and measurements. The problem is analog to the problem of solving for unkowns from a set of algebraic equations. The number of independent equations must be the same as the number of unknowns in order to have a unique solution. If the number of equations are less, there is no longer only one solution, but a set of solutions satisfying the equations. The same principle applies to calibration of model parameters from measurements. The number of independent measurements and known relations are analogous to the number of equations in the above example, hence, basically only one parameter can be calibrated from one measurement. However, by adding additional known relations between parameters, it is possible to extend the number of parameters that can be calibrated based on a given set of measurements.

Note that this is in essence what the human mind does when tuning parameters of an advanced model manually; based on complex knowledge and experience of the system, constraints and relations are added sub-consciously, making it possible to pick a unique solution from a set of several possibilities. The challenge is to for-

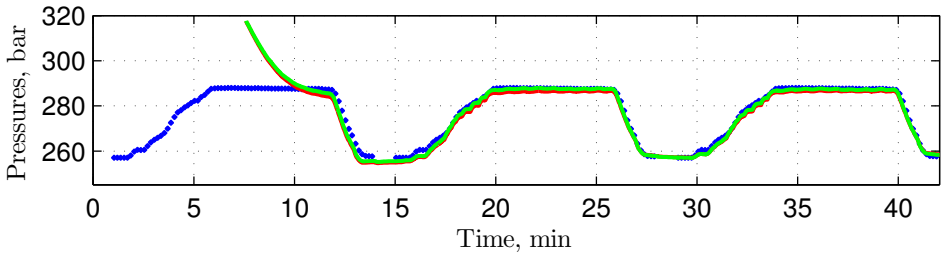

(a) Downhole pressure. Blue crosses corresponds to the logged downhole pressure, red and green lines corresponds to slow and fast adaptation respectively.

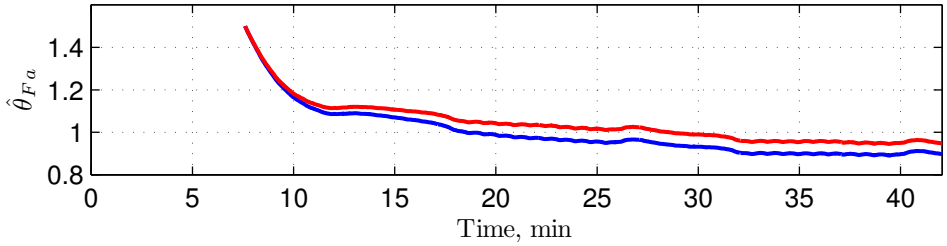

(b) Estimated annulus friction coefficient. The blue and red lines correspond to slow and fast adaptation respectively.

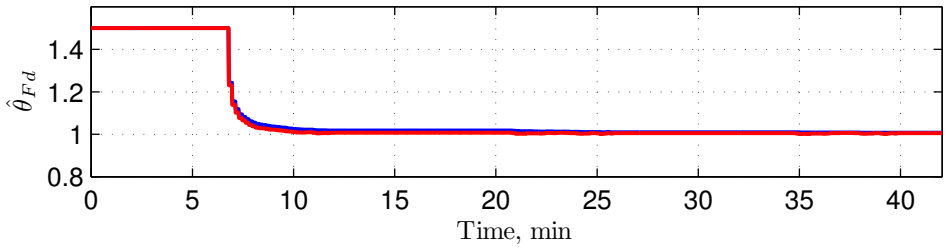

(c) Estimated drill string friction coefficient. The blue and red lines correspond to slow and fast adaptation respectively.

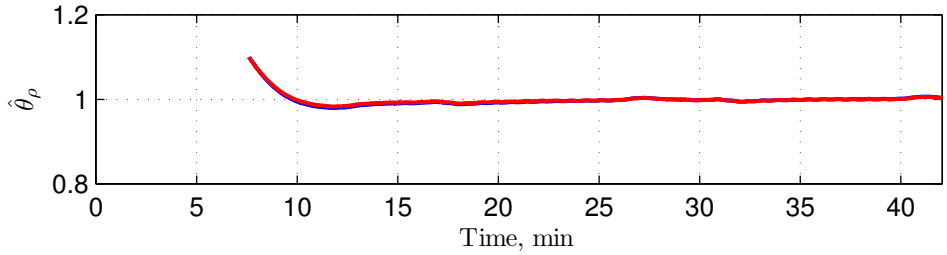

(d) Estimated density coefficient. The blue and red lines correspond to slow and fast adaptation respectively.

Figure 2.8: Estimation of downhole pressure and three parameters using both topside and downhole measurements

mulate these relations in a mathematical language so that they can be implemented in an automatic procedure. When the model becomes complex, it usually becomes impossible to rigorously assess the identifiability of different parameters under all conditions. To make this possible, the model needs to be simple and transparent, and fit the mathematical framework available.

2.4 Conclusions

In this work, we have outlined the basic assumptions behind the derivation of advanced and simplified hydraulic models, and derived in detail a simple fit-for-purpose hydraulic model for managed pressure drilling. We have briefly demonstrated that the simplified hydraulic model is able to capture the dominating hydraulics of the well, and illustrated by some examples how the model can be calibrated automatically using available measurements.

Nomenclature

HPHT	High Pressure, High Temperature
MPD	Managed Pressure Drilling
PVT	Pressure-Volume-Temperature
PWD	Pressure While Drilling
RLS	Recursive Least Squares
RPM	Revolutions Per Minute
UKF	Unsceted Kalman Filter

2.5 Appendix

2.5.1 GFC data

Data from drilling operations at Gullfaks C has been gathered. Both data available during drilling (top-side and low frequency downhole measurements) and data available after drilling (logged downhole measurements) have been collected. Based on these data we test an estimation scheme for estimation of the bottomhole pressure. A simple polynominal friction model for the drill string and the annulus was fitted to steady-state data giving

Parameter	Value	Description
N	20	Number of observers
T	45	Delay between observers
G	diag$([2.5, 3])$	Medium adaptation gain
l_1	2×10^{-4}	Feedback gain (pump)
l_2	10^{-4}	Feedback gain (choke)
α	1	Adaptation weighting gain

Table 2.2: Tuning parameters for estimation scheme from Stamnes et al. (2010a).

$$F_a(q) = 304.9q + 5188q^2 \quad (2.32a)$$
$$F_d(q) = 366.6q + 146570q^2 \quad (2.32b)$$

where $F_a(q) = F(l_{bit}, L, q, \mu)$ corresponds to the frictional pressure loss from the bit to the choke and $F_d(q) = F(0, l_{bit}, q, \mu)$ corresponds to the frictional pressure loss from the main pump to the bit. The fit is shown in Fig. 2.9 and 2.10. We see that the fit for the annulus frictional pressure is quite good for high flow rates but deviates with around 2 bars at lower flow rates. The fit for the drillstring frictional pressure is better when considering relative error but worse when considering absolute error, with maximum errors around 5 bar.

Based on the model (2.21)–(2.22) and (2.29) an adaptive observer has been derived in Stamnes et al. (2010a). The gains and tuning parameters for the observer used when only topside measurements are available are summarized in Table 2.2. The low adaption gain corresponds to $0.5G$ while the high adaptive gain corresponds to $1.5G$. When both topside and downhole measurements are available we use the same parameter values except for the adaptation gain G which is chosen to be diag$([40, 0.5])$. When downhole pressure measurements are available we use an additional RLS algorithm to estimate an aditional parameter, the RLS algorithm is included in Appendix 2.5.2 and the gains for the RLS algorithm are $P(0) = 0.1\hat{}2$ and $\lambda = \{0.90, 0.99\}$ with $\lambda = 0.99$ corresponding to slow adaptation and $\lambda = 0.90$ corresponding to fast adaptation.

2.5.2 RLS algorithm

The recursive least squares algorithm used in the estimation scheme in Section 2.3.2 is taken from Ljung (1999) and summarized in Table 2.3. The RLS algorithm has a

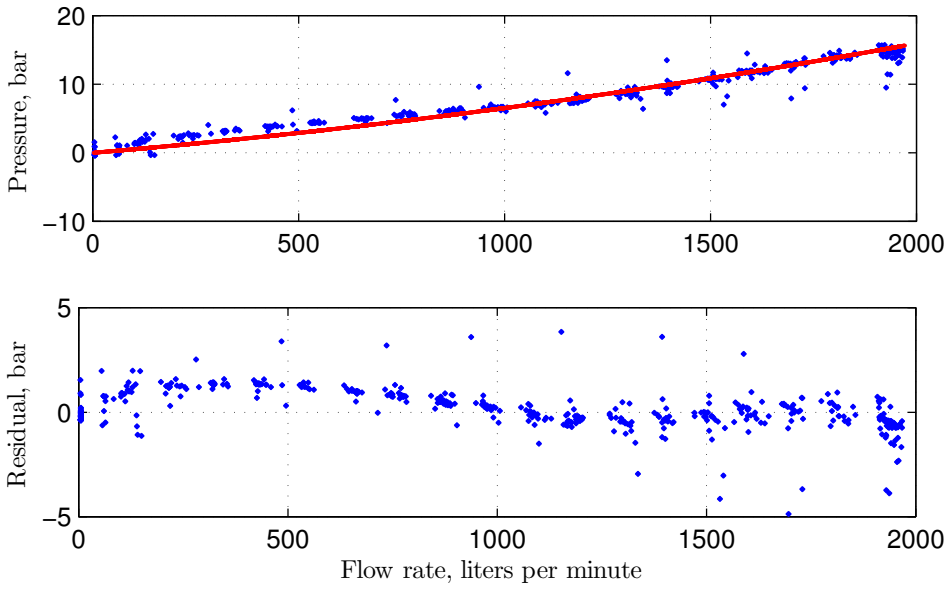

Figure 2.9: Polynominal fit of the friction in the annulus.

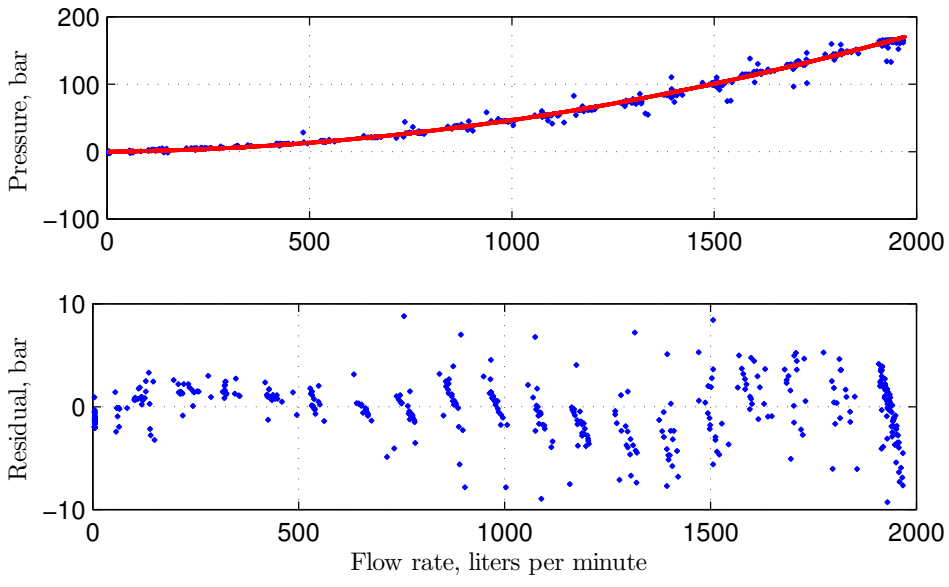

Figure 2.10: Polynominal fit of the friction in the drillstring.

Parametric Model	$\theta^T \phi(q) = z(t)$
Criterion	$\hat{\theta}(t) = \arg\min_\theta \sum_{k=1}^{t} \beta(t,k) \left[z(k) - \phi^T(q(k)) \theta \right]^2$ $\beta(t,k) = \lambda(t) \beta(t-T,k), 0 \leq k \leq t-T$ $\beta(t,t) = 1$
Algorithm	$\hat{\theta}(t) = \hat{\theta}(t-T) + L(t) \left[z(t) - \phi^T(q(t)) \hat{\theta}(t-T) \right]$ $L(t) = \frac{P(t-T)\phi(q(t))}{\lambda(t) + \phi^T(t) P(t-T) \phi(q(t))}$ $P(t) = \frac{1}{\lambda(t)} \left[P(t-1) - \frac{P(t-1)\phi(q(t))\phi^T(q(t))P(t-T)}{\lambda(t) + \phi^T(q(t))P(t-T)\phi(q(t))} \right]$
Initial Conditions	$\hat{\theta}(0), P(0) = P^T(0) > 0$
Design Variables	$0 < \lambda(t) \leq 1$

Table 2.3: RLS with forgetting factor

forgetting factor λ which discounts the data according to

$$\beta(t,k) = \lambda^{t-k}, \tag{2.33}$$

which implies that $\lambda = 1$ weights all the data equally while $0 < \lambda < 1$ discounts the data. For example $\lambda = 0.95$ discounts the tenth data point according to $\beta = 0.95^{10} \approx 0.60$.

Part II

Adaptive Observer Design

Chapter 3

Adaptive Redesign of Nonlinear Observers

Abstract: *To estimate unmeasured states in dynamical systems with parametric uncertainties one can use adaptive observers. In this paper a new method for adaptive redesign of reduced order observers for nonlinear systems is presented. The redesign makes the observer robust as it guarantees that the state estimation error converges to zero in the presence of parametric uncertainties. To enable parameter adaption, a new type of update law is derived using Lyapunov analysis and a nonlinear coordinate transformation. The uniqueness of the approach is that it allows terms containing both uncertainty and nonlinearity in the unmeasured states to appear in the dynamics of the unmeasured states, and still achieves convergence of the state estimate without requiring persistent excitation. Two examples are presented that demonstrate these properties.*

3.1 Introduction

It is often the case that signals needed for feedback control are not measured or the measurement quality is low due to noise or slow sampling rates. In these cases signals needed for control purposes can be estimated or filtered using state observers. Much research has been devoted to this field of study starting with observer design for linear systems (Kalman, 1960; Luenberger, 1964). For nonlinear systems satisfying a Lipschitz type condition, high-gain observers can be designed (Thau, 1973; Tornambe, 1989; Gauthier et al., 1992; Khalil, 1999). In the work by Krener and Isidori (1983), conditions are derived for when a nonlinear system can be trans-

formed into a linear system, plus a nonlinear term which only depends on measured signals, enabling linear systems theory to be used to derive an observer. More recently, Kazantzis and Kravaris (1998) extended Luenbergers original ideas (Luenberger, 1964) to the nonlinear case. In the work by Kazantzis and Kravaris (1998), conditions are derived for the existence of a local nonlinear transformation that transforms the original nonlinear system into a linear system, driven by a nonlinear measured term. Since the output map can be nonlinear in the new coordinates the method is more general than the result by Krener and Isidori (1983), where the output map is constrained to be linear. Extensions to this work has been developed in (Krener and Xiao, 2002, 2004; Andrieu and Praly, 2006; Kravaris et al., 2007). For systems satisfying a sector condition, the circle criterion can be used to derive observers (Arcak and Kokotović, 2001; Fan and Arcak, 2003). Moreno (2005) uses a diffeomorphism to turn the nonlinear system into a linear system, plus a nonlinear term depending on measured signals only, and a perturbation term. The perturbation term is dealt with by either using high-gain or sector conditions, the approach thus unifies several of the above design methods. In the work (Karagiannis et al., 2008), the observer design is reduced to finding certain mappings so that a chosen manifold, corresponding to the estimation error being equal to zero, is rendered attractive and invariant. The order of the observer can be higher than the order of the state to be estimated, so the method thus represents an immersion based design.

If, in addition to unmeasured states, there are parametric uncertainties, an observer can be made robust by adapting to these uncertainties. These observers are often called *adaptive observers*. For linear time invariant systems early results on adaptive observer design can be found in (Luders and Narendra, 1973; Kreisselmeier, 1977), and a complete theory on adaptive observers for linear systems can be found in e.g. Ioannou and Sun (1996) or Narendra and Annaswamy (1989).

For nonlinear systems, paralleling the work done in the nonadaptive case, adaptive observers have been developed using transformation techniques and exploiting certain structures/canonical forms. The design methods are often based on Lyapunov like functions containing a parameter error term. Under a strictly positive real (SPR) condition (Ioannou and Sun, 1996), the derivative of such functions can be found to be negative semidefinite, providing conditions for applying Barbălat's lemma to guarantee that the state estimation error converges to zero. An early result can be found in (Bastin and Gevers, 1988), where adaptive observers were developed for systems in the so called adaptive observer canonical form. It was also shown that several useful systems can be transformed into this form. Building on these results, all systems that are transformable into the adaptive observer canonical form through the use of filtered transformations (possibly dependent on unknown parameters) were characterized in Marino and Tomei (1992). If the filtered trans-

formations depend on unknown parameters, persistency of excitation is needed to reconstruct the actual state estimate. These approaches are thoroughly presented in Marino and Tomei (1996). An interesting comparison of different transformation based adaptive observers can be found in Zhang (2005), where the author collects several of the adaptive observers into one canonical form. Without relying on transformation techniques, the results in Cho and Rajamani (1997) apply to a class of multiple-input multiple-output nonlinear system satisfying an SPR like condition and a Lipschitz condition on the nonlinearities. In the spirit of Bastin and Gevers (1988) and Marino and Tomei (1996), Besançon (2000a) collects most of the existing results into one adaptive observer form for which design procedures are available.

In this paper we consider adaptive redesign of reduced order nonlinear observers. That is, we assume that a (nonadaptive) reduced order observer and a corresponding Lyapunov function is given, and based on this, perform an adaptive redesign to make the observer adaptive. Through Lyapunov analysis we find an update law that is driven by the unmeasured state estimation error, and thus cannot be implemented as is. However, if a solution to a certain partial differential equation (PDE) can be found, we are able to show that a new, implementable update law, is equivalent to the one found through Lyapunov analysis. We apply the method to design adaptive observers for two example systems. In the first example, we design an adaptive observer to estimate the unmeasured flow rate in a hydraulic system, while in the second example we apply the method to a system where the regressor depends nonlinearly on both the measured output and the unmeasured state. In both examples, the unmeasured state dynamics contains terms that combine parametric uncertainty and nonlinearity in the unmeasured states. Still, the proposed redesign achieves convergence of the state estimate without requiring persistent excitation. To the best of the authors knowledge, this is not achieved by any other method.

3.2 Adaptive Redesign

Given the system

$$\dot{y} = f_1(t, y, z) \tag{3.1a}$$
$$\dot{z} = f_2(t, y, z) + \phi(t, y, z)\,\theta, \tag{3.1b}$$

where f_1, f_2 and ϕ are locally Lipschitz in $y \in K_y$, $z \in K_z$ uniformly in $t \in \mathbb{R}$, $\theta \in K_\theta$ is a vector of constant, uncertain parameters, and $K_y \subset \mathbb{R}^m$, $K_z \subset \mathbb{R}^n$ and $K_\theta \subset \mathbb{R}^p$ are compact sets. We do not require knowledge of the sets K_y, K_z and K_θ for the redesign (although knowledge of some or all might be needed for the

nominal design in (3.2)–(3.4)). Suppose a reduced order observer is available for the case where θ is known in the form

$$\hat{z} = \beta(t, y, \xi), \tag{3.2a}$$

$$\dot{\xi} = \psi(t, y, \xi) + \left(\frac{\partial \beta}{\partial \xi}\right)^{-1} \phi(t, y, \hat{z})\,\theta, \tag{3.2b}$$

where $\det(\frac{\partial \beta}{\partial \xi}) \neq 0$ for any (t, y, ξ). As an example, the observer (3.2) could be found using the methodology proposed in (Arcak and Kokotović, 2001; Karagiannis et al., 2008). Defining the error $\tilde{z} = z - \hat{z}$, suppose that the error dynamics can be written as

$$\dot{\tilde{z}} = \varepsilon(\theta, t, y, z, \tilde{z}), \tag{3.3}$$

with ε locally Lipschitz uniformly in t, for all $(\theta, y, z) \in K_\theta \times K_y \times K_z$. Furthermore, we assume that we are given a differentiable Lyapunov function $V_z(t, \tilde{z}) : [0, \infty) \times D_z \longrightarrow \mathbb{R}$, with $D_z \subset \mathbb{R}^n$, satisfying

$$\alpha_1(\tilde{z}) \leq V_z(t, \tilde{z}) \leq \alpha_2(\tilde{z}) \tag{3.4a}$$

$$\frac{\partial V_z}{\partial t} + \frac{\partial V_z}{\partial \tilde{z}} \varepsilon(\theta, t, y, z, \tilde{z}) \leq -c\alpha_3(\tilde{z}), \tag{3.4b}$$

for all $t \geq 0$ and all $(\theta, y, z) \in K_\theta \times K_y \times K_z$, where α_i, $i \in \{1, ...3\}$ are continuous positive definite functions on D_z, and $c > 0$ is a design constant (observer gain). Let $B_z = \{\tilde{z} \in \mathbb{R}^n \mid V_z(t, \tilde{z}) \leq c_z\} \subset D_z$ for some $c_z > 0$ be an estimate of the region of attraction. If (3.4) holds with $D_z = \mathbb{R}^n$ and α_1 radially unbounded, then $B_z = \mathbb{R}^n$ ($c_z = \infty$), Khalil (2002).

The main result in this paper relies on the following assumption.

Assumption 3.1. *There exists $f_v(t, y, \hat{z})$ such that*

$$f_1(t, y, z) - f_1(t, y, \hat{z}) = f_v(t, y, \hat{z}) \left(\frac{\partial V_z}{\partial \tilde{z}}\right)^T. \tag{3.5}$$

For systems with f_1 nonlinear in z, Assumption 3.1 imposes a specific property on the Lyapunov function which in general will be hard to obtain. If (3.1a) has the form $\dot{y} = A(t, y)\, z + \bar{f}_1(t, y)$, then Assumption 3.1 can be satisfied with a Lyapunov function that is quadratic in $\tilde{z}$.

Theorem 3.2. *(Main result) Suppose $\eta(t, y, \hat{z})$ is a solution to the partial differential equation*

$$-\phi^T(t, y, \hat{z}) = \left(\frac{\partial \eta}{\partial y}(t, y, \hat{z}) + \frac{\partial \eta}{\partial \hat{z}}(t, y, \hat{z}) \frac{\partial \beta}{\partial y}(t, y, \xi)\right) f_v(t, y, \hat{z}). \tag{3.6}$$

Then, the adaptive observer

$$\dot{\xi} = \psi(t, y, \xi) + \left(\frac{\partial \beta}{\partial \xi}\right)^{-1} \phi(t, y, \hat{z})\,\hat{\theta}, \tag{3.7}$$

$$\hat{z} = \beta(t, y, \xi), \tag{3.8}$$

$$\begin{aligned}\dot{\hat{\sigma}} =& \Gamma \frac{\partial \eta}{\partial t}(t, y, \hat{z}) + \Gamma \frac{\partial \eta}{\partial y}(t, y, \hat{z})\, f_1(t, y, \hat{z}) \\ &+ \Gamma \frac{\partial \eta}{\partial \hat{z}}(t, y, \hat{z}) \left(\frac{\partial \beta}{\partial t}(t, y, \xi) + \frac{\partial \beta}{\partial y}(t, y, \xi)\, f_1(t, y, \hat{z}) \right. \\ &\left. + \frac{\partial \beta}{\partial \xi}(t, y, \xi)\, \psi(t, y, \xi) + \phi(t, y, \hat{z})\,\hat{\theta} \right),\end{aligned} \tag{3.9}$$

$$\hat{\theta} = \hat{\sigma} - \Gamma \eta(t, y, \hat{z}), \tag{3.10}$$

where $\Gamma = \Gamma^T > 0$, *provides the following properties for the error dynamics: All solutions starting in*

$$B = \left\{ \left(\tilde{z}, \tilde{\theta}\right) \in \mathbb{R}^n \times \mathbb{R}^p \;\middle|\; V_z(t, \tilde{z}) + \frac{1}{2}\tilde{\theta}^T \Gamma^{-1} \tilde{\theta} \leq c_z \right\}$$

are uniformly bounded and $\lim_{t\to\infty} \tilde{z} = 0$.

Remark 3.3. Equation (3.6) is a partial differential equation that cannot be solved in general. However, as we will show in Section 3.3 it has a solution for several practical examples.

The proof of Theorem 3.2 consists of the following two intermediate steps.

Proposition 3.4. *The properties of the adaptive observer in Theorem 3.2 are achieved for (3.7)–(3.8) and the update law*

$$\dot{\hat{\theta}} = \Gamma \phi^T(t, y, \hat{z}) \left(\frac{\partial V_z}{\partial \tilde{z}}\right)^T. \tag{3.11}$$

Proposition 3.5. *The dynamics of (3.11) and the dynamics of (3.9)–(3.10) are identical (in terms of trajectories of* $\hat{\theta}(t)$*). That is, (3.9)–(3.10) represents an implementable version of (3.11).*

Proof of Proposition 3.4. By differentiating (3.8) with respect to time, inserting (3.1a) and (3.7), and subtracting the result from (3.1b), we find the state estimation error dynamics to be

$$\dot{\tilde{z}} = \varepsilon(\theta, t, y, z, \tilde{z}) + \phi(t, y, \hat{z})\,\tilde{\theta}, \tag{3.12}$$

where $\varepsilon(\theta, t, y, z, \tilde{z})$ is the unperturbed error dynamics (see (3.3)). Using the properties (3.4a)–(3.4b), we have, for $\tilde{z} \in D_z$, that

$$\frac{\partial V_z}{\partial t} + \frac{\partial V_z}{\partial \tilde{z}} \varepsilon(\theta, t, y, z, \tilde{z}) \leq -c\alpha_3(\tilde{z}) + \frac{\partial V_z}{\partial \tilde{z}} \phi(t, y, \hat{z})\, \tilde{\theta}. \tag{3.13}$$

Taking

$$V = V_z + \frac{1}{2} \tilde{\theta}^T \Gamma^{-1} \tilde{\theta}, \tag{3.14}$$

we obtain from (3.13) and $\dot{\theta} = 0$ that

$$\dot{V} \leq -c\alpha_3(\tilde{z}) + \tilde{\theta}^T \Gamma^{-1} \left(-\dot{\hat{\theta}} + \Gamma \phi^T(t, y, \hat{z}) \left(\frac{\partial V_z}{\partial \tilde{z}} \right)^T \right). \tag{3.15}$$

Substituting the update law (3.11) into (3.15), we get

$$\dot{V} \leq -c\alpha_3(\tilde{z}), \tag{3.16}$$

which holds for $(\tilde{z}, \tilde{\theta}) \in D_z \times \mathbb{R}^p$. Since (3.16) holds for all $(\tilde{z}, \tilde{\theta}) \in B$, we have that all solutions of (3.12) and (3.11) ($\dot{\tilde{\theta}} = -\dot{\hat{\theta}}$) starting in B are uniformly bounded. That is, $\exists\, \bar{c} < \infty$, such that $\|(\tilde{z}(t), \tilde{\theta}(t))\| \leq \bar{c}$, $\forall t$. Note that since $y \in K_y$ and $z \in K_z$ this also implies that $\hat{z}$ and ξ are bounded. To prove $\lim_{t\to\infty} \tilde{z} = 0$, we use a local version of the proof for the LaSalle–Yoshizawa theorem (Krstić et al., 1995, Th. A.8), mainly based on Barbălat's lemma. Since V is non-increasing and bounded from below it has a limit $V_\infty = \lim_{t\to\infty} V(t, \tilde{z}(t), \tilde{\theta}(t))$. Integrating (3.16) with respect to time gives

$$\left[V\left(t_0, \tilde{z}_0, \tilde{\theta}_0\right) - V_\infty \right] \geq c \int_{t_0}^{\infty} \alpha_3(\tilde{z}(\tau))\, d\tau, \tag{3.17}$$

hence $\int_{t_0}^{\infty} \alpha_3(\tilde{z}(\tau))\, d\tau$ exists and is finite. Since y, z and $\tilde{z}$ are bounded the right-hand side of (3.12) is bounded so $\tilde{z}(t)$ is uniformly continuous. Since $\alpha_3(\tilde{z})$ is continuous, it is uniformly continuous on the compact set $D = \{\|\tilde{z}\| \leq \bar{c}\}$. From the uniform continuity of $\alpha_3(\tilde{z})$ and $\tilde{z}(t)$, we conclude that $\alpha_3(\tilde{z}(t))$ is uniformly continuous. By Barbălat's lemma we then have $\lim_{t\to\infty} \alpha_3(\tilde{z}) = 0$, which implies $\lim_{t\to\infty} \tilde{z} = 0$. □

Proof of Proposition 3.5. Differentiating (3.10) with respect to time and inserting (3.1a) and (3.9) we have

$$\begin{aligned}
\dot{\hat{\theta}} = {} & \Gamma \frac{\partial \eta}{\partial y}(t, y, \hat{z}) \left(f_1(t, y, \hat{z}) - f_1(t, y, z) \right) \\
& + \Gamma \frac{\partial \eta}{\partial \hat{z}}(t, y, \hat{z}) \left(\frac{\partial \beta}{\partial t}(t, y, \xi) + \frac{\partial \beta}{\partial y}(t, y, \xi)\, f_1(t, y, \hat{z}) \right. \\
& \left. + \frac{\partial \beta}{\partial \xi}(t, y, \xi)\, \psi(t, y, \xi) + \phi(t, y, \hat{z})\, \hat{\theta} - \dot{\hat{z}} \right).
\end{aligned} \tag{3.18}$$

Differentiating (3.8) with respect to time and substituting into (3.18) we get

$$\begin{aligned}\dot{\hat{\theta}} = &\Gamma \frac{\partial \eta}{\partial y}(t, y, \hat{z})\left(f_1(t, y, \hat{z}) - f_1(t, y, z)\right) \\ &+ \Gamma \frac{\partial \eta}{\partial \hat{z}}(t, y, \hat{z}) \frac{\partial \beta}{\partial y}(t, y, \xi)\left(f_1(t, y, \hat{z}) - f_1(t, y, z)\right).\end{aligned}$$

Now, from Assumption 3.1 we have

$$\dot{\hat{\theta}} = -\Gamma \left(\frac{\partial \eta}{\partial y}(t, y, \hat{z}) + \frac{\partial \eta}{\partial \hat{z}}(t, y, \hat{z}) \frac{\partial \beta}{\partial y}(t, y, \xi) \right) f_v(t, y, \hat{z}) \left(\frac{\partial V_z}{\partial \tilde{z}} \right)^T. \quad (3.19)$$

Comparing (3.19) to (3.11) we see that the expressions are identical in view of (3.6). □

Proof of Theorem 3.2. Since the dynamics of (3.11) and the dynamics of (3.9)–(3.10) are identical (in terms of trajectories of $\hat{\theta}(t)$) by Proposition 3.5, and the properties of the adaptive observer in Theorem 3.2 are achieved for (3.7)–(3.8) and the update law (3.11) by Lemma 3.4, we conclude that the properties in Theorem 3.2 hold for the adaptive observer (3.7)–(3.10). □

3.3 Applications

We illustrate the use of the proposed method by designing an adaptive observer for a drilling system from Stamnes et al. (2008), as well as for an instructive example from Besançon, Zhang, and Hammouri (2004).

3.3.1 Drilling System Example

Consider the simplified model of a managed pressure drilling system taken from Stamnes et al. (2008)

$$\frac{V_d}{\beta_d}\dot{p}_p = q_p - q_{bit}, \quad (3.20a)$$

$$M\dot{q}_{bit} = p_p - p_c - \bar{\phi}(q_{bit})\theta, \quad (3.20b)$$

$$\frac{V_a}{\beta_a}\dot{p}_c = q_{bit} - q_{choke} + q_{bpp}, \quad (3.20c)$$

where p_p is the main pump pressure, q_{bit} is the flow rate through the bit and p_c is the pressure upstream the choke. V_d and V_a are the volumes in the drill string and

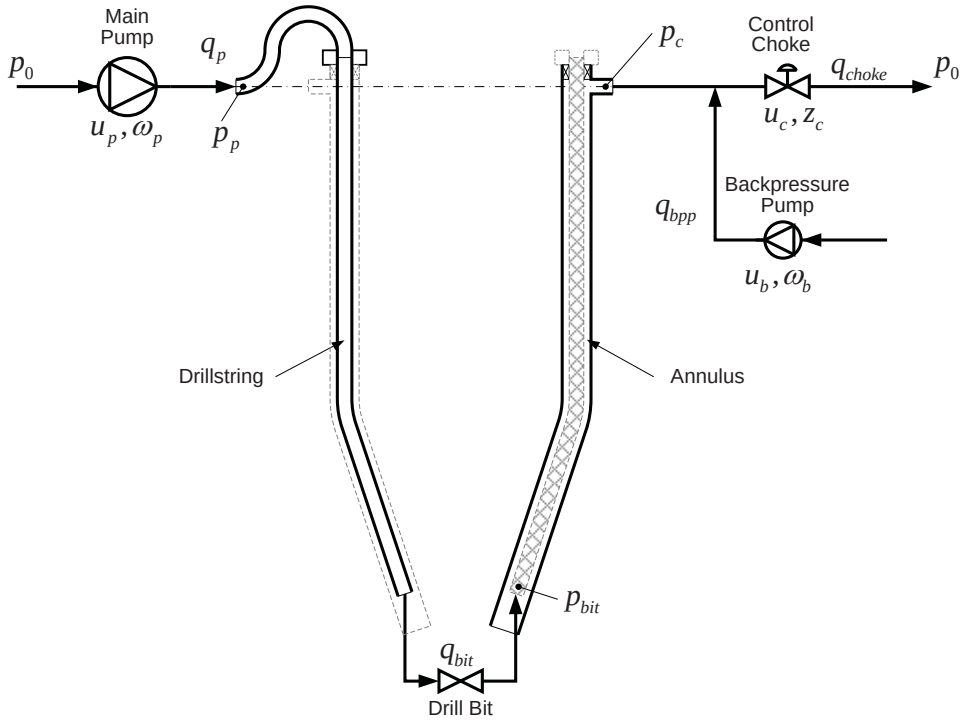

Figure 3.1: Schematic of a managed pressure drilling system. The model consists of two control volumes, one for the drill string and one for the annulus.

annulus, β_d and β_a the bulk moduli of the fluid in the drill string and the annulus and M a lumped density per length parameter. q_p, q_{choke} and q_{bpp} are the main pump, choke and back pressure pump flow rates, which are all positive measured signals. The pressures p_p and p_c are measured while the bit flow rate is not. A schematic of the system is shown in Fig. 3.1. The flow rate through the choke is modeled by a standard orifice equation (Manring, 2005)

$$q_{choke} = u_c K_c \text{sign}(p_c - p_0)\sqrt{|p_c - p_0|} \tag{3.21}$$

where $u_c \in [0, 1]$ is the normalized valve opening, p_0 is the pressure at vena contracta (which can be approximated by the pressure further downstream the choke) and $K_c > 0$ is a lumped parameter depending on the density, the discharge coefficient and the cross-sectional area of the fully open valve opening. Note that for $u_c \geq \delta > 0$ the trajectories p_p, q_{bit} and p_c remain bounded if the inputs q_p and q_{bpp} and their derivatives are bounded[1]. The objective is to estimate the bit flow rate and the uncertain parameter vector θ. In Stamnes et al. (2008), only turbulent flow was considered so the friction pressure was modeled as $\bar{\phi}(q_{bit})\,\theta = \theta\,|q_{bit}|\,q_{bit}$. Here we consider the more general case where $\theta \in \mathbb{R}^3$ is a vector of uncertain parameters and $\bar{\phi}(q_{bit}) = \begin{bmatrix} q_{bit} & |q_{bit}|\,q_{bit} & q_{bit}^3 \end{bmatrix}$. We require $\bar{\phi}(q_{bit})\,\theta$ to be monotonically increasing in q_{bit} which is the case in practice. To be consistent with the notation we rewrite (3.20) into the form (3.1) by defining

$$\begin{aligned} y &= \begin{bmatrix} p_p \\ p_c \end{bmatrix},\ f_1(t, z) = \begin{bmatrix} \frac{\beta_d}{V_d}\left(q_p(t) - z\right) \\ \frac{\beta_a}{V_a}\left(z - q_{choke}(t) + q_{bpp}(t)\right) \end{bmatrix}, \\ z &= q_{bit},\ f_2(y) = \frac{1}{M}\left(p_p - p_c\right), \\ \phi(z) &= -\frac{1}{M}\begin{bmatrix} z & |z|\,z & z^3 \end{bmatrix}. \end{aligned}$$

[1]The boundedness of p_c and q_{bit} can be proved by differentiating $V = \frac{V_d}{2\beta_d}(p_p - p_0)^2 + \frac{V_a}{2\beta_a}(p_c - p_0)^2 + \frac{M}{2}(q_{bit} - q_p)^2$ with respect to time using (3.20), the monotonicity of $\bar{\phi}(q_{bit})\,\theta$ and (3.21). Boundedness of p_p follows from the boundedness of q_{bit} and p_c.

Observer Design for the Nominal Case

In the known parameter case a reduced order observer of the form (3.2) is given by

$$\begin{aligned}\hat{z} =&\beta(y,\xi) = \xi - l_1 p_p - l_2 p_c \qquad (3.22)\\ \dot{\xi} =&\psi(t,y,\xi) + \phi(\hat{z})\,\theta\\ =&f_2(y) + l_1\frac{\beta_d}{V_d}\left(q_p(t) - \beta(y,\xi)\right)\\ &+ l_2\frac{\beta_a}{V_a}\left(\beta(y,\xi) - q_{choke}(t) + q_{bpp}(t)\right) + \phi(\hat{z})\,\theta, \qquad (3.23)\end{aligned}$$

and $\frac{\partial\beta}{\partial\xi} = 1$. To verify that the observer (3.22)–(3.23) satisfies the necessary properties stated in Section 3.2, we take the derivative of (3.22) with respect to time, use (3.20a) and (3.20c), and subtract the result from from (3.20b), giving

$$\dot{\tilde{z}} = \left[\phi(z) - \phi(\hat{z})\right]\theta - l_1\frac{\beta_d}{V_d}\tilde{z} + l_2\frac{\beta_a}{V_a}\tilde{z}.$$

Taking $V_z = \frac{1}{2}\tilde{z}^2$ and using the fact that $\left[\phi(z) - \phi(\hat{z})\right]\theta\tilde{z} \leq 0$ by the monotonicity of $\bar{\phi}(q_{bit})\,\theta$, we get

$$\dot{V}_z \leq -\left(l_1\frac{\beta_d}{V_d} - l_2\frac{\beta_a}{V_a}\right)\tilde{z}^2 \qquad (3.24)$$

and so (3.4) is satisfied with $c = \left(l_1\frac{\beta_d}{V_d} - l_2\frac{\beta_a}{V_a}\right)$ and l_1 and l_2 chosen so that $c > 0$.

Adaptive Redesign

To apply Theorem 3.2, we select $f_v = \begin{bmatrix}-\frac{\beta_d}{V_d} & \frac{\beta_a}{V_a}\end{bmatrix}^T$ which satisfies Assumption 3.1, and so the partial differential equation (3.6) is given as

$$\frac{1}{M}\begin{bmatrix}\hat{z}\\ |\hat{z}|\,\hat{z}\\ \hat{z}^3\end{bmatrix} = \left(\frac{\partial\eta}{\partial y} + \frac{\partial\eta}{\partial\hat{z}}\begin{bmatrix}-l_1 & -l_2\end{bmatrix}\right)\begin{bmatrix}-\frac{\beta_d}{V_d}\\ \frac{\beta_a}{V_a}\end{bmatrix}. \qquad (3.25)$$

Choosing $\frac{\partial\eta}{\partial y} \equiv 0$, (3.25) reduces to

$$\frac{\partial\eta}{\partial\hat{z}}(\hat{z}) = \frac{1}{cM}\begin{bmatrix}\hat{z}\\ |\hat{z}|\,\hat{z}\\ \hat{z}^3\end{bmatrix} \qquad (3.26)$$

for which a solution $\eta(\hat{z})$ is

$$\eta(\hat{z}) = \frac{1}{cM} \begin{bmatrix} \frac{1}{2}\hat{z}^2 \\ \frac{1}{3}|\hat{z}|\hat{z}^2 \\ \frac{1}{4}\hat{z}^4 \end{bmatrix}. \tag{3.27}$$

By Theorem 3.2 an adaptive observer is

$$\hat{z} = \beta(y, \xi) \tag{3.28a}$$

$$\dot{\xi} = \psi(t, y, \xi) + \phi(\hat{z})\hat{\theta} \tag{3.28b}$$

$$\dot{\hat{\sigma}} = \Gamma \frac{\partial \eta}{\partial \hat{z}} \left(\frac{\partial \beta}{\partial y} f_1(t, \hat{z}) + \psi(t, y, \xi) + \phi(\hat{z})\hat{\theta} \right) \tag{3.28c}$$

$$\hat{\theta} = \hat{\sigma} - \Gamma \eta(\hat{z}), \tag{3.28d}$$

where $\frac{\partial \beta}{\partial y} = -\begin{bmatrix} l_1 & l_2 \end{bmatrix}$ and $\frac{\partial \eta}{\partial \hat{z}}$ and $\eta(\hat{z})$ are specified in (3.26) and (3.27).

Simulation Results

To illustrate the use of the adaptive observer we simulate a common drilling scenario known as a pipe connection. During a pipe connection the back pressure pump flow rate, q_{bpp}, is ramped up while the main pump flow rate, q_p, is ramped down to zero so that a new stand of drill pipe can be connected to the drill string. After the connection, q_{bpp} is ramped down while q_p is ramped up again. The parameters used in the simulation are $V_a = 100m^3$, $V_d = 28m^3$, $\beta_a = \beta_d = 14000$bar, $M = 8.3 \times 10^3 \frac{kg}{m^4}$, $K_c = \frac{1}{180}$, $\theta_1 = 3 \times 10^3$, $\theta_2 = -1.4 \times 10^5$ and $\theta_3 = 5.1 \times 10^6$ while the valve is left fully open $u_c \equiv 1$. We choose $l_1 = 0.5\frac{V_d}{\beta_d}$ and $l_2 = -0.5\frac{V_a}{\beta_a}$ so that $c = 1$ and $\Gamma = 10^6 M \text{diag}([1,\ 10^4,\ 10^7])$. The initial conditions for the model are $p_p(0) = 50$bar, $p_c(0) = 10$bar, $z(0) = \frac{1}{60}\frac{m^3}{s}$, and for the observer $\xi(0) = 2z(0) + l_1 p_p(0) + l_2 p_c(0)$ and $\hat{\sigma}(0) = 1.5\theta + \Gamma\eta(2z(0))$. Fig. 3.2a and 3.2b show the measured pressures and flow rates. Fig. 3.2c shows that in the non-adaptive case ($\Gamma \equiv 0$), the flow rate estimate $\hat{z}$ deviates from the true flow rate z, while Fig. 3.2d shows that the adaptive observer estimate quickly converges to the true state. Fig. 3.3 shows that the parameter estimation errors remain bounded.

3.3.2 Example with Uncertainties Depending on y and z

The regressor ϕ in the previous example did not depend on y. To illustrate that the method can be applied to such cases, we apply it to an instructive example from

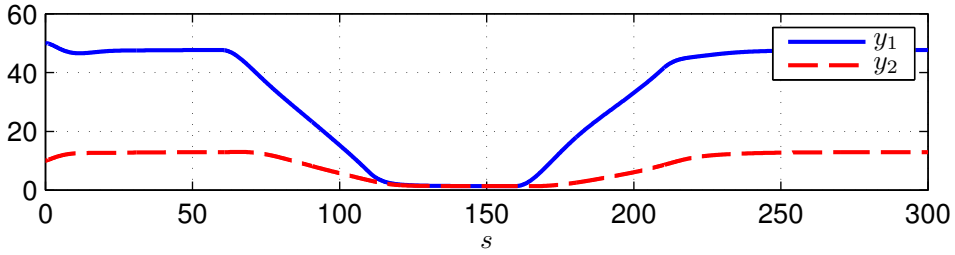

(a) Measured pressures y_1 and y_2 in bar.

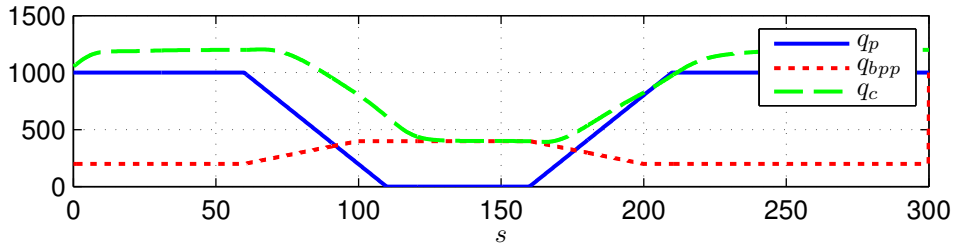

(b) Measured flow rates q_p, q_{bpp} and q_c in liters per minute.

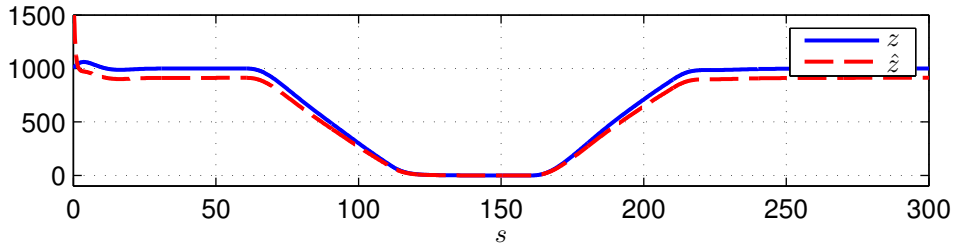

(c) Unmeasured flow rate z and its estimate $\hat{z}$ in liters per minute, no adaption.

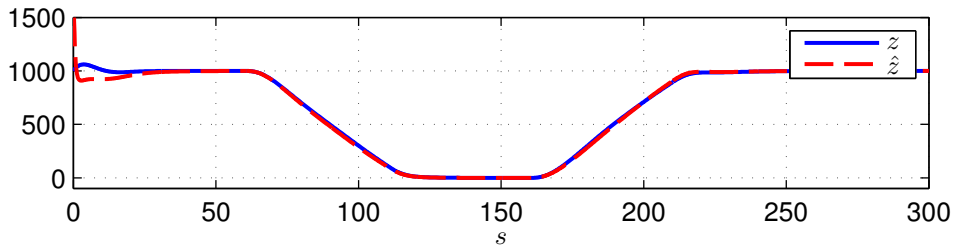

(d) Unmeasured flow rate z and its estimate $\hat{z}$ in liters per minute, with adaptation

Figure 3.2: Simulation of pipe connection

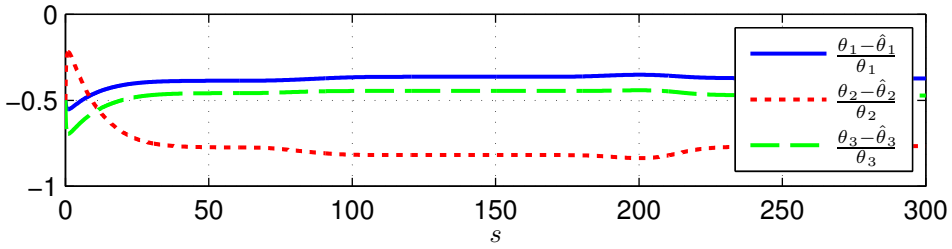

Figure 3.3: Normalized parameter estimation errors

Besançon et al. (2004). The system considered is of the form (3.1) with $f_1(t,z) = z + u(t)$, $f_2(y,z) = -y - 2\sin(z)$ and $\phi(y,z) = \begin{bmatrix}\arctan(z) & \cos(yz)\end{bmatrix}^T$. As in Besançon et al. (2004) we assume that the input $u(t)$ ensures that the states are bounded.

Observer Design for the Nominal Case

For the case where θ is known, an observer is given as

$$\hat{z} = \beta(y,\xi) = \xi + ly, \tag{3.29}$$

$$\dot{\xi} = \psi(y, \xi - ly) + \phi(y,\hat{z})\theta, \tag{3.30}$$

where $\psi(y, \hat{z} - ly) = -l(\hat{z} + u(t)) - y - 2\sin(\hat{z})$ and the gain l is appropriately chosen. As $\sin(z), \cos(yz)$ and $\arctan(z)$ are all globally Lipschitz in z (recall that y is bounded) it is straightforward to use the Lyapunov function $V_z = \frac{1}{2}\tilde{z}^2$, to prove that, for sufficiently large l, we get $\dot{V}_z \leq c\tilde{z}^2$, for some $c < 0$. Note that to find such an l, knowledge of $\|y\|_\infty$ is needed.

Adaptive Redesign

Since we have $\frac{\partial V_z}{\partial \tilde{z}} = \tilde{z}$ we see that Assumption 3.1 is satisfied with $f_v(t,y,\hat{z}) = 1$. To apply Theorem 3.2, we need to find $\eta(y,\hat{z})$ that satisfies (3.6). Since $\frac{\partial \beta}{\partial y} = l$, we need to solve

$$\frac{\partial \eta_1}{\partial y} + l\frac{\partial \eta_1}{\partial \hat{z}} = -\arctan(z), \tag{3.31a}$$

$$\frac{\partial \eta_2}{\partial y} + l\frac{\partial \eta_2}{\partial \hat{z}} = -\cos(yz), \tag{3.31b}$$

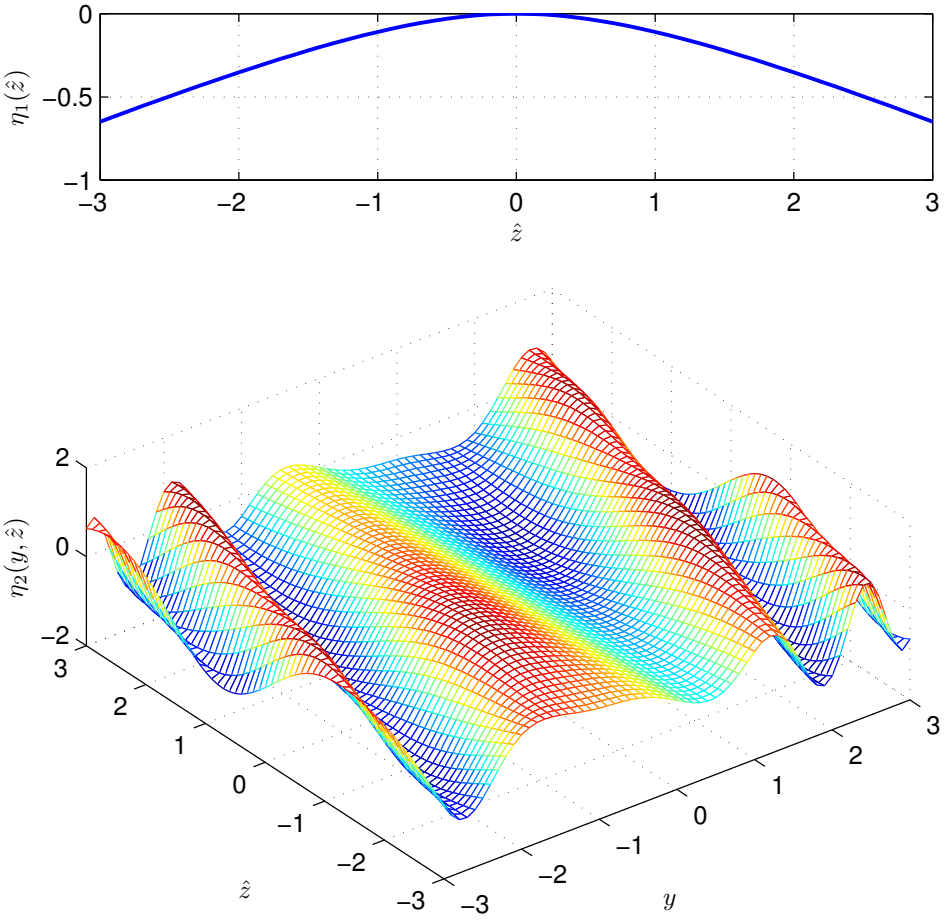

Figure 3.4: $\eta_1(\hat{z})$ and $\eta_2(y,\hat{z})$

for $\eta_1(y,\hat{z})$ and $\eta_2(y,\hat{z})$. Both of these equations can be transformed into solvable ODEs. The solution to the first one is

$$\eta_1(\hat{z}) = \frac{1}{2l}\left(\log\left(\hat{z}^2+1\right) - 2\hat{z}\arctan(\hat{z})\right), \tag{3.32}$$

and according to (3.9)–(3.10) the update law is

$$\dot{\hat{\sigma}}_1 = -\gamma_1 \arctan(z)\left[\hat{z} + u(t) + l^{-1}(\psi(t,y,\hat{z}-ly) + \phi(y,\hat{z})\,\hat{\theta})\right], \tag{3.33}$$

$$\hat{\theta} = \hat{\sigma}_1 - \gamma_1\eta_1(\hat{z}). \tag{3.34}$$

Solving (3.31b) is a bit more involved. Let $\hat{z} = ly + b$, for some b, and define $\lambda_b(y) = \eta_2(y, ly+b)$. Then, we have $\lambda_b'(y) = -\cos(y(ly+b))$ which we can integrate to obtain $\lambda_b(y) = \lambda_b(0) + F(y,b) - F(0,b)$, where $F(y,b) =$

$\int -\cos\left(y\left(ly+b\right)\right)dy$. We then have that

$$\eta_2\left(y,\hat{z}\right) = \lambda_{\hat{z}-ly}\left(y\right) = \eta_2\left(0,\hat{z}\right) + F\left(y,\hat{z}-ly\right) - F\left(0,\hat{z}-ly\right), \tag{3.35}$$

where we are free to select $\eta_2\left(0,\hat{z}\right)=0$. In this particular case, we have

$$\begin{aligned} F\left(y,b\right) = -\sqrt{\frac{\pi}{2l}}\Bigg[&\cos\left(\frac{b^2}{4l}\right)\mathcal{C}\left(\frac{b+2ly}{\sqrt{2\pi l}}\right) \\ &+\sin\left(\frac{b^2}{4l}\right)\mathcal{S}\left(\frac{b+2ly}{\sqrt{2\pi l}}\right)\Bigg], \end{aligned} \tag{3.36}$$

where $\mathcal{S}$ and $\mathcal{C}$ are the Fresnel sine and cosine, respectively. So we obtain

$$\eta_2\left(y,\hat{z}\right) = \sqrt{\frac{\pi}{2l}}\cos\left(\frac{\left(\hat{z}-ly\right)^2}{4l}\right)\Delta\mathcal{C}\left(y,\hat{z}\right) \tag{3.37}$$

$$+\sqrt{\frac{\pi}{2l}}\sin\left(\frac{\left(\hat{z}-ly\right)^2}{4l}\right)\Delta\mathcal{S}\left(y,\hat{z}\right), \tag{3.38}$$

where we have defined

$$\Delta\mathcal{C}\left(y,\hat{z}\right) = \mathcal{C}\left(\frac{\hat{z}-ly}{\sqrt{2\pi l}}\right) - \mathcal{C}\left(\frac{\hat{z}+ly}{\sqrt{2\pi l}}\right) \tag{3.39}$$

$$\Delta\mathcal{S}\left(y,\hat{z}\right) = \mathcal{S}\left(\frac{\hat{z}-ly}{\sqrt{2\pi l}}\right) - \mathcal{S}\left(\frac{\hat{z}+ly}{\sqrt{2\pi l}}\right). \tag{3.40}$$

The update law in this case is

$$\dot{\hat{\sigma}}_2 = -\gamma_2\cos\left(yz\right)\left(\hat{z}+u\left(t\right)\right) + \gamma_2\frac{\partial\eta_2}{\partial\hat{z}}\left(\psi\left(t,y,\xi\right)+\phi\left(y,\hat{z}\right)\hat{\theta}\right), \tag{3.41}$$

$$\hat{\theta}_2 = \hat{\sigma}_2 - \gamma_2\eta_2\left(y,\hat{z}\right), \tag{3.42}$$

where

$$\frac{\partial\eta_2}{\partial\hat{z}} = -\sqrt{\frac{\pi}{2l}}\frac{\hat{z}-ly}{2l}\sin\left(\frac{\left(\hat{z}-ly\right)^2}{4l}\right)\Delta\mathcal{C}\left(y,\hat{z}\right) \tag{3.43}$$

$$\sqrt{\frac{\pi}{2l}}\frac{\hat{z}-ly}{2l}\cos\left(\frac{\left(\hat{z}-ly\right)^2}{4l}\right)\Delta\mathcal{S}\left(y,\hat{z}\right) \tag{3.44}$$

$$+\frac{1}{2l}(1-cos(y\hat{z})). \tag{3.45}$$

Fig. 3.4 shows the graphs of $\eta_1\left(\hat{z}\right)$ and $\eta_2\left(y,\hat{z}\right)$.

Simulation Results

Simulation results with initial conditions $y(0) = z(0) = 1$, input $u(t) = \sin(2t) + \frac{1}{10}\cos(10t)$ and uncertain parameter $\theta = [1, 2]$, as in Besançon et al. (2004), can be seen in Fig. 3.5a and Fig. 3.5b. The observer gains were chosen as $l = 4$, $\gamma_1 = 3$, $\gamma_2 = 1$ and the initial conditions as $\hat{z}(0) = -1$, $\hat{\theta}(0) = [0, 0]$. From Fig. 3.5a and Fig. 3.5b we see that both the state estimation error and parameter estimation error converges to zero. Parameter convergence is achieved due to the persistently exciting (of sufficient order) input signal. To illustrate that the observer can estimate z without parameter identification we ran the same simulation, only this time we choose $u(t) = -\hat{z} - y$. The results can be seen in Fig. 3.5c and Fig. 3.5d. which shows that the state estimation error converges to zero without identifying the unknown parameters. This is not guaranteed with the observer found in Besançon et al. (2004).

3.4 Conclusions

We have presented a new method for adaptive redesign of reduced order nonlinear observers. Contrary to other adaptive observer design procedures the method does not require a strictly positive real condition but requires the solution of a partial differential equation. Two examples show that the method extends existing theory on adaptive observer design, and is of practical usefulness.

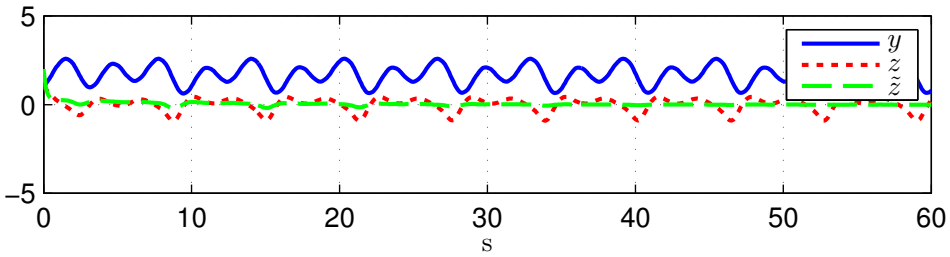

(a) y, z and estimation error $\tilde{z}$ with persistently exciting input.

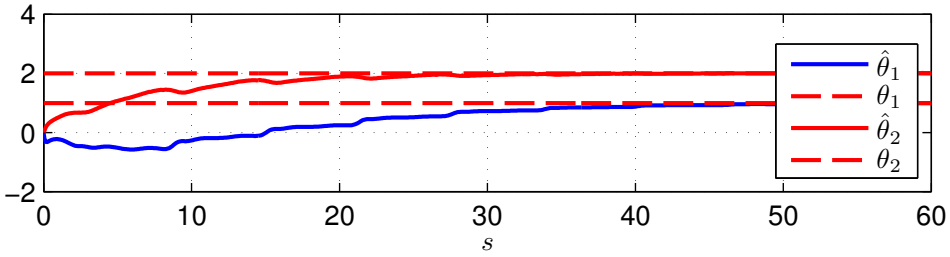

(b) Estimated and actual parameters, $\hat{\theta}$ and θ with persistently exciting input.

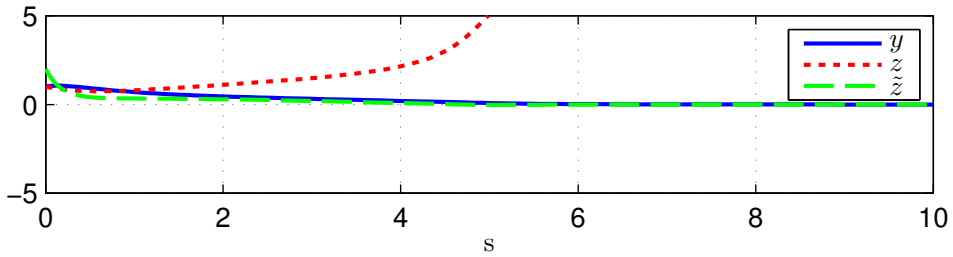

(c) y, z and estimation error $\tilde{z}$ without persistently exciting input.

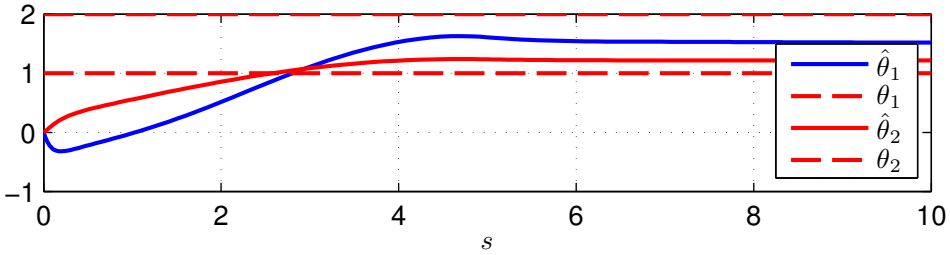

(d) Estimated and actual parameters, $\hat{\theta}$ and θ without persistently exciting input.

Figure 3.5: Simulation results for the example with uncertainties depending on y and z.

Chapter 4

Redesign of Adaptive Observers for Improved Parameter Identification in Nonlinear Systems

Abstract: *We propose a method for redesigning adaptive observers for nonlinear systems. The redesign uses an adaptive law that is based on delayed observers. This increases the computational burden, but gives significantly better parameter identification and robustness properties. In particular, given that a special persistency of excitation condition is satisfied, we prove uniform global asymptotic stability and semi-global exponential stability of the origin of the state and parameter estimation error, and give explicit lower bounds on the convergence rate of both the state and parameter estimation error dynamics. For initial conditions with a known upper bound, we prove tunable exponential convergence rate. To illustrate the use of the proposed method, we apply it to estimate the unmeasured flow rate and the uncertain friction parameters in a model of a managed pressure drilling system. The simulation results clearly show the improved performance of the redesigned adaptive observer compared to a traditional design.*

4.1 Introduction

In practical applications it is often the case that unmeasured states and uncertain parameters are needed for control purposes. In these cases it is necessary to generate real time estimates of these unknown quantities. If the system is persistently excited (PE), one can estimate both parameters and states simultaneously by using adaptive

observers.

For linear systems the parameter and state estimation problem can be separated into two parts. The first part is to design a Luenberger type observer for the unmeasured state while the second part consists of selecting an appropriate adaptive law for the unknown parameters (Kreisselmeier, 1977; Narendra and Annaswamy, 1989; Ioannou and Sun, 1996). If the regressor is persistently exciting both the state and the parameter estimation error will converge to zero.

For nonlinear systems it might not be possible to parameterize the plant so that it is suitable for this modular approach, but one can instead attempt a Lyapunov based design. Such designs usually require that the unknown parameters enter in such a way (possibly after a transformation) that the system is strictly positive real (SPR) from the unknown parameters to the measured output (Marino and Tomei, 1996; Cho and Rajamani, 1997; Besançon, 2000a). Again, as in the linear case, if the regressor is persistently exciting one can prove that both the state and the parameter estimation error will converge to zero. In some cases the SPR condition can be relaxed to systems with higher relative degree from the measured output to the unknown parameter, as shown in Stamnes et al. (2009). We should also mention that for the class of systems considered in Marino and Tomei (1996), one can design adaptive observers with arbitrary rate of convergence (Marino and Tomei, 1995) if the system is sufficiently excited (PE). The design in Marino and Tomei (1995) is based on several additional filters and does not guarantee that the state estimation error goes to zero when the system is not persistently excited.

Experience has shown that the parameter identification properties of Lyapunov based adaptive laws often are poor, in particular when the number of uncertain parameters is high compared to the number of measurements (Krstić, 2009). Even if uniform exponential stability of the state and parameter estimation error is proved, the convergence rate can be small, which severely limits the practical usefulness of such schemes. Motivated by Xu and Zhang (2004), we introduce delayed observers to remedy this lack of performance. Using the delayed observers we are able to obtain easily tunable convergence rates, which is generally not possible in existing adaptive schemes. The price to pay for the improved performance is increased computational burden due to several delayed observers.

The rest of the paper is organized as follows. In Sections 4.2.1 and 4.2.2 we specify the class of systems under consideration and further motivate our work. Section 4.2.3 contains the new design and the stability proofs. In Section 4.3 we apply the proposed method to estimate the unmeasured flow rate and uncertain friction parameters in a model of a managed pressure drilling system from Stamnes et al. (2008). Finally, conclusions are given in Section 3.4.

4.2 Observer Design

4.2.1 Standard Design and Motivation

Given the system

$$\dot{y} = f_1(t, y, z) \tag{4.1a}$$
$$\dot{z} = f_2(t, y, z) + \phi(t, y, z)\,\theta, \tag{4.1b}$$

where $y \in \mathbb{R}^m$ is measured, $z \in \mathbb{R}^n$ is unmeasured, f_1 and f_2 are locally Lipschitz in y, z uniformly in $t \in \mathbb{R}$, and $\theta \in \mathbb{R}^p$ is a vector of constant, uncertain parameters. We assume that the states y and z are bounded but do not require knowledge of the value of the upper bound. We also require $\phi(t, y, z)$ to be continuously differentiable in y and z, uniformly in t. Suppose a reduced order adaptive observer is available in the form

$$\hat{z} = \beta(t, y, \xi), \tag{4.2a}$$
$$\dot{\xi} = \psi(t, y, \xi) + \left(\frac{\partial \beta}{\partial \xi}\right)^{+} \phi(t, y, \hat{z})\,\hat{\theta}, \tag{4.2b}$$

with $\xi \in \mathbb{R}^l$ for $l \geq n$, and rank $\left(\frac{\partial \beta}{\partial \xi}\right) = n$ so that the right inverse $\left(\frac{\partial \beta}{\partial \xi}\right)^{+}$ exists. The parameter $\hat{\theta}$ is generated from a system that satisfies

$$\dot{\hat{\theta}} = -\dot{\tilde{\theta}} = \Gamma \phi^T(t, y, \hat{z}) \left(\frac{\partial V_z}{\partial \tilde{z}}\right)^T \tag{4.3}$$

with $\tilde{\theta} = \theta - \hat{\theta}$, $\Gamma = \Gamma^T > 0$ and V_z a Lyapunov function specified in Assumption 4.1 below. Defining the error $\tilde{z} = z - \hat{z}$, suppose that the error dynamics can be written as

$$\dot{\tilde{z}} = \varepsilon(\theta, t, y, z, \tilde{z}) + \phi(t, y, \hat{z})\,\tilde{\theta}, \tag{4.4}$$

with ε locally Lipschitz in $\tilde{z}$ uniformly in t for bounded y and z. Furthermore, we assume that we are given a differentiable Lyapunov function $V_z(t, \tilde{z}) : [0, \infty) \times \mathbb{R}^n \longrightarrow \mathbb{R}$, satisfying

Assumption 4.1.

$$k_1 \|\tilde{z}\|^2 \leq V_z(t, \tilde{z}) \leq k_2 \|\tilde{z}\|^2, \tag{4.5a}$$
$$\frac{\partial V_z}{\partial t} + \frac{\partial V_z(t, \tilde{z})}{\partial \tilde{z}} \varepsilon(\theta, t, y, z, \tilde{z}) \leq -k_3 \|\tilde{z}\|^2, \tag{4.5b}$$
$$\left\| \frac{\partial V_z(t, \tilde{z})}{\partial \tilde{z}} \right\| \leq k_4 \|\tilde{z}\|, \tag{4.5c}$$

where $k_i > 0$ $i \in \{1, ...4\}$.

Remark 4.2. Notice that the adaptation law is not implemented in the form (4.3) since $\frac{\partial V_z}{\partial \tilde{z}}$ depends on the unmeasured error $\tilde{z}$, but requires a design based on a change of coordinate in the parameters. Adaptive laws of this form satisfying Assumption 4.1 have been proposed in Stamnes et al. (2009, 2011a). See the example in Section 4.2.2 for further details on how (4.3) can be implemented.
Remark 4.3. Taking $V_1 = V_z + \frac{1}{2}\tilde{\theta}^T \Gamma^{-1} \tilde{\theta}$ and differentiating with respect to time along the trajectories of (4.3)–(4.4) gives

$$\dot{V}_1 \leq -k_3 \left\| \tilde{z} \right\|^2, \tag{4.6}$$

so the origin of (4.3)–(4.4) is uniformly globally stable and $\lim_{t\to\infty} \tilde{z} = 0$ by the LaSalle-Yoshizawa Theorem Krstić et al. (1995).
Remark 4.4. If θ is known so that $\tilde{\theta} \equiv 0$, then (4.5) implies that the origin of (4.4) is uniformly globally exponentially stable. Moreover, if k_3 can be increased arbitrarily without increasing k_2 or k_4, or decreasing k_1, then the convergence rate of the state estimation error can be tuned arbitrarily large, see Th. 4.10 Khalil (2002).

Systems of the form (4.3)–(4.4) have been studied extensively in the adaptive control/observer literature. For linear systems where ϕ only depends on t it is well known that if, and only if, the regressor is persistently exciting, that is

$$\int_t^{t+T} \phi^T(\tau)\, \phi(\tau)\, d\tau \geq k_1 I, \tag{4.7}$$

then the origin is globally exponentially stable (GES) (Narendra and Annaswamy, 1989; Ioannou and Sun, 1996; Loría, 2004). In the case where ϕ depends not only on time, but also on the state of the system, more sophisticated tools, such as Matrosov's theorem and its generalizations (Loría et al., 2005), can be used to conclude uniform global asymptotic stability (UGAS).

Even in the linear case, where ϕ only depends on t, adaptive laws of the form (4.3) are hard to tune and have poor parameter convergence properties (Krstić, 2009), in particular if the number of uncertain parameters is high compared to the number of measurements. One might hope that explicit convergence rates, such as the one presented in Loría (2004), would help in tuning. Unfortunately, this is not the case as the expressions in Loría (2004) are complex, and do not show how the gains affect performance.

Due to the shortcomings of adaptive laws of the form (4.3), algorithms with better parameter estimation properties, such as least squares type algorithms, are preferred when parameter estimation is important (Krstić, 2009). However, for nonlinear systems of the form (4.1) least squares type algorithms are not available. Therefore, motivated by Xu and Zhang (2004) we try to remedy this lack of performance by introducing delayed observers.

4.2.2 Example

To further illustrate the poor parameter identification properties of (4.3), and to illustrate how an adaptive observer of the form (4.2)–(4.3) can be designed, consider the nonlinear mass-spring-damper dynamics

$$\dot{y} = z, \tag{4.8a}$$
$$\dot{z} = -y - \theta_1 z - \theta_2 |z| z + u(t), \tag{4.8b}$$

where y is the measured position, z the unmeasured velocity, u is the control input, θ_1 and θ_2 are positive but otherwise uncertain damping coefficients. System (4.8) is in the form (4.1) with $f_1(z) = z$, $f_2(t, y) = -y + u(t)$ and $\phi(z) = [-z, \ -|z| z]$. In the known parameter case ($\hat{\theta} \equiv \theta$), a reduced order observer for system (4.8) of the form (4.2) can be derived using existing results in e.g. (Arcak and Kokotović, 2001; Karagiannis et al., 2008) leading to

$$\hat{z} = \xi + k_3 y, \tag{4.9}$$
$$\dot{\xi} = -y + u(t) - k_3 \hat{z} + \phi(\hat{z})\hat{\theta} \tag{4.10}$$

with $k_3 > 0$. Taking the derivative of (4.9) with respect to time, using (4.8a), and subtracting the result from (4.8b), we obtain the error dynamics

$$\dot{\tilde{z}} = -k_3 \tilde{z} + (\phi(z) - \phi(\hat{z}))\theta + \phi(\hat{z})\tilde{\theta}, \tag{4.11}$$

and so (4.4) is satisfied with $\varepsilon(\theta, y, z, \tilde{z}) = -k_3 \tilde{z} + (\phi(z) - \phi(z - \tilde{z}))\theta$. Using the monotonicity of $\phi(z)\theta$ it is straight forward to verify that $V_z(\tilde{z}) = \frac{1}{2}\tilde{z}^2$ is a Lyapunov function that satisfies Assumption 4.1. Augmenting the Lyapunov function with the term $\frac{1}{2}\tilde{\theta}^T \Gamma \tilde{\theta}$ gives the adaptive law (4.3), which is not implementable. Following the procedures in Stamnes et al. (2011a, 2009) we let the implementable adaptive law be of the form

$$\hat{\theta} = \sigma - \eta(y, \xi), \tag{4.12a}$$
$$\dot{\sigma} = \frac{\partial \eta}{\partial y}\hat{z} + \frac{\partial \eta}{\partial \xi}\dot{\xi} \tag{4.12b}$$

with $\eta(y, \xi)$ to be designed so that $\hat{\theta}$ has the desired dynamics (4.3). To that purpose we take the derivative of (4.12a) with respect to time using (4.8a) and (4.12b) giving

$$\dot{\hat{\theta}} = -\frac{\partial \eta}{\partial y}\tilde{z}. \tag{4.13}$$

Comparing (4.13) to (4.3) we choose $\eta(y,\xi)$ as the solution to the differential equation

$$-\frac{\partial \eta(y,\xi)}{\partial y} = \Gamma \phi^T(\xi + k_3 y). \tag{4.14}$$

Selecting $\Gamma = \text{diag}([\gamma_1, \gamma_2])$ a solution is

$$\eta_1(y,\xi) = \frac{\gamma_1}{2k_3}(\xi + k_3 y)^2, \tag{4.15a}$$

$$\eta_2(y,\xi) = \frac{\gamma_2}{3k_3}|\xi + k_3 y|^3. \tag{4.15b}$$

(4.12) and (4.15) now represent an implementable adaptive law that satisfies (4.3).

Following Remark 4.3 it is straight forward to show that the origin, $\left(\tilde{z}, \tilde{\theta}\right) = 0$, is uniformly globally stable and that $\lim_{t\to\infty} \tilde{z} = 0$. If the regressor is persistently exciting, then the origin is uniformly globally asymptotically stable and uniformly locally exponentially stable (Loría, Panteley, Popović, and Teel (2002); Stamnes et al. (2009)). However, as the simulation results below demonstrate, the convergence of the parameter estimation error can be very slow. Using the parameters $\theta_1 = 0.5$, $\theta_2 = 1$, $k_3 = 2$, $\gamma_1 = \gamma_2 = 10$ and initial conditions $y(0) = z(0) = 1$, $\hat{z}(0) = 0$ and $\hat{\theta}(0) = 2\theta$ we simulate system (4.8) with the observer (4.9)–(4.15). Fig. 4.1a shows the measured position y and the input u. The input u is designed in such a way that the regressor is PE. Fig. 4.1b shows that the state estimate, $\hat{z}$, converges rapidly to the state, z. Since z reaches steady state twice during the simulation, we can set $\dot{z} = 0$ in (4.8b) to obtain the two equations

$$0 = f_2(t_1, y(t_1)) + \phi(\hat{z}(t_1))\theta, \tag{4.16a}$$

$$0 = f_2(t_2, y(t_2)) + \phi(\hat{z}(t_2))\theta, \tag{4.16b}$$

which can be solved for θ provided the matrix

$$\Phi(t_1, t_2) = \begin{bmatrix} \phi(\hat{z}(t_1)) \\ \phi(\hat{z}(t_2)) \end{bmatrix} \tag{4.16c}$$

is nonsingular. For $t_1 = 12$ and $t_2 = 20$ we have $z(t_1) \approx -0.5$ and $z(t_2) \approx 1$ so

$$\Phi(12, 20) \approx \begin{bmatrix} 0.5 & 0.5^2 \\ -1 & -1 \end{bmatrix}, \tag{4.16d}$$

which has full rank and so it is easy to calculate θ. Despite this fact, as Fig. 4.1c shows, the adaptive law is not able to identify the two parameters within the simulation time. The corresponding result for the new method proposed in this paper is shown in Fig. 4.1d. It is clear that the new method is able to quickly identify the uncertain parameters.

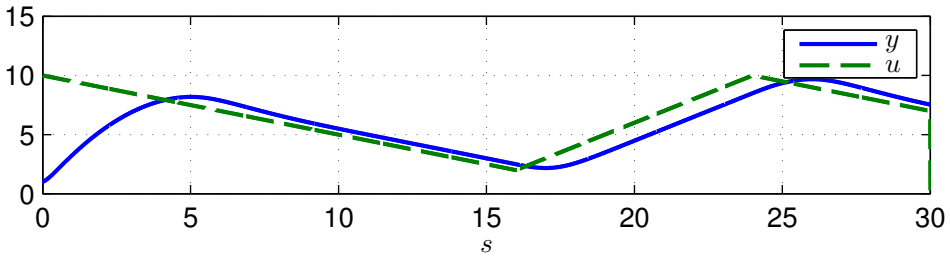

(a) Measured position y and input u.

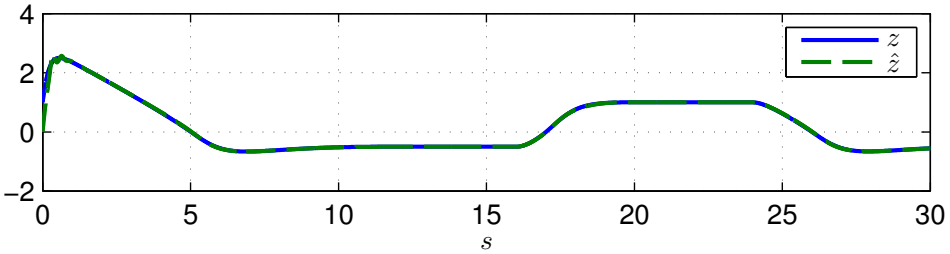

(b) Unmeasured state and its estimate.

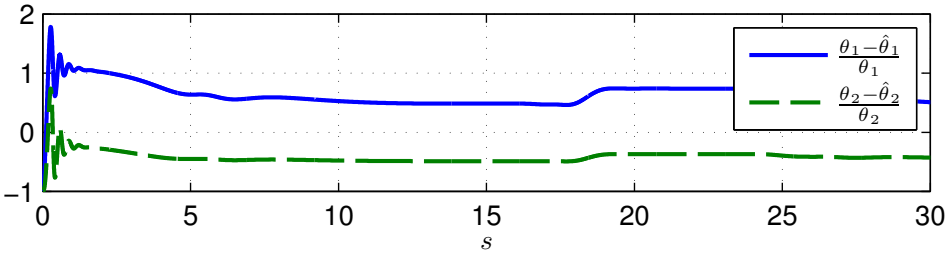

(c) Normalized parameter estimation error.

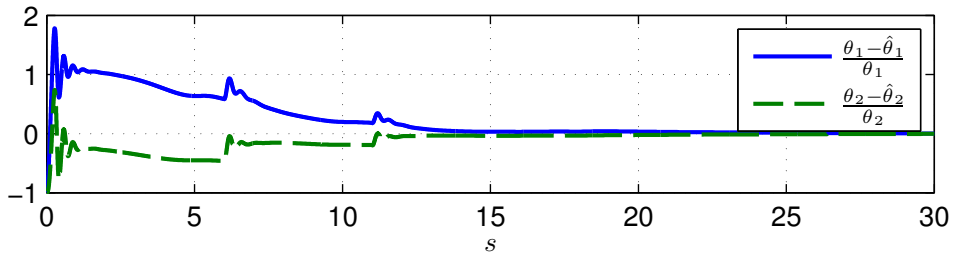

(d) Normalized parameter estimation error, method based on delayed observers.

Figure 4.1: Simulation results for the nonlinear mass-spring-damper.

4.2.3 New Design

To improve the parameter estimation properties of the observer (4.2)–(4.3) we propose using multiple delayed observers. That is, we propose to estimate the unmeasured state not only at the current time t, but also at $t-\tau^1$, $t-\tau^2$, ..., $t-\tau^N$, with $\tau^0 = 0$ and $\tau^0 < \tau^1 < \tau^2 \ldots \tau^{N-1} < \tau^N$. The motivation behind this scheme is to bring more "memory" into the parameter estimation algorithm. To make the idea rigid we introduce some notation. Define $K_N = \{0, 1, ..., N\}$, and let $k \in K_N$

$$y^k = y^k(t) = y\left(t-\tau^k\right), \tag{4.17}$$
$$z^k = z^k(t) = z\left(t-\tau^k\right), \tag{4.18}$$
$$\hat{z}^k = \hat{z}^k(t) = \beta\left(t-\tau^k, y^k, \xi^k\right), \tag{4.19}$$
$$\tilde{z}^k = z^k(t) - \hat{z}^k(t), \tag{4.20}$$
$$\varepsilon^k(t) = \varepsilon\left(\theta, t-\tau^k, y^k, z^k, \tilde{z}^k\right), \tag{4.21}$$
$$\phi^k(t) = \phi\left(t-\tau^k, y^k(t), z^k(t)\right), \tag{4.22}$$
$$\hat{\phi}^k(t) = \phi\left(t-\tau^k, y^k(t), \hat{z}^k(t)\right), \tag{4.23}$$
$$\tilde{z}^T = \left[\left(\tilde{z}^0\right)^T, .., \left(\tilde{z}^N\right)^T\right]^T \tag{4.24}$$

with $\xi^k = \xi^k(t)$ the solution to

$$\dot{\xi}^k = \psi\left(t-\tau^k, y^k, \xi^k\right) + \left(\frac{\partial\beta}{\partial\xi^k}\right)^+ \hat{\phi}^k(t)\,\hat{\theta}(t). \tag{4.25}$$

Although (4.25) looks like a shifted (in time) version (4.2b) it is not due to the fact that we use the same parameter estimate $\hat{\theta}(t)$ for all k. The proposed parameter update law is

$$\dot{\hat{\theta}} = -\dot{\tilde{\theta}} = \Gamma \sum_{k=0}^{N} \left(\hat{\phi}^k(t)\right)^T \left(\frac{\partial V_z\left(t-\tau^k, \tilde{z}^k\right)}{\partial \tilde{z}^k}\right)^T. \tag{4.26}$$

Indeed we see that (4.26) reduces to (4.3) for $N = 0$, however for $N > 0$ it contains more "memory" than (4.3). Later, we will prove that this gives us better convergence rates for the parameter estimation error, given that a PE condition is satisfied. Before we state our main result we derive the appropriate error system. Consider the change of coordinates

$$x = L^{-1}\tilde{\theta}, \tag{4.27}$$

where $\Gamma = \frac{1}{2k_2} LL^T$ and $L = L^T > 0$. In the new coordinate system we have from (4.4) and (4.26) that

$$\dot{\tilde{z}}^k = \varepsilon^k(t) + \hat{\phi}^k(t)\, Lx, \quad \forall k \in K_N, \tag{4.28a}$$

$$\dot{x} = -\frac{1}{2k_2} L^T \sum_{k=0}^{N} \left[\left(\hat{\phi}^k(t) \right)^T \left(\frac{\partial V_z\left(t - \tau^k, \tilde{z}^k\right)}{\partial \tilde{z}^k} \right)^T \right],$$

and we define for future reference the state vector

$$w = \left[\left(\tilde{z}^0\right)^T \quad \left(\tilde{z}^1\right)^T \quad \dots \quad \left(\tilde{z}^N\right)^T \quad x^T \right]^T = \left[\tilde{z}^T \quad x^T \right]^T. \tag{4.29}$$

Note also that from (4.5) we have a differentiable Lyapunov function $V_z\left(t - \tau^k, \tilde{z}^k\right) : [0, \infty) \times \mathbb{R}^n \to \mathbb{R}$ that satisfies

$$k_1 \left\|\tilde{z}^k\right\|^2 \leq V_z\left(t - \tau^k, \tilde{z}^k\right) \leq k_2 \left\|\tilde{z}^k\right\|^2 \tag{4.30a}$$

$$\frac{\partial V_z\left(t - \tau^k, \tilde{z}^k\right)}{\partial t} + \frac{\partial V_z\left(t - \tau^k, \tilde{z}^k\right)}{\partial \tilde{z}} \varepsilon^k(t) \leq -k_3 \left\|\tilde{z}^k\right\|^2, \tag{4.30b}$$

$$\left\| \frac{\partial V_z\left(t - \tau^k, \tilde{z}^k\right)}{\partial \tilde{z}^k} \right\| \leq k_4 \left\|\tilde{z}^k\right\|, \tag{4.30c}$$

for all $k \in K_N$. Our main result relies on the following assumptions.

Assumption 4.5. *There exists $c_G > 0$ such that*

$$\max\left(\left\| \dot{\phi}^k(t) \right\| \right) \leq c_G. \tag{4.31}$$

Assumption 4.6 (PE)**.** *Furthermore, there exists $b_M \geq b_m > 0$ such that*

$$b_m I \leq \sum_{k=0}^{N} \left(\phi^k(t)\right)^T \phi^k(t) \leq b_M I \tag{4.32}$$

for all $t \in \mathbb{R}^+$.

Assumption 4.7. *k_3 can be chosen arbitrarily large in the way indicated in Remark 4.4.*

Assumption 4.6 is a discretized version of the persistency of excitation condition (4.7) and depends on the input applied to the system. To the authors best knowledge a systematic method for guaranteeing that the regressor is persistently excited in general nonlinear systems remains an open problem.

Theorem 4.8 (Main Result)**.** *The origin of (4.28) is uniformly globally stable and $\lim_{t\to\infty} \tilde{z} = 0$. Moreover,*

- *if Assumptions 4.1, 4.5–4.6 hold, then the origin is uniformly globally asymptotically stable, semi-globally exponentially stable and solutions satisfy*

$$\|w(t)\| \leq \kappa \|w(t_0)\| e^{-\alpha(\|w(t_0)\|)(t-t_0)}, \tag{4.33}$$

with $\kappa = \sqrt{\frac{3k_2}{k_1}}$ *and* $\alpha(\|w(t_0)\|) > 0$.

- *if, in addition, Assumption 4.7 holds, then for any positive constant* $\bar{w}$*, and all initial conditions* $\|w(t_0)\| \leq \bar{w}$*, the bound (4.33) holds for any desirable value of* α *by appropriate choice of* k_3 *and* L *(that depend on* $\bar{w}$*).*

Remark 4.9. From (4.27) we see that

$$\left\| \begin{bmatrix} \tilde{z}(t) \\ \lambda_M^{-1}\tilde{\theta}(t) \end{bmatrix} \right\| \leq \left\| \begin{bmatrix} \tilde{z}(t) \\ x(t) \end{bmatrix} \right\| \leq \left\| \begin{bmatrix} \tilde{z}(t) \\ \lambda_m^{-1}\tilde{\theta}(t) \end{bmatrix} \right\|, \tag{4.34}$$

where $\lambda_m I \leq L \leq \lambda_M I$, which implies that

$$\left\| \begin{bmatrix} \tilde{z}(t) \\ \tilde{\theta}(t) \end{bmatrix} \right\| \leq \bar{\kappa} \left\| \begin{bmatrix} \tilde{z}(t_0) \\ \tilde{\theta}(t_0) \end{bmatrix} \right\| \exp\left(-\alpha(t-t_0)\right), \tag{4.35}$$

with $\bar{\kappa} = \kappa \frac{\max(1,\lambda_M)}{\min(1,\lambda_m)}$. From (4.35) we see that the convergence rate in terms of the original coordinates, $\tilde{z}$ and $\tilde{\theta}$, is the same as in (4.33) while the overshoot is affected by the spread in the eigenvalues of L.

Remark 4.10. Assumption 4.6 can only be satisfied if the system is persistently excited, and a systematic choice of N and τ^k can only be performed if prior knowledge of $\phi(t)$ is available. For instance, in the example in Section 4.2.2, we see that the velocity z is approximately constant over periods of $5-10$ seconds. Choosing $N = 2$ and $\tau^k = 5k$ for $k = 0, 1, 2$ we ensure that the observers cover a window of 15s so that at least one z^k differs from the other two and so Assumption 4.6 is satisfied. As the proof of Theorem 4.8 shows, N and τ^k affect the convergence rate in a complicated way. Thus, if one can satisfy Assumption 4.6 for some b_m, the convergence rate should be controlled using k_3 and L.

Proof. The proof of Theorem 4.8 follows a similar approach as in the proof of Theorem 1 in Fossen et al. (2001) and consists of three steps. First we prove overall stability and convergence of the state estimation error, then we introduce a cross term in the Lyapuov function which enables us to prove convergence of the parameter estimation error. The last part of the proof deals with the ability to tune the convergence rate. Consider the Lyapunov-like function

$$V_2(t, w) = \sum_{k=0}^{N} V_z\left(t - \tau^k, \tilde{z}^k\right) + k_2 \|x\|^2. \tag{4.36}$$

From (4.30a) it is clear that

$$k_1 \|w\|^2 \leq V_2(t,w) \leq k_2 \|w\|^2 . \tag{4.37}$$

Differentiating (4.36) with respect to time and using (4.28) we get

$$\begin{aligned}
\dot{V}_2 =& \sum_{k=0}^{N} \left[\frac{\partial V_z\left(t-\tau^k, \tilde{z}^k\right)}{\partial t} + \frac{\partial V_z\left(t-\tau^k, \tilde{z}^k\right)}{\partial \tilde{z}^k} \varepsilon^k(t) \right. \\
& \left. + \frac{\partial V_z\left(t-\tau^k, \tilde{z}^k\right)}{\partial \tilde{z}^k} \hat{\phi}^k(t) Lx \right] \\
& - x^T \sum_{k=0}^{N} L^T \left(\hat{\phi}^k(t)\right)^T \left(\frac{\partial V_z\left(t-\tau^k, \tilde{z}^k\right)}{\partial \tilde{z}^k} \right)^T \\
=& \sum_{k=0}^{N} \left[\frac{\partial V_z\left(t-\tau^k, \tilde{z}^k\right)}{\partial t} + \frac{\partial V_z\left(t-\tau^k, \tilde{z}^k\right)}{\partial \tilde{z}^k} \varepsilon^k(t) \right].
\end{aligned} \tag{4.38}$$

Substituting (4.30b) into (4.38), we obtain

$$\dot{V}_2 \leq -k_3 \sum_{k=0}^{N} \left\|\tilde{z}^k\right\|^2 = -k_3 \|\tilde{z}\|^2 , \tag{4.39}$$

which implies that the origin of (4.28) is uniformly globally stable, that is

$$\|w(t)\| \leq \sqrt{\frac{k_2}{k_1}} \|w(t_0)\| . \tag{4.40}$$

Inequalities (4.37) and (4.39) imply that $\lim_{t\to\infty} \tilde{z} = 0$ by the LaSalle-Yoshizawa Theorem Krstić et al. (1995). This completes the first part of the proof.

Let λ_M and λ_m be the largest and smallest eigenvalues of L and $\mu \geq \frac{2(N+1)\lambda_M \sqrt{b_M}}{k_1}$, a Lyapunov function is

$$V_3(t,w) = \mu V_2(t,w) - \sum_{k=0}^{N} \left(\tilde{z}^k\right)^T \phi^k(t) Lx. \tag{4.41}$$

From the choice of μ, $V_3(t,w)$ satisfies

$$c_1 \|w\|^2 \leq V_3(t,w) \leq c_2 \|w\|^2 , \tag{4.42}$$

with

$$c_1 = \frac{\mu}{2} k_1, \; c_2 = \frac{3}{2} \mu k_2. \tag{4.43}$$

We differentiate (4.41) along the trajectories of (4.28) to get

$$\begin{aligned}\dot{V}_3 \leq & -\mu k_3 \|\tilde{z}\|^2 - \sum_{k=0}^{N} \left(\varepsilon^k(t)\right)^T \phi^k(t) Lx \\ & - \sum_{k=0}^{N} x^T L^T \left(\phi^k(t)\right)^T \phi^k(t) Lx \\ & + \sum_{k=0}^{N} x^T L^T \left(\phi^k(t) - \hat{\phi}^k(t)\right)^T \phi^k(t) Lx \\ & - \sum_{k=0}^{N} \left(\tilde{z}^k\right)^T \dot{\phi}^k(t) Lx + \frac{1}{2k_2} \sum_{k=0}^{N} \left(\tilde{z}^k\right)^T \phi^k(t) LL^T \\ & \times \sum_{k=0}^{N} \left(\hat{\phi}^k(t)\right)^T \left(\frac{\partial V_z\left(t-\tau^k, \tilde{z}^k\right)}{\partial \tilde{z}^k}\right)^T . \end{aligned} \tag{4.44}$$

Since y and z are bounded $\varepsilon(\theta, t, y, z, \tilde{z})$ is locally Lipschitz in $\tilde{z}$ uniformly in t, and similarly $\phi(t, y, z)$ is locally Lipschitz in z uniformly in t, so there exists a continuous nondecreasing function $\rho_1 : \mathbb{R}^+ \to \mathbb{R}^+$, such that

$$\max\left\{\left\|\left(\varepsilon^k(t)\right)^T\right\|, \left\|\phi^k(t) - \hat{\phi}^k(t)\right\|\right\} \leq \rho_1\left(\left\|\tilde{z}^k\right\|\right)\left\|\tilde{z}^k\right\|. \tag{4.45}$$

Letting $\bar{\gamma} = \sqrt{\frac{k_2}{k_1}}\|w(t_0)\|$ and $\bar{\rho}_1 = \rho_1(\bar{\gamma})$, we bound the time-varying terms based on Assumptions 4.5–4.6, (4.30c) and (4.45) giving

$$\lambda_m^2 b_m \|x\|^2 \leq \sum_{k=0}^{N} x^T L^T \left(\phi^k(t)\right)^T \phi^k(t) Lx, \tag{4.46}$$

$$\left\|\dot{\phi}^k(t)\right\| \leq c_G, \tag{4.47}$$

$$\left\|\sum_{k=0}^{N} \left(\varepsilon^k(t)\right)^T \phi^k(t) L\right\| \leq \lambda_M \bar{\rho}_1 (N+1)\sqrt{b_M}\|\tilde{z}\|, \tag{4.48}$$

$$\left\|\sum_{k=0}^{N} L^T \left(\phi^k(t) - \hat{\phi}^k(t)\right)^T \phi^k(t) L\right\| \leq \lambda_M^2 \bar{\rho}_1 (N+1)\sqrt{b_M}\|\tilde{z}\|, \tag{4.49}$$

$$\left\|\sum_{k=0}^{N} \left(\tilde{z}^k\right)^T \phi^k(t) LL^T\right\| \leq \lambda_M^2 (N+1)\sqrt{b_M}\|\tilde{z}\|, \tag{4.50}$$

$$\left\|\sum_{k=0}^{N} \hat{\phi}^T(t) \left(\frac{\partial V_z\left(t-\tau^k, \tilde{z}^k\right)}{\partial \tilde{z}^k}\right)^T\right\| \leq k_4 (N+1)\left(\sqrt{b_M} + \bar{\rho}_1\bar{\gamma}\right)\|\tilde{z}\|. \tag{4.51}$$

The bounds imply

$$\begin{aligned}\dot{V}_3 \leq & -\mu k_3 \|\tilde{z}\|^2 + \lambda_M \bar{\rho}_1 (N+1) \sqrt{b_M} \|\tilde{z}\| \|x\| \\ & - \lambda_m^2 b_m \|x\|^2 + \lambda_M^2 \bar{\rho}_1 (N+1) \sqrt{b_M} \bar{\gamma} \|\tilde{z}\| \|x\| \\ & + \lambda_M (N+1) c_g \|\tilde{z}\| \|x\| + \frac{1}{2k_2} \lambda_M^2 k_4 (N+1)^2 \\ & \times \sqrt{b_M} \left(\sqrt{b_M} + \bar{\rho}_1 \bar{\gamma} \right) \|\tilde{z}\|^2 . \end{aligned} \tag{4.52}$$

Defining

$$M_1 = \frac{1}{2k_2} \lambda_M^2 k_4 (N+1)^2 \sqrt{b_M} \left(\sqrt{b_M} + \bar{\rho}_1 \bar{\gamma} \right), \tag{4.53a}$$

$$M_2 = \lambda_M (N+1) \left(\bar{\rho}_1 \sqrt{b_M} + \lambda_M \bar{\rho}_1 \sqrt{b_M} \bar{\gamma} + c_g \right), \tag{4.53b}$$

gives

$$\dot{V}_3 \leq - (\mu k_3 - M_1) \|\tilde{z}\|^2 + M_2 \|\tilde{z}\| \|x\| - \lambda_m^2 b_m \|x\|^2 . \tag{4.54}$$

By Young's inequality we have

$$\frac{\mu k_3}{4} \|\tilde{z}\|^2 + \frac{\lambda_m^2 b_m}{2} \|x\|^2 \geq \sqrt{\frac{\mu k_3}{2}} \lambda_m \sqrt{b_m} \|\tilde{z}\| \|x\| , \tag{4.55}$$

so we choose $\mu > \max \left(\frac{2M_2^2}{k_3 \lambda_m^2 b_m}, \frac{4M_1}{k_3}, \frac{2(N+1)\lambda_M \sqrt{b_M}}{k_1} \right)$ so that

$$\dot{V}_3 \leq -\frac{\mu k_3}{2} \|\tilde{z}\|^2 - \frac{\lambda_m^2 b_m}{2} \|x\|^2 \tag{4.56}$$

$$\leq -c_3 \|w\|^2 , \tag{4.57}$$

with $c_3 = \frac{1}{2} \min (\mu k_3, \lambda_m^2 b_m)$. Finally, (4.42) and (4.57) imply that

$$\|w(t)\| \leq \kappa \|w(t_0)\| \exp (-\alpha (t - t_0)) , \tag{4.58}$$

with

$$\kappa = \sqrt{\frac{c_2}{c_1}} = \sqrt{\frac{3k_2}{k_1}}, \tag{4.59}$$

$$\begin{aligned}\alpha (\|w(t_0)\|) &= \frac{c_3 (\|w(t_0)\|)}{2c_2} \\ &= \frac{\min (\mu (\|w(t_0)\|) k_3, \lambda_m^2 b_m)}{6\mu (\|w(t_0)\|) k_2}. \end{aligned} \tag{4.60}$$

In (4.60) we have made the dependence of the convergence rate α on the initial condition $w(t_0)$ explicit. The reason for this dependence can be traced from (4.53) where we see that M_1 and M_2 depends on $\bar{\rho}_1$ and $\bar{\gamma}$, and since μ must be chosen to satisfy

$$\mu > \max\left(\frac{2M_2^2}{k_3\lambda_m^2 b_m}, \frac{4M_1}{k_3}, \frac{2(N+1)\lambda_M\sqrt{b_M}}{k_1}\right), \tag{4.61}$$

it will also depend on $w(t_0)$. Since we obtain a lower bound for α only when $\|w(t_0)\|$ is bounded, we conclude that the origin of (4.28) is uniformly globally asymptotically stable and semi-globally exponentially stable (since $\alpha \to 0$ as $\|w(t_0)\| \to \infty$ we cannot conclude that the origin is uniformly globally exponentially stable). This proves the second part of Theorem 4.8.

Now, to prove the last part of the theorem we consider two cases. The first is the case where $\mu k_3 < \lambda_m^2 b_m$ and in the second case $\mu k_3 \geq \lambda_m^2 b_m$. In the first case $\alpha = \frac{k_3}{6k_2}$ and we see that, since Assumption 4.7 is satisfied, α can be increased arbitrarily by increasing k_3 without increasing κ. In the second case we first consider the case where M_1 and M_2 are small, so that $\max\left(\frac{2M_2^2}{k_3\lambda_m^2 b_m}, \frac{4M_1}{k_3}, \frac{2(N+1)\lambda_M\sqrt{b_M}}{k_1}\right) = \frac{2(N+1)\lambda_M\sqrt{b_M}}{k_1}$. In this case $\alpha = \frac{\lambda_m^2 b_m k_1}{2(N+1)\lambda_M\sqrt{b_M}}$ and so α can be increased arbitrarily, without affecting κ, by increasing $\frac{\lambda_m^2}{\lambda_M}$. Next we consider the case where M_1 or M_2 are large so that

$$\begin{aligned}\mu &> \max\left(\frac{2M_2^2}{k_3\lambda_m^2 b_m}, \frac{4M_1}{k_3}, \frac{2(N+1)\lambda_M\sqrt{b_M}}{k_1}\right)\\ &= \max\left(\frac{2M_2^2}{k_3\lambda_m^2 b_m}, \frac{4M_1}{k_3}\right).\end{aligned} \tag{4.62}$$

Observing that M_1 and M_2 are independent of k_3 we choose k_3 so that μ is kept constant so we have $\alpha = \frac{\lambda_m^2 b_m}{6\mu k_2}$, and we see that increasing λ_m gives arbitrarily large convergence rate α while κ is kept constant. This completes the proof of Theorem 4.8. □

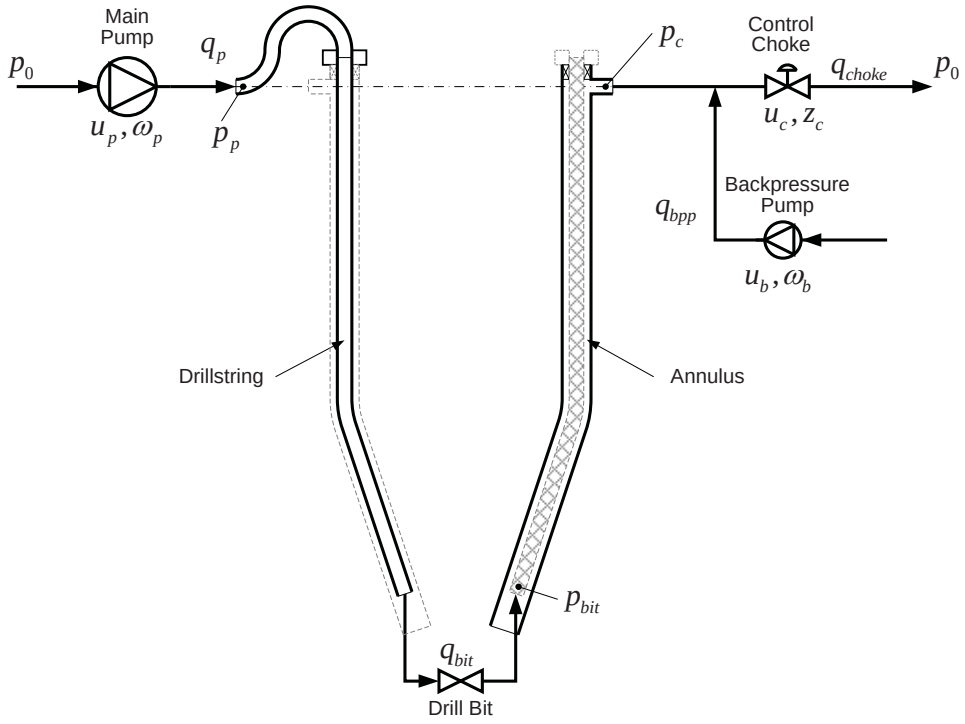

Figure 4.2: Schematic of a managed pressure drilling system. The model consists of two control volumes, one for the drill string and one for the annulus.

4.3 Drilling System Example

4.3.1 Adaptive Observer Design

Consider the simplified model of a managed pressure drilling system from Stamnes et al. (2008)

$$\frac{V_d}{\beta_d}\dot{p}_p = q_p - q_{bit}, \tag{4.63a}$$

$$M\dot{q}_{bit} = p_p - p_c - \phi\left(q_{bit}\right)\theta, \tag{4.63b}$$

$$\frac{V_a}{\beta_a}\dot{p}_c = q_{bit} - q_{choke} + q_{bpp}, \tag{4.63c}$$

where p_p is the main pump pressure, q_{bit} is the flow rate through the bit and p_c is the pressure upstream the choke. V_d and V_a are the volumes in the drill string and annulus, β_d and β_a the bulk moduli of the fluid in the drill string and the annulus and M a lumped density per length parameter. q_p, q_{choke} and q_{bpp} are the main pump, choke and back pressure pump flow rates, which are all measured signals. The pressures p_p and p_c are measured while the bit flow rate is not. A schematic of the system is shown in Fig. 4.2. The flow rate through the choke is modeled by a standard orifice equation (Manring, 2005)

$$q_{choke} = u_c K_c \sqrt{\max(p_c - p_0, 0)} \tag{4.64}$$

where $u_c \in [0, 1]$ is the normalized valve opening and $K_c > 0$ is a lumped parameter depending on the density, the discharge coefficient and the cross-sectional area of the fully open valve opening. Note that for u_c positive and bounded away from zero, the states p_p, q_{bit} and p_c remain bounded if the inputs q_p and q_{bpp} are bounded. The objective is to estimate the bit flow rate and the uncertain parameter vector θ. In Stamnes et al. (2008) only turbulent flow was considered so the friction pressure was modeled as $\phi\left(q_{bit}\right)\theta = \theta\left|q_{bit}\right| q_{bit}$. Here we consider the more general case where $\theta \in \mathbb{R}^3$ is a vector of uncertain parameters and $\phi\left(q_{bit}\right) = [q_{bit},\ \left|q_{bit}\right| q_{bit},\ q_{bit}^3]$. We require $\phi\left(q_{bit}\right)\theta$ to be monotonically increasing in q_{bit} which is the case in practice. To be consistent with the notation we rewrite (4.63) into the form (4.1) by defining

$$y = \begin{bmatrix} p_p \\ p_c \end{bmatrix},\ f_1\left(t, z\right) = \begin{bmatrix} \frac{\beta_d}{V_d}\left(q_p\left(t\right) - z\right) \\ \frac{\beta_a}{V_a}\left(z - q_{choke}\left(t\right) + q_{bpp}\left(t\right)\right) \end{bmatrix}, \tag{4.65}$$

$$z = q_{bit},\ f_2\left(y\right) = \frac{1}{M}\left(p_p - p_c\right), \tag{4.66}$$

$$\phi\left(z\right) = -\frac{1}{M}\begin{bmatrix} z & \left|z\right| z & z^3 \end{bmatrix}. \tag{4.67}$$

Similar to Stamnes et al. (2008) an adaptive observer for (4.63) of the form (4.2) is given by

$$\hat{z} = \beta(y, \xi), \tag{4.68a}$$

$$\dot{\xi} = \psi(t, y, \xi) + \phi(\hat{z})\hat{\theta}, \tag{4.68b}$$

with

$$\beta(y, \xi) = \xi - l_1 p_p - l_2 p_c \tag{4.69}$$

and

$$\begin{aligned}\psi(t, y, \xi) =& f_2(y) + l_1 \frac{\beta_d}{V_d}(q_p(t) - \hat{z}) \\ &+ l_2 \frac{\beta_a}{V_a}(\hat{z} - q_{choke}(t) + q_{bpp}(t)).\end{aligned} \tag{4.70}$$

The adaptive law is given as

$$\hat{\theta} = \sigma - \eta(\xi, y), \tag{4.71a}$$

$$\begin{aligned}\dot{\sigma} =& \frac{\partial \eta}{\partial \xi}\dot{\xi} + \frac{\partial \eta}{\partial y_1}\frac{\beta_d}{V_d}(q_p(t) - \hat{z}) \\ &+ \frac{\partial \eta}{\partial y_2}\frac{\beta_a}{V_a}(\hat{z} - q_{choke}(t) + q_{bpp}(t)),\end{aligned} \tag{4.71b}$$

where

$$\eta_1 = -\gamma_1 \xi\left(\alpha \frac{V_d}{\beta_d} y_1 - (1-\alpha)\frac{V_a}{\beta_a} y_2\right) + \frac{\gamma_1}{2}\left(\frac{l_1 V_d}{\beta_d} y_1^2 - \frac{l_2 V_a}{\beta_a} y_2^2\right) \tag{4.72a}$$

$$\eta_2 = \gamma_2 \begin{cases} \xi|\xi|\left(-\alpha\frac{V_d}{\beta_d} y_1 + (1-\alpha)\frac{V_a}{\beta_a} y_2\right) & l_1 = l_2 = 0 \\ \frac{1}{3\left(l_1 \frac{\beta_d}{V_d} - l_2 \frac{\beta_a}{V_a}\right)}|\xi - l_1 y_1 - l_2 y_2|^3 & |l_1| + |l_2| \neq 0 \end{cases} \tag{4.72b}$$

$$\eta_3 = \gamma_3 \begin{cases} \xi^3\left(-\alpha\frac{V_d}{\beta_d} y_1 + (1-\alpha)\frac{V_a}{\beta_a} y_2\right) & l_1 = l_2 = 0 \\ \frac{1}{4\left(l_1 \frac{\beta_d}{V_d} - l_2 \frac{\beta_a}{V_a}\right)}(\xi - l_1 y_1 - l_2 y_2)^4 & |l_1| + |l_2| \neq 0 \end{cases}. \tag{4.72c}$$

To apply Theorem 4.8 we need to verify that the adaptive observer (4.68)– (4.72) satisfies the assumptions in Sections 4.2.1 and 4.2.3. Towards that end, we differentiate (4.71a) with respect to time giving

$$\begin{aligned}\dot{\hat{\theta}} =& \frac{\partial \eta}{\partial \xi}\dot{\xi} + \frac{\partial \eta}{\partial y_1}\frac{\beta_d}{V_d}(q_p(t) - \hat{z}) + \frac{\partial \eta}{\partial y_2}\frac{\beta_a}{V_a}(\hat{z} - q_{choke}(t) + q_{bpp}(t)) \\ &- \frac{\partial \eta}{\partial \xi}\dot{\xi} - \frac{\partial \eta}{\partial y_1}\frac{\beta_d}{V_d}(q_p(t) - z) - \frac{\partial \eta}{\partial y_2}\frac{\beta_a}{V_a}(z - q_{choke}(t) + q_{bpp}(t))\end{aligned} \tag{4.73}$$

$$= \frac{\partial \eta}{\partial y_1}\frac{\beta_d}{V_d}\tilde{z} - \frac{\partial \eta}{\partial y_2}\frac{\beta_a}{V_a}\tilde{z} \tag{4.74}$$

$$= \Gamma\phi(\hat{z})\tilde{z}, \tag{4.75}$$

where the last step was taken by differentiating (4.72), using the relationships (4.68a) and (4.69), and defining $\Gamma = diag([\gamma_1, \gamma_2, \gamma_3])$. Selecting $V_z = \frac{1}{2}\tilde{z}^2$, it is clear that (4.75) satisfies (4.3). From (4.63b) and (4.68) we have

$$\dot{\tilde{z}} = f_2(y) + \phi(z)\theta - \left(f_2(y) + l_1 \frac{\beta_d}{V_d}\tilde{z} - l_2 \frac{\beta_a}{V_a}\tilde{z} + \phi(\hat{z})\hat{\theta} \right), \tag{4.76}$$

$$= \varepsilon(\theta, y, z, \tilde{z}) + \phi(\hat{z})\tilde{\theta}, \tag{4.77}$$

with $\varepsilon(\theta, y, z, \tilde{z}) = (\phi(z)) - \phi(z - \tilde{z}))\theta - l_1 \frac{\beta_d}{V_d}\tilde{z} + l_2 \frac{\beta_a}{V_a}\tilde{z}$. Note that due to the monotonicity of $\phi(z)\theta$, $(\phi(z) - \phi(z - \tilde{z}))\theta\tilde{z} \leq 0$. Using this property, it is straightforward to show that $\dot{V}_z \leq -l_1 \frac{\beta_d}{V_d}\tilde{z} + l_2 \frac{\beta_a}{V_a}\tilde{z}$, and so Assumption 4.1 is satisfied with arbitrary k_3. Assumption 4.5 is satisfied since z and y (and so $\dot{z}$) are bounded.

4.3.2 Simulation Results

Using the parameters $K_c = 0.0056\frac{m^3}{s\sqrt{bar}}$, $V_a = 100m^3$, $V_d = 28m^3$, $\beta_a = \beta_d = 14000bar$, $M = 8.3 \times 10^3 \frac{s^2 bar}{m^3}$, $\theta_1 = 0.3\frac{sbar}{m^3}$, $\theta_2 = -17\frac{s^2 bar}{m^6}$ and $\theta_3 = 512\frac{s^3 bar}{m^9}$, a typical operational procedure was simulated in which the driller ramps down the main pump flow rate, q_p. The variation in flow rate during such a procedure introduces PE. We know that it takes about 1-3 minutes to ramp the pump down or up. Based on this knowledge we choose $\tau^k = kT$ for $k \in \{0, ..., N\}$ with $T = 30s$ and $N = 19$, so that the delayed observers "cover" the entire procedure. For the algorithm based on delayed observers, we use only one state observer for $t < \tau^1$, two for $\tau^1 \leq t < \tau^2$, three for $\tau^2 \leq t < \tau^3$, and so forth until $t \geq \tau^N$ at which time all the observers are operational. The adaptive law (4.26) is implemented as

$$\hat{\theta} = \sigma - \sum_{k=0}^{N} \eta\left(\xi^k, y^k\right), \tag{4.78}$$

$$\dot{\sigma} = \sum_{k=0}^{N} \left[\frac{\partial \eta(\xi^k, y^k)}{\partial \xi^k}\dot{\xi}^k + \frac{\partial \eta(\xi^k, y^k)}{\partial y_1^k}\frac{\beta_d}{V_d}\left(q_p^k - \hat{z}^k\right) + \frac{\partial \eta(\xi^k, y^k)}{\partial y_2^k}\frac{\beta_a}{V_a}\left(\hat{z}^k - q_{choke}^k + q_{bpp}^k\right) \right], \tag{4.79}$$

where $q_p^k = q_p(t - \tau^k)$, $q_{choke}^k = q_{choke}(t - \tau^k)$ and $q_{bpp}^k = q_{bpp}(t - \tau^k)$. The gains used were $l_1 = \frac{1}{2500}$, $l_2 = -\frac{4}{2500}$ and $\Gamma = diag(10, 10^5, 10^8)$ for $t < \tau^N$ and $\Gamma = 20diag(10, 10^5, 10^8)$ for $t \geq \tau^N$. For comparison purposes we include simulation results using a standard approach, which corresponds to selecting $N = 0$. Fig. 4.3a shows the pressure measurements, while Fig. 4.3b compares the bit flow with its

estimate $\hat{q}_{bit}^0$, and the most delayed estimate $\hat{q}_{bit}^N$. It can be seen that $\hat{q}_{bit}^0$ quickly converges to q_{bit}, as proved in Section 4.2.3. Fig. 4.3c and Fig. 4.3d clearly show the improved parameter identification properties of the algorithm based on multiple observers. Fig. 4.4 plots the time evolution of the sum from the PE condition (4.32). We can see that the PE condition is satisfied and so Theorem 4.8 implies convergence of both states and parameters.

4.4 Conclusions

We have presented a method to redesign adaptive observers for systems of the form (4.1). The redesign uses an adaptive law based on delayed observers. This increases the computational burden, but gives significantly better parameter identification and robustness properties. Explicit performance guarantees are given for both the state and parameter estimation error. The results include simple tuning rules that allow arbitrarily fast convergence rates for the errors, which is uncommon for nonlinear adaptive observers. Simulation results verify the significantly improved parameter identification properties of the redesigned observer compared to the original design.

Acknowledgements

This work was funded by Statoil ASA under R&D project 'Intelligent Drilling'

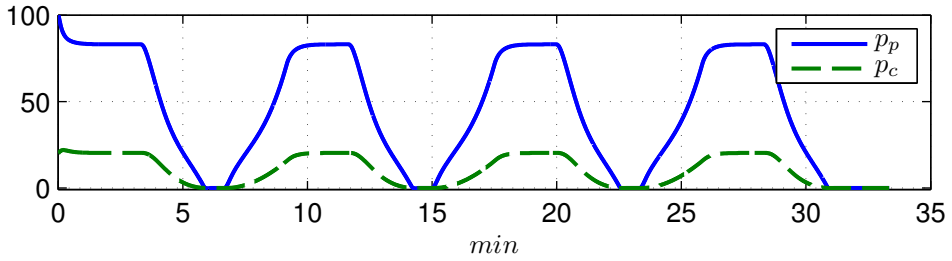

(a) Pressures, bar

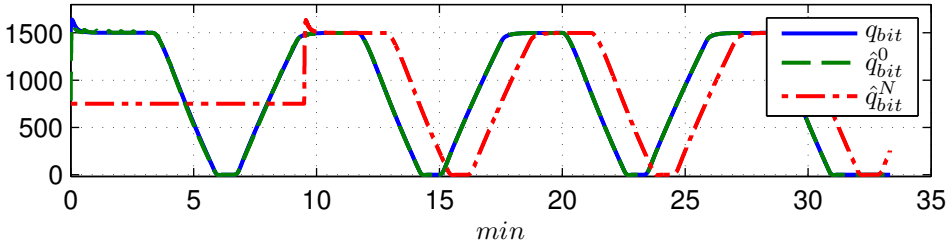

(b) Flow rates, liters per minute

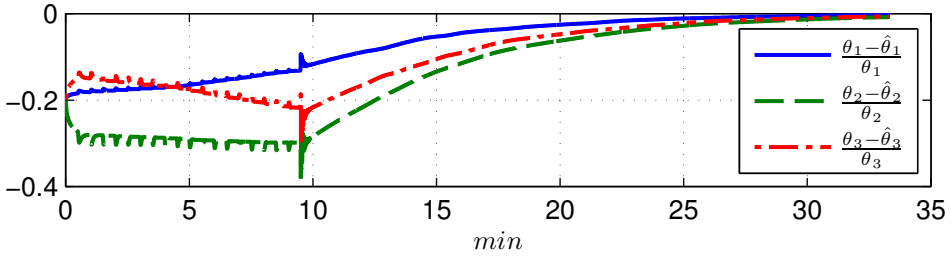

(c) Parameter estimation error, multiple observers

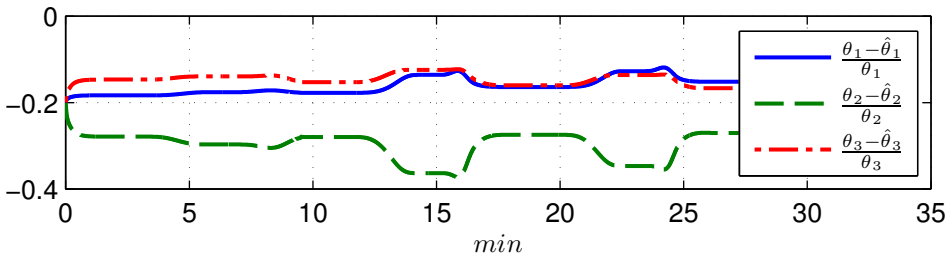

(d) Parameter estimation error, standard approach

Figure 4.3: Simulation results for the drilling system example

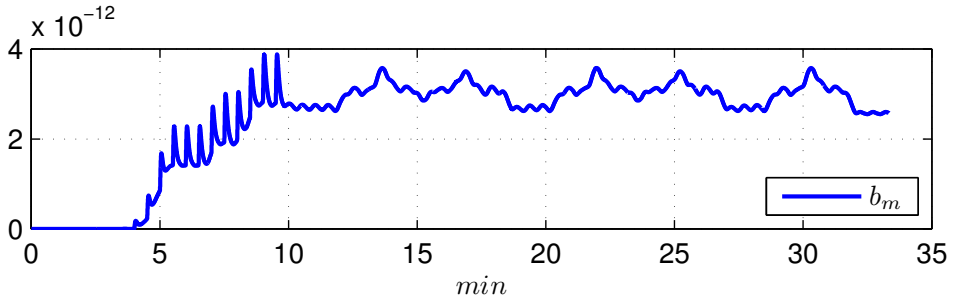

Figure 4.4: The level of excitation b_m in (4.32)

Part III

PART 3: Observer Based Output Feedback Control of Euler-Lagrange Systems

Chapter 5

A Constructive Speed Observer Design for General Euler-Lagrange Systems

Abstract: *Astolfi et al. recently proved the existence of a globally exponentially convergent speed observer for general Euler-Lagrange systems Astolfi et al. (2010). Key to their result, is a function defined by certain integrals which cannot be solved a priori, and may not have explicit analytic solutions. In this paper, this obstacle to a constructive design is removed and equations that solve the speed observer problem are given in closed form. The design is further simplified by removing up to one third of the observer states used in Astolfi et al. (2010). With the significant reduction in complexity, the new observer is easily applied to a robot example.*

5.1 Introduction

The speed observation problem for mechanical systems with only position measurements has been addressed in numerous papers, see Astolfi et al. (2010) and references therein. Recently, the first globally exponentially convergent observer for a general Euler-Lagrange system was presented in Astolfi, Ortega, and Venkatraman (2009). In Astolfi et al. (2010), it was further generalized to mechanical systems with non-holonomic constraints. The main tools that enabled Astolfi et al. to solve the problem was the Immersion and Invariance (I&I) design philosophy from Astolfi, Karagiannis, and Ortega (2008) and Karagiannis et al. (2008) combined with dynamic scaling, (Praly, 2003; Krishnamurthy and Khorrami, 2004; Lei, Wei, and

Lin, 2007; Andrieu, Praly, and Astolfi, 2009; Karagiannis, Sassano, and Astolfi, 2009). There are three major drawbacks to the design by Astolfi et. al. First, the resulting observer has fairly high dimension, namely $3n - 2k + 1$, where n is the dimension of the unmeasured velocity, and k is the number of constraints. Secondly, it requires the solution to certain integrals which cannot be derived explicitly a priori, and may even have to be computed numerically. Thirdly all the partial derivatives of these integrals are required in the implementation, which add to the already high complexity of the observer. While the solutions to these integrals and the partial derivatives may be computed numerically in real-time, this increases the computational burden of the observer significantly. In this note, using ideas from Astolfi et al. (2010), we derive a uniformly globally asymptotically stable and semi-globally exponentially stable observer of dimension $2n - k + 2$, only two states in excess of full order. The two extra states are needed to dominate the Coriolis and centrifugal forces. Furthermore, and more importantly, our observer is given by explicit expressions and does not require solutions to integrals of the kind needed in Astolfi et al. (2010).

The paper is organized as follows. The class of systems considered is defined in Section 5.2, and Section 5.3 states the main result. Section 5.4 demonstrates the performance of the observer by applying it to estimate the unmeasured angular velocities in a Furuta pendulum example taken from (Furuta, Yamakita, and Kobayashi, 1992; Xu, Iwase, and Furuta, 2001).

5.2 Class of Systems

We consider systems that can be transformed into the form

$$\dot{y} = L(y)\, x \tag{5.1a}$$

$$\dot{x} = S(y, x)\, x + F(y, x, u) \tag{5.1b}$$

where $y \in \mathbb{R}^n$ is measured, $x \in \mathbb{R}^{n-k}$ is unmeasured, $n > k \geq 0$, and $u \in \mathbb{R}^m$ is such that y, x exist for all time(the system is forward complete). We require the elements of $S(y, x) \in \mathbb{R}^{(n-k)\times(n-k)}$ and $L(y) \in \mathbb{R}^{n\times(n-k)}$ to be continuously differentiable and L to be left-invertible. Furthermore, we require S and F to satisfy the following properties:

P1 Skew-symmetry: $S(y, x) + S^T(y, x) = 0$ for all $y \in \mathbb{R}^n$, $x \in \mathbb{R}^{n-k}$,

P2 Linearity: $S(y, a_1 x + a_2 \bar{x}) = a_1 S(y, x) + a_2 S(y, \bar{x})$ for all $y \in \mathbb{R}^n$, $x, \bar{x} \in \mathbb{R}^{n-k}$ and scalar a_1, a_2,

P3 Sector Condition: There exists $c_F < \infty$ so that $[F(y,x,u) - F(y,\bar{x},u)]^T (x-\bar{x}) \leq c_F \|(x-\bar{x})\|^2$ for all $x, \bar{x} \in \mathbb{R}^{n-k}$, $y \in \mathbb{R}^n$ and $u \in \mathbb{R}^m$.

The main motivation for studying the class of systems (1) is that the class contains general Euler-Lagrange systems with k non-holonomic constraints, without velocity measurements. For details on how to transform general Euler-Lagrange systems into the form (1) see Astolfi et al. (2010).

5.3 Main Result

We denote the estimates of y and x as $\hat{y} \in \mathbb{R}^n$ and $\hat{x} \in \mathbb{R}^{n-k}$, respectively, and the corresponding estimation errors as $\tilde{y} = y - \hat{y}$ and $\tilde{x} = x - \hat{x}$. Define $\sigma = \|\hat{x}\|^2$, let $\hat{\sigma}$ be its estimate and $\tilde{\sigma} = \sigma - \hat{\sigma}$. Let $c_S : \mathbb{R}^n \to \mathbb{R}^+$ be a continuously differentiable function satisfying

$$c_S(y) \geq \sup_{\|x\|=1} \|S(y,x)\| \tag{5.2}$$

The supremum in (5.2) is taken over all $\|x\| = 1$ for fixed y. c_S is easily constructed using S. Our observer is given by

$$\hat{x} = \xi + K_x(\hat{\sigma}, \hat{y})\, y \tag{5.3}$$

$$\dot{\hat{y}} = L(y)\,\hat{x} + K_y(y, \hat{y}, r, \hat{\sigma})\,\tilde{y} \tag{5.4}$$

$$\dot{\xi} = S(y,\hat{x})\,\hat{x} + F(y,\hat{x},u) - K_x L(y)\,\hat{x} - \frac{\partial K_x}{\partial \hat{y}}\dot{\hat{y}} y - \frac{\partial K_x}{\partial \hat{\sigma}}\dot{\hat{\sigma}} y \tag{5.5}$$

$$\dot{r} = -\frac{\bar{k}_x}{2}(r - c_r) + r\left(\bar{\Delta}_y(y,\hat{y},\hat{\sigma})\,\|\tilde{y}\| + \bar{\Delta}_\sigma(y,\hat{x},\hat{\sigma})\,\|\tilde{\sigma}\|\right),\ r(t_0) \geq c_r \tag{5.6}$$

$$\dot{\hat{\sigma}} = \text{Proj}_{\hat{\sigma}}\left(2\left[\hat{x}^T F(y,\hat{x},u) + k_\sigma(y,\hat{y},\hat{x},r,\hat{\sigma},\sigma)\,\tilde{\sigma}\right]\right),\ \hat{\sigma}(t_0) \geq 0 \tag{5.7}$$

where $c_r > 0$ is a design constant, and

$$\bar{\Delta}_y(y,\hat{y},\hat{\sigma}) = \begin{cases} \frac{\Delta_y(y,\hat{y},\hat{\sigma})}{\|\tilde{y}\|} & \Delta_y(y,\hat{y},\hat{\sigma}) > \varepsilon_y \\ \frac{\Delta_y(y,\hat{y},\hat{\sigma})}{\|\Delta_y - \varepsilon_y\| + \|\tilde{y}\|} & else \end{cases} \tag{5.8}$$

$$\bar{\Delta}_\sigma(y,\sigma,\hat{\sigma}) = \begin{cases} \frac{\Delta_\sigma(y,\sigma,\hat{\sigma})}{\|\tilde{\sigma}\|} & \Delta_\sigma(y,\sigma,\hat{\sigma}) > \varepsilon_\sigma \\ \frac{\Delta_\sigma(y,\sigma,\hat{\sigma})}{\|\Delta_\sigma - \varepsilon_\sigma\| + \|\tilde{\sigma}\|} & else \end{cases} \tag{5.9}$$

$$\Delta_y(y,\hat{y},\hat{\sigma}) = \|c_S(y) - c_S(\hat{y})\|\sqrt{1+\hat{\sigma}} + \|K_x(\hat{\sigma},\hat{y})(L(y) - L(\hat{y}))\| \tag{5.10}$$

$$\Delta_\sigma(y,\sigma,\hat{\sigma}) = c_S(y)\left\|\sqrt{1+\sigma} - \sqrt{1+\hat{\sigma}}\right\|, \tag{5.11}$$

for some chosen $\varepsilon_y > 0$ and $\varepsilon_\sigma > 0$. The gains K_x, K_y, and k_σ are

$$K_x(\hat{\sigma}, \hat{y}) = \left[\bar{k}_x + c_F + \varepsilon_y + \varepsilon_\sigma + c_S(\hat{y})\sqrt{1+\hat{\sigma}}\right] L^+(\hat{y}) \tag{5.12}$$

$$K_y(y, \hat{y}, r, \hat{\sigma}) = \left[\bar{k}_y + \frac{2}{\bar{k}_x} r^2 \left(\|L(y)\|^2 + \bar{\Delta}_y^2(y, \hat{y}, \hat{\sigma})\right)\right] I_{n\times n} \tag{5.13}$$

$$k_\sigma(y, \hat{y}, \hat{x}, r, \hat{\sigma}, \sigma) = \bar{k}_\sigma + \frac{2}{\bar{k}_x} r^2 \left(\left\|\hat{x}^T K_x(\hat{\sigma}, \hat{y}) L(y)\right\|^2 + \bar{\Delta}_\sigma^2(y, \sigma, \hat{\sigma})\right) \tag{5.14}$$

with $\bar{k}_x > 0$, $\bar{k}_y > 0$ and $\bar{k}_\sigma > 0$. L^+ denotes the left inverse of L, defined as $L^+ = \left(L^T L\right)^{-1} L^T$, and $\text{Proj}_{\hat{\sigma}}(\tau)$ denotes the standard smooth projection operator known from adaptive control (Krstić et al., 1995, Appendix E), defined as

$$\text{Proj}_{\hat{\sigma}}(\tau) = \begin{cases} \tau & \hat{\sigma} > 0 \text{ or } \tau \geq 0 \\ \left(1 - \min\left\{1, \frac{-\hat{\sigma}}{\varepsilon}\right\}\right)\tau & -\varepsilon \leq \hat{\sigma} \leq 0 \text{ and } \tau < 0 \end{cases} \tag{5.15}$$

for a chosen $0 < \varepsilon < 1$.

The main result in this paper is summarized in the following Theorem.

Theorem 5.1. *Suppose u is such that system (5.1) is forward complete, and consider the observer (5.3)–(5.14). There exist a strictly positive constant k (given in (5.67)) and a continuous function $\alpha(s) : \mathbb{R}^+ \to \mathbb{R}^+$ (given in (5.68)) such that for any initial condition $y(t_0), \hat{y}(t_0) \in \mathbb{R}^n$, $x(t_0), \xi(t_0) \in \mathbb{R}^{n-k}$, $r(t_0) \geq c_r$ and $\hat{\sigma}(t_0) \geq 0$,*

$$\|w(t)\| \leq \alpha(\|w(t_0)\|) e^{-k(t-t_0)}, \tag{5.16}$$

where $w = \left[\tilde{x}^T, \tilde{y}^T, \tilde{\sigma}, r - c_r\right]^T$.

The proof of Theorem 5.1 is included in the Appendix.

Remark 5.2. The construction (5.8)–(5.9) is based on the numerical consideration of avoiding division by small numbers. Theoretically, one could let $\varepsilon_y = \varepsilon_\sigma = 0$ and replace the second lines of (5.8)–(5.9) with the appropriate limits (which exist by smoothness assumptions). By the smoothness of L and c_S there exists $\bar{\varepsilon}_y(y, \hat{y}, \hat{\sigma})$ so that $\|\Delta_y\| \geq \varepsilon_y$ implies $\|\tilde{y}\| \geq \bar{\varepsilon}_y(y, \hat{y}, \hat{\sigma}) > 0$, and so we avoid division by numbers smaller than $\bar{\varepsilon}_y(y, \hat{y}, \hat{\sigma})$ in (5.8). The same argument holds for (5.9).

Remark 5.3. The main challenge in the design is related to dominating the Coriolis and centrifugal forces, which appear as cubic nonlinearities in the time derivative of the Lyapunov function. Domination is achieved by using dynamic scaling (Praly, 2003; Krishnamurthy and Khorrami, 2004; Lei et al., 2007; Andrieu et al., 2009; Karagiannis et al., 2009), implemented through the two extra observer states r and $\hat{\sigma}$ whose dynamics is given in (5.6)–(5.7). $\hat{\sigma}$ is an estimate of $\sigma = \|\hat{x}\|$ with a known time-derivative. In particular this estimate is used in the gain K_x in (5.12) to dominate the nonlinearities caused by the Coriolis and centrifugal effects while

its time-derivate is used in the last term of (5.5). The projection operator $\text{Proj}_{\hat{\sigma}}(\cdot)$ in (5.7) guarantees that $\hat{\sigma}(t) \geq -\varepsilon$ for some $0 < \varepsilon < 1$, so that the square roots in (5.10)–(5.12) can be computed. Also, note that for $r(t_0) \geq c_r$, (5.6) ensures $r(t) \geq c_r \; \forall \, t \geq t_0$.

Remark 5.4. The signal $\hat{y}$ is a filtered estimate of y, $\hat{x} = \xi + K_x(\hat{\sigma}, \hat{y})\, y$ is an estimate of x where K_x and ξ are designed so that the manifold $\tilde{x} = x - (\xi + K_x(\hat{\sigma}, \hat{y})\, y)$ is rendered attractive and invariant.

Remark 5.5. The parameters $\bar{k}_x, \bar{k}_y, \bar{k}_\sigma$ can be used to increase the convergence rates of the estimation errors beyond what is provided by the dynamic terms in (5.12)–(5.14). c_r affects the size of r and so implicitly the size of the gains K_y and k_σ. Choosing c_r small (e.g. $c_r < 1$) therefore reduces sensitivity to measurement noise.

Remark 5.6. Comparing our observer (5.3)–(5.14) with the observer in (Astolfi et al., 2010, equations (25), (29), (37), (40) and (42)) we point out that the main differences are: *a)* (Astolfi et al., 2010, equation (42)) is replaced with the scalar (5.7), reducing the dimension of the observer; *b)* The need for solving certain integrals (Astolfi et al., 2010, equation (29)) is removed, and; *c)* Expressions (5.8)–(5.9) are given explicitly, in contrast to the corresponding expressions in (Astolfi et al., 2010, equation (47)).

5.4 Simulation Example

We consider the Furuta pendulum (Furuta et al., 1992; Xu et al., 2001). The Furuta pendulum consists of an arm attached to a motor in one end and a pendulum in the other. The arm rotates around the vertical axis and the pendulum rotates around the main axis of the arm. Let q_1 be the angle between the arm and a horizontal axis, and q_2 be the angle between the pendulum and the vertical axis with $q_2 = 0$ corresponding to the pendulum being in the upright position. The dynamics for the Furuta pendulum are governed by (Furuta et al., 1992; Xu et al., 2001)

$$M(q)\,\ddot{q} + C(q, \dot{q})\,\dot{q} + G(q) = Bu \tag{5.17}$$

where $q = [q_1, q_2]^T$ and

$$M(q) = \begin{bmatrix} p_1 + p_2 \sin^2 q_2 & p_3 \cos q_2 \\ p_3 \cos q_2 & p_4 \end{bmatrix} \tag{5.18}$$

$$C(q, \dot{q}) = \begin{bmatrix} \frac{1}{2} p_2 \sin(2q_2)\,\dot{q}_2 & -p_3 \sin q_2 \dot{q}_2 + \frac{1}{2} p_2 \sin(2q_2)\,\dot{q}_1 \\ -\frac{1}{2} p_2 \sin(2q_2)\,\dot{q}_1 & 0 \end{bmatrix} \tag{5.19}$$

$$G(q) = \begin{bmatrix} 0 \\ -p_5 \sin q_2 \end{bmatrix}, \; B = \begin{bmatrix} 1 \\ 0 \end{bmatrix} \tag{5.20}$$

The constants p_i for $i = 1, 2.., 5$ are

$$p_1 = I_0 + m_1 L_0^2,\ p_2 = m_1 l_1^2 \tag{5.21}$$
$$p_3 = m_1 l_1 L_0,\ p_4 = J_1 + m_1 l_1^2 \tag{5.22}$$
$$p_5 = m_1 l_1 g, \tag{5.23}$$

where I_0 is the arm's inertia, L_0 is the arms length, m_1 is the mass of the pendulum, l_1 is the length of the pendulum, J_1 is the inertia of the pendulum and g is the gravitational acceleration. To transform system (5.17) into the form (5.1) we follow Lemma 1 in Astolfi et al. (2009) and define the coordinates $y = q$ and $x = T(y)\dot{q}$, with $T(y) \in \mathbb{R}^{2\times 2}$ being the upper triangular Cholesky factorization of $M(y)$, that is $M(y) = T^T(y)T(y)$ with

$$T(y) = \begin{bmatrix} t_{11}(y) & \frac{p_3 \cos(y_2)}{t_{11}(y)} \\ 0 & t_{22}(y) \end{bmatrix}$$
$$t_{11}(y) = \sqrt{p_1 + p_2 \sin^2(y_2)}$$
$$t_{22}(y) = \sqrt{p_4 - \frac{\left(p_3 \cos(y_2)\right)^2}{t_{11}^2(y)}}.$$

It is straight forward to find the matrices $L(y)$, $S(y, x)$ and $F(y, u)$ as

$$L(y) = T^{-1}(y) = \begin{bmatrix} \frac{1}{t_{11}(y)} & -\frac{p_3 \cos(y_2)}{t_{11}^2(y) t_{22}(y)} \\ 0 & \frac{1}{t_{22}(y)} \end{bmatrix} \tag{5.24}$$
$$\begin{aligned} S\left(y, x\right) &= \left(\dot{T}(y) - L^T(y) C(y, L(y)x)\right) L(y) \\ &= \frac{p_2 \cos\left(y_2\right) \sin\left(y_2\right) x_1}{t_{22}(y) t_{11}^2(y)} \begin{bmatrix} 0 & -1 \\ 1 & 0 \end{bmatrix} \end{aligned} \tag{5.25}$$
$$F\left(y, u\right) = L^T(y)\left(Bu - G(y)\right) \tag{5.26}$$
$$= \begin{bmatrix} \frac{1}{t_{11}(y)} u \\ -\frac{p_3 \cos(q_2)}{t_{11}^2(y) t_{22}(y)} u - \frac{p_5 \sin q_2}{t_{22}(q)}. \end{bmatrix} \tag{5.27}$$

The parameters for the Furuta pendulum are the same as in Xu et al. (2001) and are given in Table 5.1. To find $c_s(y)$ that satisfies (5.2) we note that $\|S\left(y, x\right)\| = \left|\frac{p_2 \cos(y_2) \sin(y_2)}{t_{22}(y) t_{11}^2(y)}\right| |x_1|$ so any

$$c_S(y) \geq \left|\frac{p_2 \cos\left(y_2\right) \sin\left(y_2\right)}{t_{22}(y) t_{11}^2(y)}\right| \tag{5.28}$$

$I_0 = 0.0256kgm^2$	$L_0 = 0.0223m$
$m_1 = 0.0831kg$	$l_1 = 0.104m$
$J_1 = 2.77 \times 10^{-4}kgm^2$	$g = 9.81\frac{m}{s^2}$

Table 5.1: Parameters for the Furuta pendulum.

satisfies (5.2). For the parameter values chosen, $c_S = 0.55$ satisfies (5.28). In order to implement (5.5) we need to calculate the partial derivatives $\frac{\partial K_x}{\partial \hat{y}_1}$, $\frac{\partial K_x}{\partial \hat{y}_2}$ and $\frac{\partial K_x}{\partial \hat{\sigma}}$. For that purpose we note that $\frac{\partial K_x}{\partial \hat{y}_1} = 0$ and find

$$\frac{\partial K_x}{\partial \hat{y}_2} = \left[\bar{k}_x + \varepsilon_y + \varepsilon_\sigma + c_S\sqrt{1+\hat{\sigma}}\right]\frac{\partial T}{\partial \hat{y}_2} \tag{5.29}$$

$$\frac{\partial T}{\partial \hat{y}_2} = \begin{bmatrix} \frac{p_2\cos(\hat{y}_2)\sin(\hat{y}_2)}{t_{11}(\hat{y})} & -\left[\frac{p_3\sin(\hat{y}_2)}{t_{11}(\hat{y})} + \frac{p_2p_3\cos^2(\hat{y}_2)\sin(\hat{y}_2)}{t_{11}^3(\hat{y})}\right] \\ 0 & \frac{2p_3^2\cos(\hat{y}_2)\sin(\hat{y}_2)}{2t_{22}(\hat{y})t_{11}^2(\hat{y})} + \frac{2p_2p_3^2\cos^3(\hat{y}_2)\sin(\hat{y}_2)}{2t_{22}(\hat{y})t_{11}^4(\hat{y})} \end{bmatrix} \tag{5.30}$$

$$\frac{\partial K_x}{\partial \hat{\sigma}} = \frac{c_S}{2\sqrt{1+\hat{\sigma}}}T(\hat{y}) \tag{5.31}$$

where we have used $L^+(\hat{y}) = T(\hat{y})$. To illustrate the performance of the observer in the presence of measurement noise we assume that we measure

$$q^m = q + d \tag{5.32}$$

where $d = [d_1, d_2]$ is zero mean normally distributed random noise with standard deviation $\frac{\pi}{100}$. For comparison purposes we also implement an approximate differentiation scheme as

$$\hat{\dot{q}}_1^{num} = \frac{s}{T_{d1}s+1}q_1^m \tag{5.33}$$

$$\hat{\dot{q}}_2^{num} = \frac{s}{T_{d2}s+1}q_2^m \tag{5.34}$$

where T_{d1} and T_{d2} are chosen based on a trade off between an exact derivative for $T_{d1} = T_{d2} = 0$ and sensitivity towards measurement noise. The gains and initial conditions for the simulation are given in Table 5.2. The input torque u is shown in Fig. 5.3 and corresponds to pushing the arm first in one direction and then in the other direction. Fig. 5.1 shows the measured position, q^m and the observer estimate $\hat{q}$. From the bottom figures we see that the observer estimate converges quickly to a neighborhood around the true value as expected. Fig. 5.2 shows the velocity $\dot{q}$, the observer estimate $\hat{\dot{q}} = L(\hat{y})\hat{x}$ and the approximate derivative $\hat{\dot{q}}^{num}$. We see that the observer estimate converges quickly to a neighborhood around the true velocity while the approximate derivative has phase lag and is more sensitive to the measurement noise. Finally we would like to point out that to apply the method in Astolfi

$y(0) = 0$	$\xi(0) = \hat{x}(0) - K_x(\hat{\sigma}(0), \hat{y}(0))\hat{y}(0)$
$x(0) = 0$	$r(0) = 5c_r$, $\hat{\sigma}(0) = \|\hat{x}(0)\|^2$
$\hat{y}_1(0) = \hat{y}_2(0) = 1$	$k_x = 2$, $k_y = 1$, $k_\sigma = 0.1$,
$\hat{x}_1(0) = \hat{x}_2(0) = 1$	$c_r = 0.1$, $\varepsilon_y = \varepsilon_\sigma = 0.01$
$T_{d1} = 0.2$	$T_{d2} = 0.1$

Table 5.2: Initial conditions, gains and tuning parameters.

et al. (2010, 2009) it is necessary to solve an integral (with respect to y) containing the product of $S(y, x)$ and $T(y)$, a daunting task for this two degrees-of-freedom example. For general higher order systems this will be practically impossible.

5.5 Conclusion

We have presented a constructive globally convergent speed observer design for general Euler-Lagrange systems. The observer is given by explicit expressions and is easily applied to estimate angular velocities in a Furuta pendulum example with measurement noise. Future work should focus on the robustness of the observer towards measurement errors, robustness towards parametric uncertainties and application of the observer for output feedback control.

Acknowledgements

This work was funded by Statoil ASA under R&D project "Intelligent Drilling" and was performed while the first and second authors were visiting the Center for Control, Dynamical Systems and Computation, University of California Santa Barbara. The authors would like to thank professor João P. Hespanha for constructive comments.

5.A Appendix

To streamline the presentation of the proof of Theorem 5.1 we first point out some relevant properties of the projection operator in (5.15) and the Coriolis and centrifugal matrix S in Section 5.A.1. Various error dynamics with partial Lyapunov functions are derived in Sections 5.A.2-5.A.4, and put together into a complete

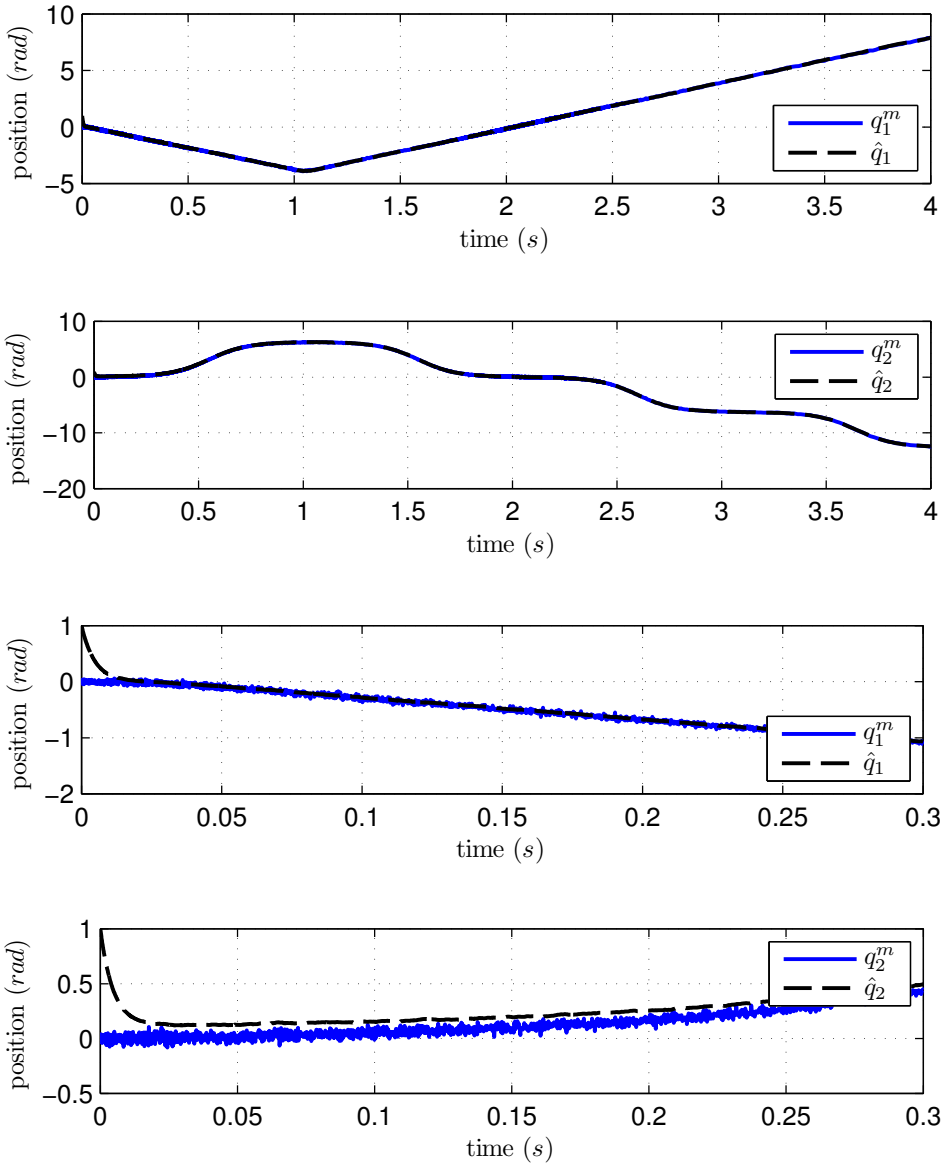

Figure 5.1: Measured joint angles q^m and the estimated joint angles $\hat{q}$ from the observer (top figures). Close-up of q^m and $\hat{q}$ for the first 0.3s (bottom figures).

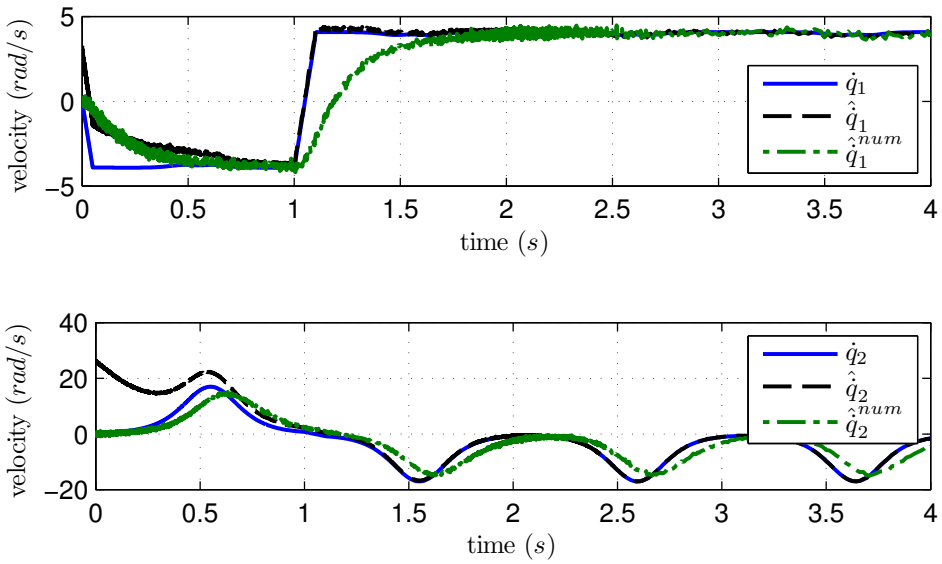

Figure 5.2: Joint angular velocities $\dot{q}$, estimates $\hat{\dot{q}} = L(\hat{y})\hat{x}$ and numerical derivative $\hat{\dot{q}}^{num}$.

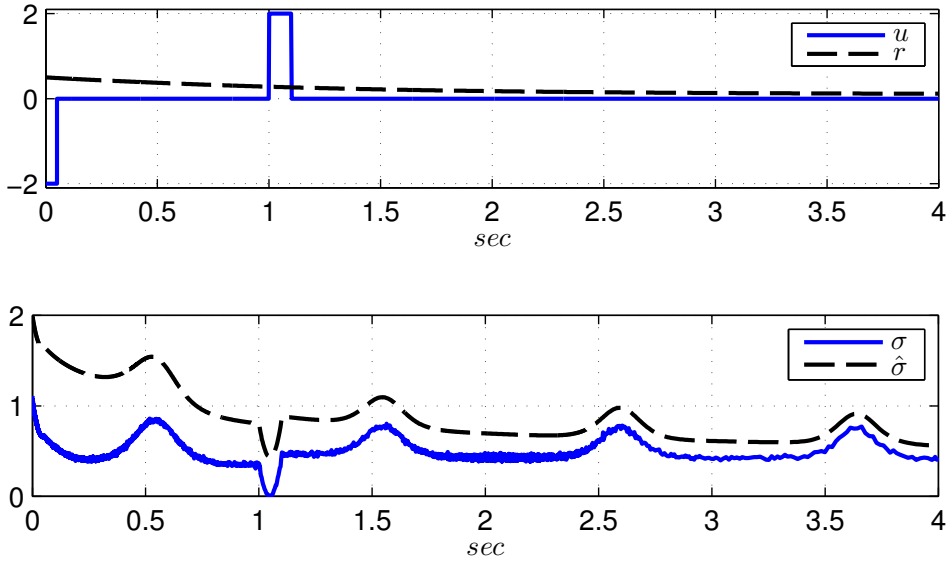

Figure 5.3: Input u, dynamic scaling factor r, σ and its estimate $\hat{\sigma}$.

Lyapunov based proof in Section 5.A.5. To simplify notation, the arguments of the functions defined in (5.8)–(5.14) are omitted.

5.A.1 Preliminaries

From (Krstić et al., 1995, Appendix E) we know that the projection operator in (5.15) guarantees that, on its domain of definition, $\hat{\sigma}(t)$, the solution to

$$\dot{\hat{\sigma}} = \text{Proj}_{\hat{\sigma}}(\tau), \ \hat{\sigma}(t_0) \geq -\varepsilon, \tag{5.35}$$

satisfies $\hat{\sigma}(t) \geq -\varepsilon$. It also has the following useful property

$$[\tau - \text{Proj}_{\hat{\sigma}}(\tau)]\,\tilde{\sigma} \leq 0 \ \forall\ \sigma \geq 0, \ \hat{\sigma} \geq -\varepsilon. \tag{5.36}$$

This follows trivially when $\hat{\sigma} > 0$ or $\tau \geq 0$ while for $\hat{\sigma} \leq 0$ and $\tau < 0$, we have $\tilde{\sigma} \geq 0$ and

$$\tau - \left(1 - \min\left\{1, \frac{-\hat{\sigma}}{\varepsilon}\right\}\right)\tau = \min\left\{1, \frac{-\hat{\sigma}}{\varepsilon}\right\}\tau \leq 0. \tag{5.37}$$

From P2 we have

$$S(y,x)\,x - S(y,\hat{x})\,\hat{x} = S(y,x)\,\tilde{x} + S(y,\tilde{x})\,\hat{x}, \tag{5.38}$$

and from P2 and (5.2) we have

$$\|S(y,x)\| \leq c_S(y)\,\|x\|. \tag{5.39}$$

5.A.2 $\tilde{y}$ dynamics

Subtracting (5.4) from (5.1a) we see that the dynamics for $\tilde{y}$ are governed by

$$\dot{\tilde{y}} = L(y)\,\tilde{x} - K_y\tilde{y}. \tag{5.40}$$

Let $V_y(\tilde{y}) = \frac{1}{2}\|\tilde{y}\|^2$, so using (5.40) gives

$$\dot{V}_y = -\tilde{y}^T K_y(y,\hat{y},r,\hat{\sigma})\,\tilde{y} + \tilde{y}^T L(y)\,\tilde{x}. \tag{5.41}$$

5.A.3 Norm estimate of $\|\hat{x}\|$ and $\tilde{\sigma}$ dynamics

For later use it is necessary to provide an estimate of the upper bound of $\|\hat{x}\|$, with known time derivative. We will use $\hat{\sigma}$, the solution to (5.7) to estimate $\sigma = \|\hat{x}\|^2$. Differentiating (5.3) with respect to time and using (5.1a) and (5.5) gives

$$\dot{\hat{x}} = S(y,\hat{x})\,\hat{x} + F(y,\hat{x},u) + K_x L(y)\,\tilde{x} \tag{5.42}$$

so σ satisfies

$$\dot{\sigma} = 2\left[\hat{x}^T F(y,\hat{x},u) + \hat{x}^T K_x L(y)\,\tilde{x}\right] \tag{5.43}$$

where P1 has been used. Subtracting (5.7) from (5.43) the dynamics for $\tilde{\sigma} = \sigma - \hat{\sigma}$ is

$$\dot{\tilde{\sigma}} = 2\left[\hat{x}^T K_x L(y)\,\tilde{x} - k_\sigma \tilde{\sigma}\right] + 2\Delta_1, \tag{5.44}$$

where

$$\Delta_1 = \left[\hat{x}^T F(y,\hat{x},u) + k_\sigma\tilde{\sigma}\right] - \text{Proj}_{\hat{\sigma}}\left(\left[\hat{x}^T F(y,\hat{x},u) + k_\sigma\tilde{\sigma}\right]\right). \tag{5.45}$$

Defining $V_\sigma(\tilde{\sigma}) = \frac{1}{4}\|\tilde{\sigma}\|^2$, and noticing that $\Delta_1\tilde{\sigma} \leq 0$ by (5.36), we get

$$\dot{V}_\sigma \leq \hat{x}^T K_x L(y)\,\tilde{x}\tilde{\sigma} - k_\sigma\tilde{\sigma}^2. \tag{5.46}$$

5.A.4 $\tilde{x}$ dynamics and dynamic scaling

Subtracting (5.42) from (5.1b) and using (5.38) gives

$$\dot{\tilde{x}} = S(y,x)\,\tilde{x} + S(y,\tilde{x})\,\hat{x} + F(y,x,u) - F(y,\hat{x},u) - K_x L(y)\,\tilde{x}. \tag{5.47}$$

Due to the skew-symmetric property of S (P1) the first term in (5.47) will disappear when using $\|\tilde{x}\|^2$ as a Lyapunov function while $F(y,x,u) - F(y,\hat{x},u)$ can be bounded using P3. The difficult term[1] is $S(y,\tilde{x})\,\hat{x}$ which by (5.39) satisfies $\|S(y,\tilde{x})\,\hat{x}\| \leq c_S(y)\,\|\tilde{x}\|\,\|\hat{x}\|$. Since the bound is linear in the unknown $\tilde{x}$ it could be possible to dominate it using K_x. However, since $\dot{y}$ and $\dot{\hat{x}}$ are unknown signals, K_x cannot depend on y or $\hat{x}$ (see the last two terms of (5.5)). To deal with this we will use the estimate $\hat{\sigma}$ derived in the previous section. First, note that by the definition of σ

$$\|S(y,\tilde{x})\,\hat{x}\| \leq c_S(y)\,\|\tilde{x}\|\,\|\hat{x}\| \leq c_S(y)\,\|\tilde{x}\|\,\sqrt{1+\sigma}. \tag{5.48}$$

[1] In Astolfi et al. (2010) this term is dealt with using an approximated solution to a partial differential equation (see (27) and (29) in the cited paper), making the resulting observer significantly more complex.

Using the estimates $\hat{\sigma}$, $\hat{y}$, and Δ_σ defined in (5.11) we get

$$\|S(y,\tilde{x})\,\hat{x}\| \leq c_S(\hat{y})\,\|\tilde{x}\|\sqrt{1+\hat{\sigma}} + \|c_S(y)-c_S(\hat{y})\|\,\|\tilde{x}\|\sqrt{1+\hat{\sigma}} + \Delta_\sigma\,\|\tilde{x}\|. \tag{5.49}$$

Note that $\sigma \geq 0$ by definition and $\hat{\sigma} > -1$ due to the projection operator in (5.7), so the expressions under the square roots are positive. The first term in (5.49) can be dominated by the use of K_x while the second and third terms require the use of dynamic scaling. As in (Karagiannis et al., 2009; Astolfi et al., 2010) consider the scaled error variable

$$\eta = \frac{1}{r}\tilde{x}, \tag{5.50}$$

where $r(t) \geq c_r$ is guaranteed by the dynamics (5.6). Taking the time derivative of (5.50) using (5.47) and P2 gives

$$\dot{\eta} = S(y,x)\,\eta + S(y,\eta)\,\hat{x} + \frac{1}{r}\left[F(y,x,u) - F(y,\hat{x},u)\right] - K_x L(y)\,\eta - \frac{\dot{r}}{r}\eta. \tag{5.51}$$

Defining $V_\eta(\eta) = \frac{1}{2}\|\eta\|^2$, and using P1, P3 and (5.51) we obtain

$$\begin{aligned}\dot{V}_\eta &= \eta^T S(y,\eta)\,\hat{x} + \frac{c_F}{r^2}\|\tilde{x}\|^2 - \eta^T K_x L(y)\,\eta - \frac{\dot{r}}{r}\|\eta\|^2 &(5.52)\\ &\leq \|S(y,\eta)\,\hat{x}\|\,\|\eta\| + c_F\|\eta\|^2 - \eta^T K_x L(\hat{y})\,\eta \\ &\quad + \|K_x(L(y)-L(\hat{y}))\|\,\|\eta\|^2 - \frac{\dot{r}}{r}\|\eta\|^2. &(5.53)\end{aligned}$$

Using the fact $\|S(y,\eta)\hat{x}\| = \frac{1}{r}\|S(y,\tilde{x})\hat{x}\|$ and (5.49) we get

$$\begin{aligned}\dot{V}_\eta &\leq c_S(\hat{y})\sqrt{1+\hat{\sigma}}\,\|\eta\|^2 + \|c_S(y)-c_S(\hat{y})\|\sqrt{1+\hat{\sigma}}\,\|\eta\|^2 + \Delta_\sigma\|\eta\|^2 \\ &\quad + c_F\|\eta\|^2 - \eta^T K_x L(\hat{y})\,\eta + \|K_x(L(y)-L(\hat{y}))\|\,\|\eta\|^2 - \frac{\dot{r}}{r}\|\eta\|^2 \\ &= c_S(\hat{y})\sqrt{1+\hat{\sigma}}\,\|\eta\|^2 + c_F\|\eta\|^2 - \eta^T K_x L(\hat{y})\,\eta \\ &\quad + \left(\Delta_\sigma + \Delta_y - \frac{\dot{r}}{r}\right)\|\eta\|^2, &(5.54)\end{aligned}$$

where Δ_y and Δ_σ are defined in (5.10) and (5.11). Using the facts $\Delta_\sigma \leq \varepsilon_\sigma + \bar{\Delta}_\sigma \|\tilde{\sigma}\|$ and $\Delta_y \leq \varepsilon_y + \bar{\Delta}_y \|\tilde{y}\|$, and (5.6) we get

$$\begin{aligned}
\dot{V}_\eta &\leq \left(c_S(\hat{y})\sqrt{1+\hat{\sigma}} + c_F + \varepsilon_y + \varepsilon_\sigma\right)\|\eta\|^2 - \eta^T K_x L(\hat{y})\,\eta \\
&\quad + \left(\bar{\Delta}_\sigma \|\tilde{\sigma}\| + \bar{\Delta}_y \|\tilde{y}\| - \frac{\dot{r}}{r}\right)\|\eta\|^2 \\
&= \left(c_S(\hat{y})\sqrt{1+\hat{\sigma}} + c_F + \varepsilon_y + \varepsilon_\sigma\right)\|\eta\|^2 - \eta^T K_x L(\hat{y})\,\eta + \frac{\bar{k}_x}{2}\frac{(r-c_r)}{r}\|\eta\|^2 \\
&\leq \left(\frac{\bar{k}_x}{2} + c_F + \varepsilon_y + \varepsilon_\sigma + c_S(\hat{y})\sqrt{1+\hat{\sigma}}\right)\|\eta\|^2 - \eta^T K_x L(\hat{y})\,\eta. \qquad (5.55)
\end{aligned}$$

We now choose K_x as in (5.12) so

$$\dot{V}_\eta \leq -\frac{\bar{k}_x}{2}\|\eta\|^2. \qquad (5.56)$$

5.A.5 Lyapunov Function

In this section we present a Lyapunov function for $\eta, \tilde{y}, \tilde{\sigma}$ and $(r - c_r)$. The Lyapunov function is

$$V_2(\eta, \tilde{y}, \tilde{\sigma}, r - c_r) = V_1(\eta, \tilde{y}, \tilde{\sigma}) + \frac{1}{2}(r - c_r)^2. \qquad (5.57)$$

with $V_1(\eta, \tilde{y}, \tilde{\sigma}) = V_\eta(\eta) + V_y(\tilde{y}) + V_\sigma(\tilde{\sigma})$. To simplify the derivations we consider V_1 first and then $V_1 + \frac{1}{2}(r - c_r)^2$. Using (5.41), (5.46), (5.50) and (5.56) we get

$$\begin{aligned}
\dot{V}_1 &\leq -\frac{\bar{k}_x}{2}\|\eta\|^2 - \tilde{y}^T K_y \tilde{y} + r\tilde{y}^T L(y)\,\eta \qquad (5.58)\\
&\quad + \hat{x}^T K_x L(y)\,\eta r\tilde{\sigma} - k_\sigma \tilde{\sigma}^2. \qquad (5.59)
\end{aligned}$$

From Young's inequality we have

$$\left\|\hat{x}^T K_x L(y)\,\eta r\tilde{\sigma}\right\| \leq \frac{\bar{k}_x}{8}\|\eta\|^2 + \frac{2}{\bar{k}_x}\tilde{\sigma}^2 r^2 \left\|\hat{x}^T K_x L(y)\right\|^2 \qquad (5.60)$$

$$\left\|r\tilde{y}^T L(y)\,\eta\right\| \leq \frac{2}{\bar{k}_x} r^2 \|L(y)\|^2 \|\tilde{y}\|^2 + \frac{\bar{k}_x}{8}\|\eta\|^2. \qquad (5.61)$$

Now we choose K_y as in (5.13) and k_σ as in (5.14) so that

$$\dot{V}_1 \leq -\frac{\bar{k}_x}{4}\|\eta\|^2 - \bar{k}_y\|\tilde{y}\|^2 - \frac{2r^2}{\bar{k}_x}\bar{\Delta}_y^2\|\tilde{y}\|^2 - \bar{k}_\sigma\tilde{\sigma}^2 - \frac{2r^2}{\bar{k}_x}\bar{\Delta}_\sigma^2\tilde{\sigma}^2. \qquad (5.62)$$

We are now ready to consider V_2. Differentiating (5.57) with respect to time using (5.62) and (5.6) gives

$$\dot{V}_2 \leq -\frac{\bar{k}_x}{4}\|\eta\|^2 - \bar{k}_y\|\tilde{y}\|^2 - \frac{2r^2}{\bar{k}_x}\bar{\Delta}_y^2\|\tilde{y}\|^2 - \bar{k}_\sigma\tilde{\sigma}^2 - \frac{2r^2}{\bar{k}_x}\bar{\Delta}_\sigma^2\tilde{\sigma}^2 - \frac{\bar{k}_x}{2}(r-c_r)^2 + r\left(\bar{\Delta}_y\|\tilde{y}\| + \bar{\Delta}_\sigma\|\tilde{\sigma}\|\right)(r-c_r). \tag{5.63}$$

By Young's inequality

$$r\bar{\Delta}_\sigma\|\tilde{\sigma}\|(r-c_r) \leq \frac{\bar{k}_x}{8}(r-c_r)^2 + \frac{2r^2}{\bar{k}_x}\bar{\Delta}_\sigma^2\|\tilde{\sigma}\|^2 \tag{5.64}$$

$$r\bar{\Delta}_y\|\tilde{y}\|(r-c_r) \leq \frac{\bar{k}_x}{8}(r-c_r)^2 + \frac{2r^2}{\bar{k}_x}\bar{\Delta}_y^2\|\tilde{y}\|^2, \tag{5.65}$$

so (5.63) reduces to

$$\dot{V}_2 \leq -\frac{\bar{k}_x}{4}\|\eta\|^2 - \bar{k}_y\|\tilde{y}\|^2 - \bar{k}_\sigma\tilde{\sigma}^2 - \frac{\bar{k}_x}{4}(r-c_r)^2. \tag{5.66}$$

By (5.57) and (5.66) we have $\dot{V}_2 \leq -\lambda V_2$ for some positive λ which implies that the equilibrium $(\eta, \tilde{y}, \tilde{\sigma}, r) = (0, 0, 0, c_r)$ of (5.40), (5.44) (5.51) and (5.6) is uniformly globally exponentially stable, and that there exists a finite upper bound for r. Since r also is bounded below by $c_r > 0$, the norms $\|\eta\|$ and $\|\tilde{x}\|$ are equivalent, and (5.16) follows with

$$k = \min\left(\frac{\bar{k}_x}{4}, \bar{k}_y, \bar{k}_\sigma\right) \tag{5.67}$$

$$\alpha(v) = \left(\sqrt{2}c_r + 2v\right)\left(\frac{c_r+1}{c_r}\right)^2 v. \tag{5.68}$$

Notice that $\alpha(s)$ is not linear due to the fact that the relation between the equivalent norms $\|\eta\|$ and $\|\tilde{x}\|$ depend on the upper bound of r, which in turn depends on initial conditions.

Chapter 6

Global Output Feedback Tracking Control of Euler-Lagrange Systems

Abstract: *We solve the problem of global output feedback tracking control of general Euler-Lagrange systems without velocity measurement. The output feedback scheme consists of a novel nonlinear observer and any certainty equivalence tracking controller satisfying certain assumptions. Using theory for cascaded systems we guarantee uniform stability and convergence of the certainty equivalence output feedback scheme. Simulation results are included to illustrate the performance of the popular Slotine and Li controller together with our proposed observer.*

6.1 Introduction

High performance tracking control of Euler-Lagrange (EL) systems requires feedback from velocities (derivative action). Velocity "measurements" can be obtained by tachometers or by numerical differentiation of position measurements. Unfortunately this limits performance as the "measurements" are sensitive to high-frequency noise on the position measurements and introduce phase lag. In addition there are no theoretical performance guarantees when using these methods. In output feedback tracking control the (dynamic) control law guarantees stability of the closed loop without the use of velocity measurements thus addressing the above performance limiting issues. Early results on output feedback tracking of EL systems are reported in Nicosia and Tomei (1990) and Berghuis and Nijmeijer (1993) where observers with semi-global region of attraction are used to generate estimates of the unmeasured velocity. The pursuit of results with global performance guarantees first

yielded partial results for some classes of EL systems, in particular for one degrees-of-freedom (DOF) systems (Loría, 1996), for EL systems that can be made linear in the unmeasured velocity (Loria and Panteley, 1999; Besançon, 2000b; Do, Jiang, and Pan, 2005), and systems satisfying a monotone damping condition (Aamo, Arcak, Fossen, and Kokotović, 2000). The first general global result was reported in Zhang, Dawson, de Queiroz, and Dixon (2000) where the ideas in Loría (1996) were extended to the n-DOF case. Due to the presence of hyperbolic functions the control input in Zhang et al. (2000) increases exponentially in the tracking error making it very aggressive. More recently, the problem of observer-based output feedback has been approached in (Børhaug and Pettersen, 2006; Carnevale, Karagiannis, and Astolfi, 2010). The results in Børhaug and Pettersen (2006) seem promising, but require the differentiation of an estimated signal in the implementation. In Carnevale et al. (2010), an immersion and invariance observer was used in collaboration with a certainty equivalence PD controller to yield a global result for general 2-DOF EL-systems.

In this paper we derive a novel nonlinear observer for general EL systems with upper and lower bounded inertia matrix. The observer is based on ideas in (Astolfi et al., 2010; Stamnes et al., 2011b), where dynamic scaling (Praly, 2003; Krishnamurthy and Khorrami, 2004; Lei et al., 2007; Andrieu et al., 2009; Karagiannis et al., 2009) is used to overcome the difficulties in deriving an observer with global region of attraction. Using the strong stability properties of the novel observer we show that a certainty equivalence controller satisfying certain assumptions ensures global asymptotic stability of the closed loop. Both the commonly used PD+ controller proposed by Paden and Panja (1988), and the "SL controller" proposed by Slotine and Li (1987), satisfy our assumption. When the SL controller is used, we also guarantee semi-global exponential stability. To the best of our knowledge the result presented here is the first observer-based output feedback tracking control solution that guarantees a global region of attraction for general EL systems. As the observer has a simple structure, and commonly used tracking controllers can be used, the resulting complexity is kept low compared to the existing global results in Zhang et al. (2000).

6.2 System and Control Objective

We consider Euler-Lagrange systems of the form

$$M(q)\ddot{q} + C(q,\dot{q})\dot{q} + G(q) = u \tag{6.1}$$

where $q \in \mathbb{R}^n$ is a vector of generalized coordinates, $M(q) \in \mathbb{R}^{n \times n}$ is the generalized inertia matrix, $C(q, \dot{q}) \in \mathbb{R}^{n \times n}$ is the Coriolis/centrifugal matrix, $G(q) \in \mathbb{R}^n$ is a vector of potential forces and $u \in \mathbb{R}^n$ is the control input. We assume that q is measured, $\dot{q}$ and $\ddot{q}$ are not measured, and that the system satisfies the following properties

P1 $0 < m_l I_{n \times n} \leq M(q) \leq m_u I_{n \times n}$ for all $q \in \mathbb{R}^n$.

P2 $\dot{M}(q) - 2C(q, \dot{q})$ is skew-symmetric for all $q, \dot{q} \in \mathbb{R}^n$.

P3 $C(q, \dot{q})\, \bar{q} = C(q, \bar{q})\, \dot{q}$ and $\|C(q, \dot{q})\| \leq \bar{c} \|\dot{q}\|$ for some $\bar{c} > 0$ and all $q, \dot{q}, \bar{q} \in \mathbb{R}^n$.

P1-**P3** are quite standard in the literature on EL systems (Ortega, Loría, Nicklasson, and Sira-Ramirez, 1998; Spong, Hutchinson, and Vidyasagar, 2006), and many different systems satisfy these properties. There are however systems that do not satisfy **P1**, such as robots with prismatic joints. Although we do not consider such systems here it is believed that the key ideas presented can be extended to systems for which $M(q)$ is potentially unbounded.

Defining $y = q$, $x = \dot{q}$ system (6.1) can be put into the form

$$\dot{y} = x \tag{6.2a}$$

$$M(y)\, \dot{x} = -C(y, x)\, x - G(y) + u. \tag{6.2b}$$

Let a twice continuously differentiable desired trajectory $y_d(t)$ with bounded $\dot{y}_d(t)$ be given. We define the controller tracking errors as

$$\tilde{y}_c = y - y_d \tag{6.3}$$

$$\tilde{x}_c = \dot{\tilde{y}}_c = x - \dot{y}_d \tag{6.4}$$

$$w_c = \begin{bmatrix} \tilde{y}_c \\ \tilde{x}_c \end{bmatrix}. \tag{6.5}$$

The objective of this paper is to show that two commonly used full state feedback tracking controllers together with a novel nonlinear velocity observer can be used in a certainty equivalence output feedback scheme without loss of stability. More precisely, we assume that a full state feedback controller $\tau(t, y, x)$ satisfying certain assumptions is given, and show that the output feedback controller $u = \tau(t, y, \hat{x})$, where $\hat{x}$ is a state estimate generated by our proposed observer, ensures global stability and tracking (τ is a function of $y_d, \dot{y}_d$ and $\ddot{y}_d$, but we have omitted them as arguments for notational brevity).

To achieve this objective we start in Section 6.3 by stating an assumption on the given full state feedback controller (Assumption 6.1 below), and show that both the

PD+ controller in Paden and Panja (1988) and the SL controller in Slotine and Li (1987) satisfy this assumption. Then, in Section 6.4, we present our novel observer and its strong stability properties, before we summarize our findings in Theorem 6.7 in Section 6.5. A simulation study is provided in Section 6.6 to demonstrate the performance of our output feedback scheme. Conclusions are offered in Section 6.7.

6.3 Controller

The tracking error dynamics can be written as

$$\dot{w}_c = \psi_c\left(t, w_c, u\right) \tag{6.6}$$

with

$$\psi_c\left(t, w_c, u\right) = \begin{bmatrix} \tilde{x}_c \\ \psi_{c2}(t, w_c, u) \end{bmatrix} \tag{6.7}$$

where

$$\begin{aligned}\psi_{c2}(t, w_c, u) =& M(y_d(t) + \tilde{y}_c)^{-1}\left[-C(y_d(t) + \tilde{y}_c, \dot{y}_d(t) + \tilde{x}_d)\right. \\ &\left.\times(\dot{y}_d(t) + \tilde{x}_d) - G(y_d(t) + \tilde{y}_c) + u\right] - \dot{y}_d(t).\end{aligned}$$

Assumption 6.1.

a) There exists a smooth full-state feedback controller $\tau\left(t, y, x\right) : \mathbb{R} \times \mathbb{R}^n \times \mathbb{R}^n \to \mathbb{R}^n$, that renders the origin of the system

$$\dot{w}_c = \psi_c\left(t, w_c, \tau\left(t, y, x\right)\right) \tag{6.8}$$

uniformly globally asymptotically stable and satisfies

$$\left\|\tau\left(t, y, a\right) - \tau\left(t, y, b\right)\right\| \leq L\left(\|y\|\right)\alpha_\tau\left(\|a - b\|\right) \tag{6.9}$$

for all $t \in \mathbb{R}$, $y \in \mathbb{R}^n$, $a, b \in \mathbb{R}^n$, with $L\left(\|y\|\right)$ affine in $\|y\|$ and $\alpha_\tau\left(s\right) = \sum_{i=1}^{N} \kappa_i s^i$ for some $N \geq 1$ and $\kappa_i \geq 0$.

b) There exists a Lyapunov function $V_u\left(t, w_c\right) : \mathbb{R} \times \mathbb{R}^{2n} \to \mathbb{R}$, a positive semi-definite function $W_u\left(w_c\right) : \mathbb{R}^{2n} \to \mathbb{R}$ and positive constants k_1, k_2, k_3 such that

$$k_1\left\|w_c\right\|^2 \leq V_u\left(t, w_c\right) \leq k_2\left\|w_c\right\|^2 \tag{6.10}$$

$$\frac{\partial V_u}{\partial t} + \frac{\partial V_u}{\partial w_c}\psi_c\left(t, w_c.\tau\left(t, y, x\right)\right) \leq -W_u\left(w_c\right) \tag{6.11}$$

$$\left\|\frac{\partial V_u}{\partial w_c}\right\| \leq k_3\left\|w_c\right\|. \tag{6.12}$$

Assumption 6.1 part a) states that we know a full state feedback control law, that can be bounded by an affine function in $\|y\|$ times a polynomial in x, that stabilizes the tracking error. In part b) we only require W_u to be positive semi-definite, which allows us to include controllers where uniform global asymptotic stability is proved using invariance theorems such as Matrosov's theorem. We will now show that both the PD+ controller, and the SL controller satisfy this requirement.

Proposition 6.2. *The PD+ controller proposed in Paden and Panja (1988)*

$$\begin{aligned}\tau_{PD+}(t,y,x) =& M(y)\ddot{y}_d(t) + C(y,x)\dot{y}_d(t) \\ &+ G(y) - K_p\tilde{y}_c - K_d\tilde{x}_c\end{aligned} \tag{6.13}$$

where $K_p = K_p^T > 0$ and $K_d = K_d^T > 0$, satisfies Assumption 6.1 with $V_u(t,w_c) = V_{PD+}(t,w_c)$ where

$$V_{PD+}(t,w_c) = \frac{1}{2}w_c^T \begin{bmatrix} K_p & 0 \\ 0 & M(\tilde{y}_c + y_d(t)) \end{bmatrix} w_c \tag{6.14}$$

Proof. Using **P3** and the fact that $\dot{y}_d$ is bounded it is straight forward to show that $\tau_{PD+}(t,y,x)$ is globally Lipschitz in x, uniformly in t and y, so (6.9) is satisfied with $L(\|y\|) \equiv L = \bar{c}\max_t(\dot{y}_d(t)) + k_d^u$, where k_d^u is the largest eigenvalue of K_d, and $\alpha_\tau(s) = s$. The rest of part a) and b) is proved in Paden and Panja (1988) with $W_u(w_c)$ only positive-semidefinite, however using Matrosov's theorem Paden and Panja (1988) were able to show that the origin of (6.8) is UGAS. □

Proposition 6.3. *The SL controller proposed in Slotine and Li (1987)*

$$\begin{aligned}\tau_{SL}(t,y,x) =& M(y)\ddot{y}_r(t,x) + C(y,x)\dot{y}_r(t,y) \\ &+ G(y) - K_p\tilde{y}_c - K_d s_c(t,y,x)\end{aligned} \tag{6.15}$$

where

$$s_c(t,y,x) = \tilde{x}_c + \Lambda\tilde{y}_c \tag{6.16}$$

$$\dot{y}_r(t,y) = \dot{y}_d - \Lambda\tilde{y}_c \tag{6.17}$$

$$\ddot{y}_r(t,x) = \ddot{y}_d - \Lambda\tilde{x}_c, \tag{6.18}$$

and $K_p = K_p^T > 0$, $K_d = K_d^T > 0$ and $\Lambda = \Lambda^T > 0$, satisfies Assumption 6.1 with $V_u(t,w_c) = V_{SL}(t,w_c)$ where

$$\begin{aligned}&V_{SL}(t,w_c) = \\ &\quad\frac{1}{2}w_c^T \begin{bmatrix} \Lambda M(\tilde{y}_c + y_d(t))\Lambda + K_p & \Lambda M(\tilde{y}_c + y_d(t)) \\ M(\tilde{y}_c + y_d(t))\Lambda & M(\tilde{y}_c + y_d(t)) \end{bmatrix} w_c\end{aligned} \tag{6.19}$$

Proof. Using **P1**, **P3**, the boundedness of y_d and $\dot{y}_d$, and the affineness of $s_c, \dot{y}_r$ and $\ddot{y}_r$ with respect to y and x it is straight forward to show that $\tau_{SL}(t, y, x)$ satisfies (6.9) with $\alpha_\tau(s) = s$ and

$$L(\|y\|) = m_u \lambda_u + \bar{c}\left(\max_t(\dot{y}_d(t)) + \max_t(y_d(t))\lambda_u + \lambda_u\|y\|\right) + k_d^u \tag{6.20}$$

where λ_u and k_d^u are the largest eigenvalues of Λ and K_d respectively, the rest of part a) and b) is shown in Slotine and Li (1987). □

Remark 6.4. In the original reference Slotine and Li (1987) the proportional term $K_p\tilde{y}_c$ in (6.15) was not present. It was added later by Sadegh and Horowitz (1990) and proved to give better disturbance rejection.

Remark 6.5. For the SL controller (6.15) it is straight forward to show that $\dot{V}_{SL}(t, w_c) \leq -\gamma_{SL} V_{SL}(t, w_c)$ so exponential stability follows guaranteeing robustness properties such as Input to State Stability towards additive disturbances.

6.4 Observer

We denote the estimate of x as $\hat{x} \in \mathbb{R}^n$, $\sigma = \sqrt{1 + \hat{x}^T\hat{x}}$ an upper bound on $\|\hat{x}\|$, and $\hat{\sigma}$ its estimate with known (measured) time derivative. The estimation errors are denoted as $\tilde{x}_o = x - \hat{x}$ and $\tilde{\sigma} = \sigma - \hat{\sigma}$ and for notational convenience we define $w_o = \left[\tilde{x}_o^T, \quad \tilde{\sigma}, \quad r - c_r\right]^T$. The proposed observer is

$$\hat{x} = \xi + K_x(\hat{\sigma})\, y \tag{6.21a}$$

$$\dot{\xi} = M^{-1}(y)\left(-C(y, \hat{x})\,\hat{x} - G(y) + u\right) - K_x(\hat{\sigma})\,\hat{x} - \frac{\partial K_x}{\partial \hat{\sigma}}\dot{\hat{\sigma}} y \tag{6.21b}$$

$$\dot{\hat{\sigma}} = \frac{\hat{x}^T}{\sigma}\left[M^{-1}(y)\left(-C(y, \hat{x})\,\hat{x} - G(y) + u\right)\right] + k_\sigma(\hat{x}, r)\,\tilde{\sigma} \tag{6.21c}$$

$$\dot{r} = -\frac{\bar{k}_x}{2m_u}(r - c_r) + r\frac{2\bar{c}}{m_l}\|\tilde{\sigma}\| \tag{6.21d}$$

where $c_r > 0$ is a design constant and the gains are chosen as

$$K_x(\hat{\sigma}) = \frac{1}{m_l}\left(\bar{c}\hat{\sigma} + \bar{k}_x\right) I, \tag{6.22a}$$

$$k_\sigma(\hat{x}, r) = \bar{k}_\sigma + \frac{r}{2\bar{k}_x}\left\|\frac{\hat{x}^T K_x}{\sigma}\right\|^2 + \frac{m_u}{\bar{k}_x}\left(\frac{2\bar{c}}{m_l} r\right)^2 \tag{6.22b}$$

where the constants m_l, m_u and $\bar{c}$ are given in **P1** and **P3**, $\bar{k}_x > 0$ is a gain to be chosen. The signal $r \in \mathbb{R}$ is a dynamic scaling factor that ensures sufficiently high convergence rate of $\hat{\sigma}$ to σ. Note that (6.21d) ensures that $r(t) \geq c_r \;\forall\; t \geq t_0$ and $r(t_0) \geq c_r$.

Lemma 6.6. *Consider system (6.2) and the observer (6.21). There exist a class $\mathcal{K}$ function α_o and a positive constant k_o, such that for any initial conditions $(y(t_0), x(t_0)) \in \mathbb{R}^{2n}$, $\xi(t_0) \in \mathbb{R}^n$, $r(t_0) \geq c_r$ and $\hat{\sigma}(t_0) \geq 1$,*

$$\|w_o(t)\| \leq \alpha_o(\|w_o(t_0)\|) e^{-k_o(t-t_0)} \; \forall t \in [t_0, T), \tag{6.23}$$

where $[t_0, T)$ is the maximal interval of existence of solutions $(y(t), x(t))$ of (6.2).

Proof. To streamline the presentation of the main result we derive various observation error dynamics with partial Lyapunov functions which are put together to form a complete Lyapunov based proof. To simplify notation we omit the arguments of the gains defined in (6.22). For later use it is necessary to provide an estimate of the upper bound of $\|\hat{x}\|$ with known time derivative. We will use $\hat{\sigma}$, the solution to (6.21c), to estimate $\sigma = \sqrt{1 + \hat{x}^T \hat{x}} \geq 1$. Differentiating (6.21a) with respect to time, and using (6.21b) and (6.2a), give

$$\dot{\hat{x}} = M^{-1}(y)(-C(y, \hat{x})\hat{x} - G(y) + u) + K_x \tilde{x}_o \tag{6.24}$$

and so σ satisfies

$$\dot{\sigma} = \frac{\hat{x}^T}{\sigma}\left[M^{-1}(y)(-C(y, \hat{x})\hat{x} - G(y) + u) + K_x \tilde{x}_o\right]. \tag{6.25}$$

Subtracting (6.21c) from (6.25) we find that $\tilde{\sigma} = \sigma - \hat{\sigma}$ satisfies

$$\dot{\tilde{\sigma}} = \frac{1}{\sigma}\hat{x}^T K_x \tilde{x}_o - k_\sigma \tilde{\sigma}. \tag{6.26}$$

Let $V_\sigma(\tilde{\sigma}) = \frac{1}{2}\tilde{\sigma}^2$, then

$$\dot{V}_\sigma = \frac{\tilde{\sigma}}{\sigma}\hat{x}^T K_x \tilde{x}_o - k_\sigma \tilde{\sigma}^2. \tag{6.27}$$

Subtracting (6.24) from (6.2b) gives

$$M(y)\dot{\tilde{x}}_o = -(C(y, x)x - C(y, \hat{x})\hat{x}) - M(y)K_x \tilde{x}_o. \tag{6.28}$$

Observing that

$$C(y, x)x - C(y, \hat{x})\hat{x} = C(y, x)\tilde{x}_o + C(y, \hat{x})\tilde{x}_o \tag{6.29}$$

by **P3**, we obtain

$$M(y)\dot{\tilde{x}}_o = -(C(y, x)\tilde{x}_o + C(y, \hat{x})\tilde{x}_o) - M(y)K_x \tilde{x}_o. \tag{6.30}$$

Consider the function

$$V_x(y, \tilde{x}_o, r) = \frac{1}{2r}\tilde{x}_o^T M(y)\tilde{x}_o. \tag{6.31}$$

Differentiating (6.31), using (6.30), **P2** and **P3**, gives

$$\begin{aligned}\dot{V}_x &= -\frac{1}{r}\tilde{x}_o^T C\left(y,\hat{x}\right)\tilde{x}_o - \frac{1}{r}\tilde{x}_o^T M\left(y\right)K_x\tilde{x}_o - \frac{\dot{r}}{r}V_x \\ &\leq \frac{1}{r}\bar{c}\left\|\hat{x}\right\|\left\|\tilde{x}_o\right\|^2 - \frac{1}{r}\tilde{x}_o^T M\left(y\right)K_x\tilde{x}_o - \frac{\dot{r}}{r}V_x. \end{aligned} \tag{6.32}$$

By definition, $\sigma \geq \left\|\hat{x}\right\|$, so

$$\begin{aligned}\dot{V}_x &\leq \frac{1}{r}\bar{c}\sigma\left\|\tilde{x}_o\right\|^2 - \frac{1}{r}\tilde{x}_o^T M\left(y\right)K_x\tilde{x}_o - \frac{\dot{r}}{r}V_x \\ &\leq \frac{1}{r}\bar{c}\left\|\tilde{\sigma}\right\|\left\|\tilde{x}_o\right\|^2 + \frac{1}{r}\tilde{x}_o^T\left(\bar{c}\hat{\sigma} - M\left(y\right)K_x\right)\tilde{x}_o - \frac{\dot{r}}{r}V_x. \end{aligned} \tag{6.33}$$

Choosing K_x as in (6.22a) gives

$$\begin{aligned}\dot{V}_x &\leq \frac{1}{r}\bar{c}\left\|\tilde{\sigma}\right\|\left\|\tilde{x}_o\right\|^2 - \frac{\bar{k}_x}{r}\left\|\tilde{x}_o\right\|^2 - \frac{\dot{r}}{r}V_x \\ &\leq -\frac{\bar{k}_x}{r}\left\|\tilde{x}_o\right\|^2 - \left(\frac{\dot{r}}{r} - \frac{2\bar{c}}{m_l}\left\|\tilde{\sigma}\right\|\right)V_x. \end{aligned} \tag{6.34}$$

Consider $V_1\left(y,\tilde{x}_o,\tilde{\sigma},r\right) = V_x\left(y,\tilde{x}_o,r\right) + V_\sigma\left(\tilde{\sigma}\right)$. Using (6.34) and (6.27) we have

$$\dot{V}_1 \leq -\frac{\bar{k}_x}{r}\left\|\tilde{x}_o\right\|^2 - \left(\frac{\dot{r}}{r} - \frac{2\bar{c}}{m_l}\left\|\tilde{\sigma}\right\|\right)V_x + \frac{\tilde{\sigma}}{\sigma}\hat{x}^T K_x\tilde{x}_o - k_\sigma\tilde{\sigma}^2. \tag{6.35}$$

By Young's inequality we have

$$\left\|\frac{\tilde{\sigma}}{\sigma}\hat{x}^T K_x\tilde{x}_o\right\| \leq \frac{r}{2\bar{k}_x}\left\|\frac{\tilde{\sigma}}{\sigma}\hat{x}^T K_x\right\|^2 + \frac{\bar{k}_x}{2r}\left\|\tilde{x}_o\right\|^2. \tag{6.36}$$

Inserting (6.36) into (6.35) gives

$$\dot{V}_1 \leq -\frac{\bar{k}_x}{2r}\left\|\tilde{x}_o\right\|^2 - \left(\frac{\dot{r}}{r} - \frac{2\bar{c}}{m_l}\left\|\tilde{\sigma}\right\|\right)V_x + \frac{r}{2\bar{k}_x}\left\|\frac{\hat{x}^T K_x}{\sigma}\right\|^2\tilde{\sigma}^2 - k_\sigma\tilde{\sigma}^2. \tag{6.37}$$

Inserting (6.21d) gives

$$\begin{aligned}\dot{V}_1 &\leq -\frac{\bar{k}_x}{2r}\left\|\tilde{x}_o\right\|^2 + \left(\frac{\bar{k}_x\left(r-c_r\right)}{2m_u r}\right)V_x + \frac{r}{2\bar{k}_x}\left\|\frac{\hat{x}^T K_x}{\sigma}\right\|^2\tilde{\sigma}^2 - k_\sigma\tilde{\sigma}^2 \\ &\leq -\frac{\bar{k}_x}{2r}\left\|\tilde{x}_o\right\|^2 + \frac{\bar{k}_x}{2m_u}V_x + \frac{r}{2\bar{k}_x}\left\|\frac{\hat{x}^T K_x}{\sigma}\right\|^2\tilde{\sigma}^2 - k_\sigma\tilde{\sigma}^2 \\ &\leq -\frac{\bar{k}_x}{4r}\left\|\tilde{x}_o\right\|^2 + \frac{r}{2\bar{k}_x}\left\|\frac{\hat{x}^T K_x}{\sigma}\right\|^2\tilde{\sigma}^2 - k_\sigma\tilde{\sigma}^2 \end{aligned} \tag{6.38}$$

since $\frac{r-c_r}{r} < 1$ and $\left\| \frac{\bar{k}_x}{2m_u} V_x \right\| \leq \frac{\bar{k}_x}{4r} \left\| \tilde{x}_o \right\|^2$. Let

$$V_2 \left(y, w_o \right) = V_1 \left(y, \tilde{x}_o, \tilde{\sigma}, r \right) + \frac{1}{2} \left(r - c_r \right)^2 . \tag{6.39}$$

Using (6.38) and (6.21d) we have

$$\begin{aligned} \dot{V}_2 \leq & - \frac{\bar{k}_x}{4r} \left\| \tilde{x}_o \right\|^2 + \frac{r}{2\bar{k}_x} \left\| \frac{\hat{x}^T K_x}{\sigma} \right\|^2 \tilde{\sigma}^2 - k_\sigma \tilde{\sigma}^2 \\ & - \frac{\bar{k}_x}{2m_u} \left(r - c_r \right)^2 + \frac{2\bar{c}}{m_l} r \left(r - c_r \right) \left\| \tilde{\sigma} \right\| \end{aligned} \tag{6.40}$$

By Young's inequality

$$\frac{2\bar{c}}{m_l} r \left(r - c_r \right) \left\| \tilde{\sigma} \right\| \leq \frac{\bar{k}_x}{4m_u} \left(r - c_r \right)^2 + \frac{m_u}{\bar{k}_x} \left(\frac{2\bar{c}}{m_l} r \right)^2 \left\| \tilde{\sigma} \right\|^2 \tag{6.41}$$

so

$$\begin{aligned} \dot{V}_2 \leq & - \frac{\bar{k}_x}{4r} \left\| \tilde{x}_o \right\|^2 - \frac{\bar{k}_x}{4m_u} \left(r - c_r \right)^2 \\ & - \left(k_\sigma - \frac{r}{2\bar{k}_x} \left\| \frac{\hat{x}^T K_x}{\sigma} \right\|^2 - \frac{m_u}{\bar{k}_x} \left(\frac{2\bar{c}}{m_l} r \right)^2 \right) \tilde{\sigma}^2 \end{aligned} \tag{6.42}$$

so we choose k_σ as in (6.22b) so that

$$\dot{V}_2 \leq - \frac{\bar{k}_x}{4r} \left\| \tilde{x}_o \right\|^2 - \bar{k}_\sigma \tilde{\sigma}^2 - \frac{\bar{k}_x}{4m_u} \left(r - c_r \right)^2 . \tag{6.43}$$

Now, (6.39) and (6.43) imply that there exist positive constants $k_o^{'}$ and k_o such that

$$\left\| \bar{w}_o \left(t \right) \right\|^2 \leq k_o^{'2} \left\| \bar{w}_o \left(t_0 \right) \right\|^2 e^{-2k_o (t - t_o)} \; \forall t \in [t_0, T), \tag{6.44}$$

where $[t_0, T)$ is the maximal interval of existence of the solutions $\left(y \left(t \right), x \left(t \right) \right)$ of (6.2) and

$$\bar{w}_o \left(t \right) = \left[\frac{\tilde{x}_o^T (t)}{\sqrt{r(t)}}, \quad \tilde{\sigma} \left(t \right), \quad r \left(t \right) - c_r \right]^T .$$

From (6.44) and (6.21d), $r(t)$ is bounded from above and below so we obtain

$$c_r \leq r \left(t \right) \leq k_o^{'} \left\| \bar{w}_o \left(t_0 \right) \right\| + c_r \; \forall t \in [t_0, T) \tag{6.45}$$

which implies

$$\frac{c_r}{c_r+1}\left\|\bar{w}_o(t)\right\|^2 \leq \left\|w_o(t)\right\|^2 \tag{6.46a}$$

$$\left\|w_o(t)\right\|^2 \leq \left(k_o^{'}\left\|\bar{w}_o(t_0)\right\| + c_r + 1\right)\left\|\bar{w}_o(t)\right\|^2 \tag{6.46b}$$

Finally, (6.44) and (6.46) imply (6.23) with

$$\alpha_o(s) = k_o^{'}\sqrt{\left(\frac{1+c_r}{c_r}\right)}\sqrt{\left(k_o^{'}\sqrt{\left(\frac{1+c_r}{c_r}\right)}s + c_r + 1\right)}se^{-k_o(t-t_0)}. \tag{6.47}$$

□

6.5 Main Result

The main result is summarized in the following theorem.

Theorem 6.7. *Suppose we are given a state feedback controller $\tau(t,y,x)$ that satisfies Assumption 6.1. Then, the certainty equivalence controller $u = \tau(t,y,\hat{x})$, with $\hat{x}$ generated by the observer (6.21), ensures that there exists a class $\mathcal{KL}$ function β such that for any initial conditions $w_c(t_0) \in \mathbb{R}^{2n}$, $\xi(t_0) \in \mathbb{R}^n$, $r(t_0) \geq c_r$ and $\hat{\sigma}(t_0) \geq 1$,*

$$\left\|w_c(t), w_o(t)\right\| \leq \beta\left(\left\|w_c(t_0), w_o(t_0)\right\|, t - t_0\right) \tag{6.48}$$

for all $t \geq t_0$.

Proof. We will apply Proposition 3 in Loría (2008) to prove Theorem 6.7. To that end note that by Assumption 6.1 and the affineness of $\psi_c(t,w_c,u)$ in u we have

$$\alpha_1\left(\|w_c\|\right) \leq V_u(t,w_c) \leq \alpha_2\left(\|w_c\|\right) \tag{6.49}$$

where $\alpha_1\left(\|w_c\|\right) = k_1\left\|w_c\right\|^2$, $\alpha_2\left(\|w_c\|\right) = k_2\left\|w_c\right\|^2$, and

$$\frac{\partial V_u}{\partial t} + \frac{\partial V_u}{\partial w_c}\psi_c\left(t,w_c,\tau(t,y,\hat{x})\right) \leq \frac{k_3}{m_l}L\left(\|y\|\right)\|w_c\|\,\alpha_\tau\left(\|\tilde{x}_o\|\right) \tag{6.50}$$

Note that, due to the affineness of L and the boundedness of y_d, there exists $c_1 > 0$ and $\alpha_4\left(\|w_c\|\right) = c_1(1+\|w_c\|)\|w_c\|$ such that $\alpha_4\left(\|w_c\|\right) \geq \frac{k_3}{m_l}L\left(\|y_d + \tilde{y}_c\|\right)\|w_c\|$. Inserting this into (6.50) gives

$$\frac{\partial V_u}{\partial t} + \frac{\partial V_u}{\partial w_c}\psi_c\left(t,w_c,\alpha(t,y,\hat{x})\right) \leq \alpha_4\left(\|w_c\|\right)\alpha_\tau\left(\|\tilde{x}_o\|\right).$$

By the definition of α_1 and α_4 we have

$$\int_0^\infty \frac{dv}{\alpha_4\left(\alpha_1^{-1}(v)\right)} \propto \int_0^\infty \frac{dv}{\sqrt{v}+v} = \infty. \tag{6.51}$$

This verifies Assumption 4 in Loría (2008), Assumption 6.1 covers Assumption 1 and 5 in Loría (2008), while Lemma 6.6 satisfies Assumption 6 and 7 in Loría (2008). Since $\alpha_\tau(s)$ is a polynomial in s and $s \geq 0$, we have that $\sqrt{\alpha_\tau(s)} \leq \sum_{i=1}^N \sqrt{\kappa_i s^i}$. From Lemma 6.6 we then have the following

$$\int_{t_0}^\infty \sqrt{\alpha_\tau\left(\|\tilde{x}_o(t)\|\right)}dt \leq \int_{t_0}^\infty \sum_{i=1}^N \sqrt{\kappa_i \|\tilde{x}_o(t)\|^i}dt \tag{6.52}$$

$$\leq -\sum_{i=1}^N \frac{2}{ik_o}\sqrt{\kappa_i\left(\alpha_o\left(\|w_o(t_0)\|\right)\right)^i}\left[e^{-i\frac{k_o}{2}(t-t_0)}\right]_{t_0}^\infty \tag{6.53}$$

$$= \sum_{i=1}^N \frac{2}{ik_o}\sqrt{\kappa_i\left(\alpha_o\left(\|w_o(t_0)\|\right)\right)^i} \tag{6.54}$$

and so Theorem 3 in Loría (2008) holds with

$$\phi\left(\|w_o(t_0)\|\right) = \sum_{i=1}^N \frac{2}{ik_o}\sqrt{\kappa_i\left(\alpha_o\left(\|w_o(t_0)\|\right)\right)^i} \tag{6.55}$$

and (6.48) follows by Proposition 3 in Loría (2008). □

Proposition 6.8. *When the SL controller from Proposition 6.3 is used Theorem 6.7 holds with β strengthened to*

$$\beta(s, t-t_0) = \alpha_{SL}(s)\, e^{-k_{SL}(t-t_0)} \tag{6.56}$$

for some class $\mathcal{K}$ function α_{SL} and positive constant k_{SL}.

Proof. By the affineness of $\psi_c(t, w_c, u)$ in u, Proposition 6.3, Assumption 6.1 and Remark 6.5 we have

$$\dot{V}_{SL} \leq -\gamma_{SL}V_{SL} + \frac{k_3}{m_l}\sqrt{\frac{V_{SL}}{k_1}}L\left(\|y\|\right)\|\tilde{x}_o\|. \tag{6.57}$$

By Theorem 6.7 we know that all solutions $(y(t), x(t))$ of (6.2) exist and are bounded so that $\frac{k_3}{m_l\sqrt{k_1}}L\left(\|y\|\right) \leq l_u(w_c(t_0), w_o(t_0))$ for some positive l_u depending on intial conditions, and Lemma 6.6 is satisfied with $T = \infty$. We will thus consider $v(t) = \tilde{x}_o(t)$ as an exponentially decaying disturbance in (6.57) and apply the comparison method to draw conclusions. As in Khalil (2002) Chapter 9.3

we let $W(t) = \sqrt{V_{SL}(t, w_c(t))}$, and differentiate $W(t)$ with respect to time, using (6.57), to obtain

$$\dot{W} \leq -\frac{1}{2}\gamma_{SL} W + \frac{1}{2} l_u(w_c, w_o) \|v(t)\| \tag{6.58}$$

and so the solution $W(t)$ satisfies

$$W(t) \leq W(t_0) e^{-\frac{\gamma_{SL}}{2}(t-t_0)} + \frac{1}{2} l_u(w_c(t_0), w_o(t_0)) \int_{t_0}^{t} e^{-\frac{\gamma_{SL}}{2}(t-\tau)} \|v(\tau)\| d\tau. \tag{6.59}$$

Let $k_{SL} = \min\left(k_o, \frac{\gamma_{SL}}{4}\right)$. Since by Lemma 6.6 $\|v(\tau)\| \leq \alpha_o(\|w_o(t_0)\|) e^{-k_o(t-t_0)}$, the integral in (6.59) can be bounded above as follows

$$\begin{aligned} \int_{t_0}^{t} e^{-\frac{\gamma_{SL}}{2}(t-\tau)} e^{-k_o(\tau-t_0)} d\tau &\leq \int_{t_0}^{t} e^{-2k_{SL}(t-\tau)} e^{-k_{SL}(\tau-t_0)} d\tau \\ &\leq \frac{1}{k_{SL}} e^{-k_{SL}(t-t_0)} \end{aligned} \tag{6.60}$$

obtaining

$$W(t) \leq \left[W(t_0) + \frac{1}{2} l_u(w_c(t_0), w_o(t_0)) \frac{1}{k_{SL}} \alpha_o(\|w_o(t_0)\|) \right] e^{-k_{SL}(t-t_0)} \tag{6.61}$$

By Assumption 6.1, $W(t)$ and $\|w_c(t)\|$ are equivalent so (6.61) and (6.23) imply (6.56). □

6.6 Simulation Example

To illustrate the use of the output feedback scheme we use the SL controller from Proposition 6.3 and the observer derived in Section 6.4 to make a two-degrees-of-freedom robot manipulator track a given reference signal

$$y_d(t) = \begin{bmatrix} \cos(2t) \\ \sin(2t) \end{bmatrix}. \tag{6.62}$$

We use the manipulator dynamics from Berghuis and Nijmeijer (1993). $M(q)$, $C(q,\dot{q})$ and $G(q)$ in (6.1) are given as

$$M(q) = \begin{bmatrix} 9.77 + 2.02\cos(q_2) & 1.26 + 1.01\cos(q_2) \\ 1.26 + 1.01\cos(q_2) & 1.12 \end{bmatrix} \tag{6.63}$$

$$C(q,\dot{q}) = 1.01\sin(q_2)\begin{bmatrix} -\dot{q}_2 & -(\dot{q}_1 + \dot{q}_2) \\ \dot{q}_1 & 0 \end{bmatrix} \tag{6.64}$$

$$G(q) = g\begin{bmatrix} 8.1\sin(q_1) + 1.13\sin(q_1 + q_2) \\ 1.13\sin(q_1 + q_2) \end{bmatrix}. \tag{6.65}$$

The constants in **P1** and **P3** are $m_l = 0.65$, $m_u = 12.5$, $\bar{c} = 2.02$, and the controller and observer gains are chosen as $K_p = I$, $K_d = 10I$, $\Lambda = 2I$, $\bar{k}_x = 1$, $\bar{k}_\sigma = 1$ and $c_r = 0.1$. The initial conditions were chosen as $y(t_0) = [0, 0]$, $x(t_0) = [10, 10]$, $\xi(t_0) = [0, 0]$, $\hat{\sigma}(t_0) = 2$, $r(t_0) = 1$. Fig. 6.1a and 6.1b show the positions y_1 and y_2, and the velocities x_1 and x_2. In addition Fig. 6.1b shows that the velocity estimation errors converge quickly to zero in accordance with Lemma 6.6. Fig. 6.1c and 6.1d show that the tracking errors converge to zero in accordance with Theorem 6.7. Fig. 6.2 shows the control input while Fig. 6.3a shows that $\hat{\sigma}$ converges quickly to σ and Fig. 6.3b shows that r remains bounded while converging slowly towards c_r (due to a small gain $\frac{\bar{k}_x}{2m_u}$ in (6.21d)).

6.7 Conclusion

We have presented a novel velocity observer that enables output-feedback certainty equivalence control of general Euler-Lagrange systems without velocity measurements. The observer has a simple structure and global stability is guaranteed for two commonly used tracking controllers, namely the PD+ scheme proposed in Paden and Panja (1988) and the SL controller proposed in Slotine and Li (1987). The authors believe this to be the first result that guarantees global stability and convergence for certainty equivalence output feedback tracking control of general Euler-Lagrange systems. Future work includes investigating the performance of the scheme when measurement noise is present, possibly making a full-order observer, and deriving an adaptive scheme that allows for parametric uncertainties in model parameters.

Acknowledgements

This work was funded by Statoil ASA under R&D project 'Intelligent Drilling'

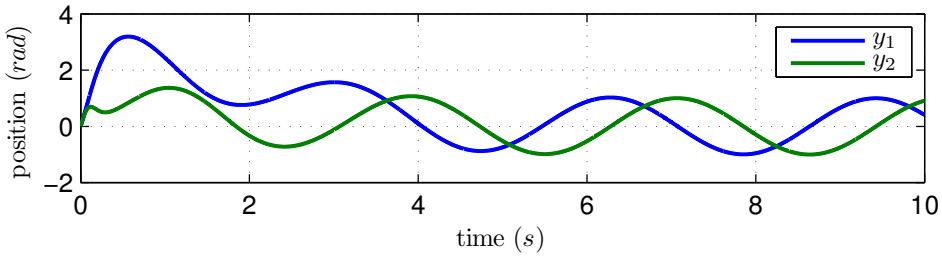

(a) Link positions.

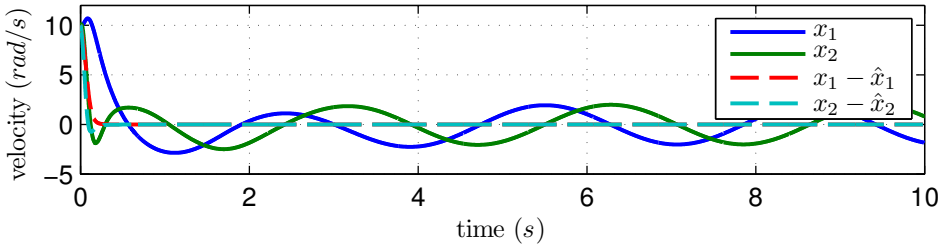

(b) Link velocities and velocity estimation errors.

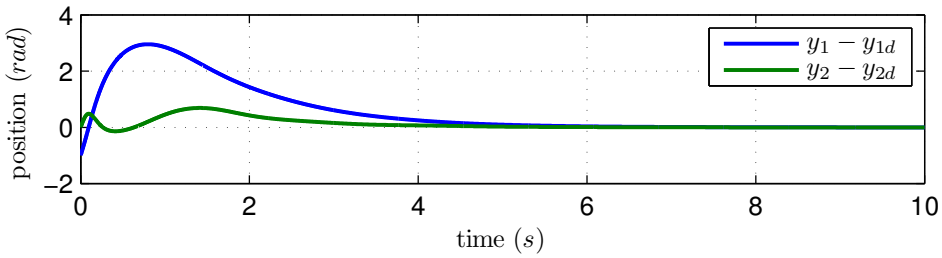

(c) Position tracking errors.

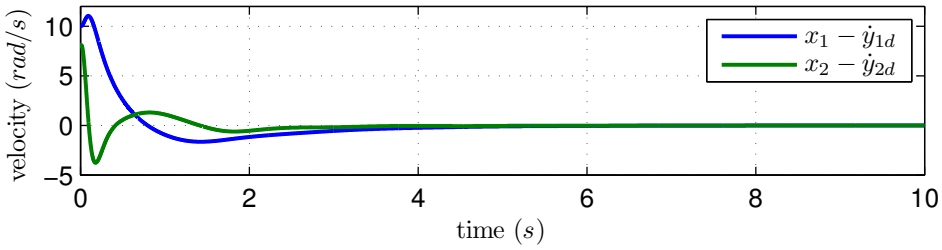

(d) Velocity tracking errors.

Figure 6.1: The top figures show position y, velocity x and velocity estimation error $\tilde{x}_o$, while the bottom figures show position and velocity tracking errors, $\tilde{y}_c$ and $\tilde{x}_c$ respectively.

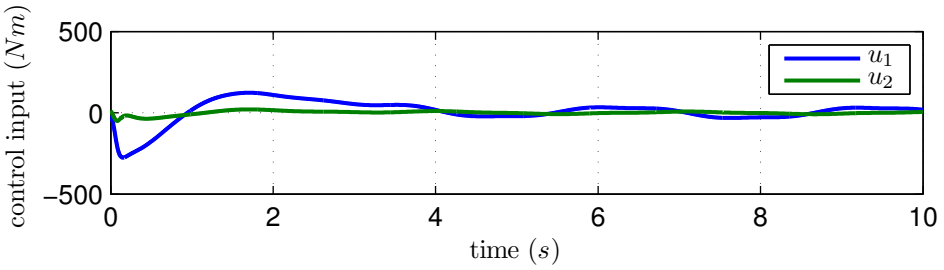

Figure 6.2: Control input u

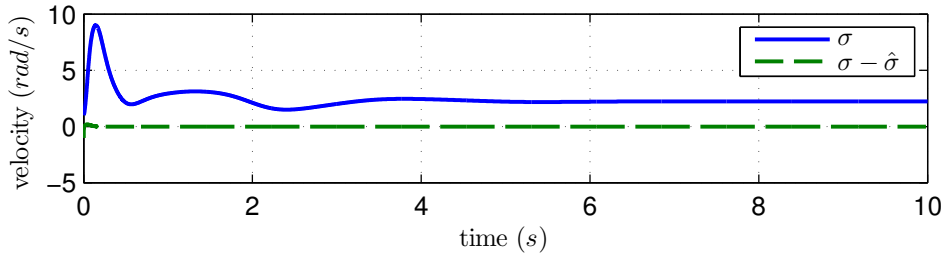

(a) $\sigma = \sqrt{1 + \hat{x}^T \hat{x}}$ and the estimation error $\tilde{\sigma} = \sigma - \hat{\sigma}$.

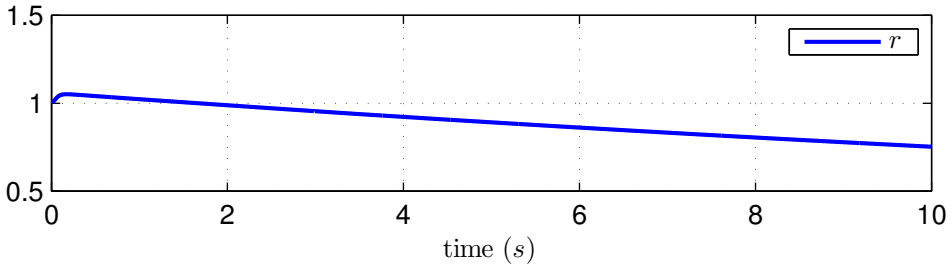

(b) The dynamic scaling factor.

Figure 6.3: σ and the estimation error $\tilde{\sigma}$, and dynamic scaling r.

Chapter 7

Conclusions and Future Work

7.1 Conclusions

This thesis addresses the topic of nonlinear observer design and its applications with particular emphasis on estimation for managed pressure drilling.

Part I of this thesis addresses the topic of estimation for managed pressure drilling. A simplified hydraulic model for a drilling system is presented and shown to capture the dominating dynamics of the well. Using adaptive observers and parameter estimation techniques we have illustrated how to calibrate the model using available real time measurements.

Part II of this thesis is concerned with the design of adaptive observers for a class of nonlinear systems including the simplified model for a drilling system. The first paper presents an adaptive observer that extends the class of systems for which adaptive observers can be designed. In particular, it allows for systems with terms containing both uncertainty and nonlinearity in the unmeasured states to appear in the dynamics of the unmeasured states, and still guarantees convergence of the state estimate without requiring persistent excitation. Instead of a commonly assumed strictly positive real condition the adaptive observer relies on the solution of a partial differential equation, to be implemented. The second paper addresses the poor parameter identification properties of commonly used Lyapunov based adaptive laws by using multiple delayed observers to improve the convergence rate of the parameter estimation error. The use of multiple delayed observers gives significantly better parameter identification and robustness properties at the cost of an increased computational burden. In particular, given that a special persistency of excitation condition is satisfied, we provide an explicit lower bound on the convergence rate of

the estimation error and show that this bound can be made arbitrarily high provided the original non-adaptive observer can achive arbitrarily high convergence rates.

Part III of this thesis addresses the topic of observer based output feedback control of Euler-Lagrange systems without velocity or acceleration measurements. In the first paper a significant obstacle to a constructive observer design for general Euler-Lagrange systems is removed. This allows for a constructive design that guarantees uniform global asymptotic stability and semi-global exponential stability. In the second paper, a similar observer is derived, and it is shown that the observer guarantees stability when used in a certainty equivalence output feedback scheme with certain types of tracking controllers, such as the PD+ controller proposed in (Paden and Panja, 1988), and the controller proposed by Slotine and Li (Slotine and Li, 1987). To the best of our knowledge this is the first observer-based output feedback tracking control solution that guarantees a global region of attraction for general Euler-Lagrange systems.

7.2 Future Work

7.2.1 Managed Pressure Drilling

The hydrostatic pressure has a significant effect on the downhole pressure so even small inaccuracies in the density estimate of the mud will affect the downhole pressure estimate significantly. Therefore a model of the density of the mud is crucial and should be added to the existing model. The model should take into account that the density of the mud is affected by pressure, temperature and the amount of cuttings and gas in the mud column, it should also handle so called multi fluid scenarios. That is, where one type of drilling fluid is displaced with a new one. When a model has been developed one should investigate how to calibrate it against the available measurements.

7.2.2 Adaptive Observer Design

One of the main limitations in the adaptive observer design proposed in Chapter 3 is that a solution to a partial differential equation must be found. In (Stamnes, Kaasa, and Aamo, 2011d) this limitation has been removed for the drilling model by extending the dimension of the observer. It is believed that the limitation be can removed for more general systems following a similar method, or by the use of

dynamic scaling (Karagiannis et al., 2009). For the observer design based on multiple observers there are several directions which can be explored. One direction is to try to reduce the computational burden by making the method more recursive. That is, to investigate for what class of systems (if any) the delayed observers can be implemented in a clever (recursive) way so that fewer integrations are needed. Another direction is to make the delays time-varying and adjustable. The objective could then be to maximize information gathering or maximize the lower bound on the persistent excitation condition in Assumption 4.6 by adjusting the delays. A third direction is to investigate the use of delayed observers to increase the robustness and parameter identification for general Lyapunov based (SPR) adaptive laws, which are ubiquitous in the literature on adaptive control.

7.2.3 Output Feedback Control of Euler-Lagrange Systems

Using the results from Part II and III and dynamic scaling it should be possible to derive adaptive observers for general Euler-Lagrange systems with uncertainties in the mass matrix. Furthermore, based on the results in Chapter 4 it should be possible to guarantee robustness and a tunable minimum convergence rate for both state and estimation error. For an adaptive observer design to work one probably needs to ensure positive definiteness of the estimated mass matrix by the use of some sort of projection operator.

Bibliography

O. M. Aamo, M. Arcak, T. I. Fossen, and P. V. Kokotović. Global output tracking control of a class of euler-lagrange systems. *International Journal of Control*, 74:649–658, 2000.

V. Andrieu and L. Praly. On the existence of a kazantzis–kravaris/luenberger observer. *SIAM J. Control Optim.*, 45(2):432–456, 2006. doi:10.1137/040617066.

V. Andrieu, L. Praly, and A. Astolfi. High gain observers with updated gain and homogeneous correction terms. *Automatica*, 45(2):422–428, 2009. doi:10.1016/j.automatica.2008.07.015.

M. Arcak and P. Kokotović. Nonlinear observers: a circle criterion design and robustness analysis. *Automatica*, 37(12):1923–1930, 2001. doi:10.1016/S0005-1098(01)00160-1.

A. Astolfi, D. Karagiannis, and R. Ortega. *Nonlinear and Adaptive Control with Applications*. Communications and Control Engineering. Springer London, 2008. doi:10.1007/978-1-84800-066-7.

A. Astolfi, R. Ortega, and A. Venkatraman. A globally exponentially convergent immersion and invariance speed observer for n degrees of freedom mechanical systems. In *Conference on Decision and Control*, pages 6508–6513, 2009. doi:10.1109/CDC.2009.5399984.

A. Astolfi, R. Ortega, and A. Venkatraman. A globally exponentially convergent immersion and invariance speed observer for mechanical systems with non-holonomic constraints. *Automatica*, 46(1):182–189, 2010. doi:10.1016/j.automatica.2009.10.027.

G. Bastin and M. R. Gevers. Stable adaptive observers for nonlinear time-varying systems. *IEEE Transactions on Automatic Control*, 33(7):650–658, 1988. doi:10.1109/9.1273.

H. Berghuis and H. Nijmeijer. A passivity approach to controller-observer design

for robots. *IEEE Transactions on Robotics and Automation*, 9(6):740–754, 1993. doi:10.1109/70.265918.

G. Besançon. Remarks on nonlinear adaptive observer design. *Systems and Control Letters*, 41(4):271–280, 2000a. doi:10.1016/S0167-6911(00)00065-7.

G. Besançon. Global output feedback tracking control for a class of lagrangian systems. *Automatica*, 36:1915–1921, 2000b. doi:10.1016/S0005-1098(00)00111-4.

G. Besançon. *Nonlinear Observers and Applications*, volume 363/2007 of *Lecture Notes in Control and Information Sciences*. Springer Berlin / Heidelberg, 2007. doi:10.1007/978-3-540-73503-8.

G. Besançon, Q. Zhang, and H. Hammouri. High gain observer based state and parameter estimation in nonlinear systems. In *6th IFAC symposium Symposium on Nonlinear Control Systems*, volume 2, pages 471–476, 2004.

K. Bjørkevoll, B.-T. Anfinsen, A. Merlo, N.-H. Eriksen, and E. Olsen. Analysis of extended reach drilling data using an advanced pressure and temperature model. In *IADC/SPE Asia Pacific Drilling Technology*, 2000. doi:10.2118/62728-MS.

K. Bjørkevoll, R. Rommetveit, A. Rønneberg, and B. Larsen. Successful field use of advanced dynamic models. In *IADC/SPE Drilling Conference*, 2006. doi:10.2118/99075-MS.

K. S. Bjørkevoll, R. Rommetveit, B. Aas, H. Gjeraldstveit, and A. Merlo. Transient gel breaking model for critical wells applications with field data verification. In *SPE/IADC Drilling Conference, Amsterdam, Netherlands*, 2003. doi:10.2118/79843-MS.

K. S. Bjørkevoll, D. O. Molde, and H. Fjeldberg. Utilize managed pressure drilling equipment and techniques to cement a severely depleted hpht reservoir in the norh sea. In *SPE Russian Oil & Gas Technical Conference and Exhibition*, 2008a. doi:10.2118/115118-RU.

K. S. Bjørkevoll, D. O. Molde, R. Rommetveit, and S. Syltøy. Mpd operation solved drilling challenges in a severely depleted hp/ht reservoir. In *IADC/SPE Drilling Conference, 4-6 March 2008, Orlando, Florida, USA*, 2008b. doi:10.2118/112739-MS.

K. S. Bjørkevoll, S. Hovland, I. B. Aas, and E. Vollen. Successful use of real time dynamic flow modelling to control a very challenging managed pressure drilling operation in the north sea. In *SPE/IADC Managed Pressure Drilling and Underbalanced Operations Conference and Exhibition*, 2010. doi:10.2118/130311-MS.

E. Børhaug and K. Pettersen. Global output feedback pid control for

n-dof euler-lagrange systems. In *American Control Conference*, 2006. doi:10.1109/ACC.2006.1657512.

J. P. Brill and H. Mukherjee. *Multiphase Flow in Wells*. Society of Petroleum Engineers Inc., 1999.

R. G. Brown and P. Y. C. Hwang. *Introduction to Random Signals and Applied Kalman Filtering*. John Wiley & Sons, 3rd edition, 1997.

E. Bullinger and F. Allgöwer. An adaptive high-gain observer for nonlinear systems. In *Proc. 36th IEEE Conference on Decision and Control*, volume 5, pages 4348–4353 vol.5, 1997. doi:10.1109/CDC.1997.649541.

A. Calderoni and G. Girola. Enbd, the proprietary eni managed pressure drilling with uninterrupted mud circulation: Technical update after the first year's activity. In *International Petroleum Technology Conference*, 2009. doi:10.2523/13867-MS.

D. Carnevale, D. Karagiannis, and A. Astolfi. A condition for certainty equivalence output feedback stabilization of nonlinear systems. *IEEE Transactions on Automatic Control*, 55(5):1180–1185, 2010. doi:10.1109/TAC.2010.2041980.

C.-T. Chen. *Linear System Theory and Design*. Oxford University Press, 1999.

Y. M. Cho and R. Rajamani. Systematic approach to adaptive observer synthesis for nonlinear systems. *IEEE Transactions on Automatic Control*, 42(4):534–537, 1997. doi:10.1109/9.566664.

M. J. Chustz, L. D. Smith, and D. Dell. Managed pressure drilling success continues on auger tlp. In *IADC/SPE Drilling Conference 4-6 March*, 2008. doi:10.2118/112662-MS.

K. Do, Z. Jiang, and J. Pan. Global partial-state feedback and output-feedback tracking controllers for underactuated ships. *Systems & Control Letters*, 54(10): 1015–1036, 2005. doi:10.1016/j.sysconle.2005.02.014.

DO-178B. Software considerations in airborne systems and equipment certification. RTCA.

J. Eck-Olsen, P.-J. Pettersen, A. Ronneberg, K. S. Bjørkevoll, and R. Rommetveit. Managing pressures during underbalanced cementing by choking the return flow; innovative design and operational modeling as well as operational lessons. In *SPE/IADC Drilling Conference*, 2005. doi:10.2118/92568-MS.

X. Fan and M. Arcak. Observer design for systems with multivariable

monotone nonlinearities. *Systems & Control Letters*, 50(4):319–330, 2003. doi:10.1016/S0167-6911(03)00170-1.

T. I. Fossen. *Marine Control Systems*. Marine Cybernetics, 2002.

T. I. Fossen, A. Loría, and A. Teel. A theorem for ugas and ules of (passive) nonautonomous systems: robust control of mechanical systems and ships. *International Journal of Robust and Nonlinear Control*, 11(2):95–108, 2001. doi:10.1002/rnc.551.

P. Fredericks, D. Reitsma, T. Runggai, N. Hudson, R. Zaeper, O. Backhaus, and M. Hernandez. Successful implementation of first closed loop, multiservice control system for automated pressure management in a shallow gas well offshore myanmar. In *IADC/SPE Drilling Conference*, 2008. doi:10.2118/112651-MS. SPE 112651.

K. Furuta, M. Yamakita, and S. Kobayashi. Swing-up control of inverted pendulum using pseudo-state feedback. *Proceedings of the Institution of Mechanical Engineers*, 206:263–269, 1992. doi:10.1243/PIME_PROC_1992_206_341_02.

J. P. Gauthier, H. Hammouri, and S. Othman. A simple observer for nonlinear systems applications to bioreactors. *IEEE Transactions on Automatic Control*, 37(6):875–880, 1992. doi:10.1109/9.256352.

J.-M. Godhavn. Control requirements for automatic managed pressure drilling system. *SPE Drilling & Completion*, 25:336–345, 2010. doi:10.2118/119442-PA.

J.-M. Godhavn and K. A. Knudsen. High performance and reliability for mpd control system ensured by extensive testing. In *IADC/SPE Drilling Conference and Exhibition*, 2010. doi:10.2118/128222-MS.

J. Gravdal, H. Lohne, G. Nygaard, E. Vefring, and R. Time. Automatic evaluation of near-well formation flow interaction during drilling operations. In *International Petroleum Technology Conference*, 2008. doi:10.2523/IPTC-12395-MS.

J. E. Gravdal, R. J. Lorentzen, K. K. Fjelde, and E. H. Vefring. Tuning of computer model parameters in managed-pressure drilling applications using an unscented-kalman-filter technique. *SPE Journal*, 15:856–866, 2010. doi:10.2118/97028-PA.

H. F. Grip. *Topics in State and Parameter Estimation for Nonlinear and Uncertain Systems*. PhD thesis, NTNU, 2010.

H. F. Grip, T. A. Johansen, L. Imsland, and G.-O. Kaasa. Parameter estimation and compensation in systems with nonlinearly parameterized perturbations. *Automatica*, 46(1):19–28, 2010. doi:10.1016/j.automatica.2009.10.013.

D. Hannegan. Case studies - offshore managed pressure drilling. In *SPE Annual Technical Conference and Exhibition*, 2006. doi:10.2118/101855-MS.

S. A. Hansen, R. Rommetveit, N. Sterri, B. Aas, and A. Merlo. A new hydraulics model for slim hole drilling applications. In *SPE/IADC Middle East Drilling Technology Conference*, 1999. doi:10.2118/57579-MS.

IEC 61508. Functional safety of electrical/electronic/programmable electronic safety-related systems. IEC.

P. A. Ioannou and J. Sun. *Robust Adaptive Control*. Prentice Hall, 1996.

P. Isambourg, B. Anfinsen, and C. Marken. Volumetric behavior of drilling muds at high pressure and high temperature. In *SPE European Petroleum Conferece*, 1996. doi:10.2118/36830-MS.

ISO 26262. Road vehicles – functional safety. ISO.

A. T. B. Jr., K. K. Millheim, M. E. Chenevert, and F. Y. Jr. *Applied Drilling Engineering*. Society of Petroleum Engineers, 1991.

S. Julier, J. Uhlmann, and H. F. Durrant-Whyte. A new method for the nonlinear transformation of means and covariances in filters and estimators. *IEEE Transactions on Automatic Control*, 45(3):477–482, 2000. doi:10.1109/9.847726.

S. J. Julier and J. K. Uhlmann. A new extension of the kalman filter to nonlinear systems. In *The Proceedings of AeroSense: The 11th International Symposium on Aerospace/Defense Sensing, Simulation and Controls*, 1997.

G.-O. Kaasa. A simple dynamic model of drilling for control. Technical report, Statoil Research Centre Porsgrunn, 2007.

G.-O. Kaasa, Ø. N. Stamnes, L. Imsland, and O. M. Aamo. Intelligent estimation of downhole pressure using a simple hydraulic model. In *IADC/SPE Managed Pressure Drilling and Underbalance Operations Conference and Exhibition*, 2011a.

G.-O. Kaasa, Ø. N. Stamnes, L. Imsland, and O. M. Aamo. Simplified hydraulic model used for intelligent estimation of downhole pressure for an mpd control system. *SPE Drilling & Completion (submitted)*, 2011b.

R. E. Kalman. A new approach to linear filtering and prediction problems. *Trans. ASME, J. Basic Engineering*, pages 35–45, 1960.

R. E. Kalman and R. S. Bucy. New results in linear filtering and prediction. *Trans. ASME, J. Basic Engineering*, 83:95–108, 1961.

D. Karagiannis, D. Carnevale, and A. Astolfi. Invariant manifold based reduced-order observer design for nonlinear systems. *IEEE Transactions on Automatic Control*, 53(11):2602–2614, 2008. doi:10.1109/TAC.2008.2007045.

D. Karagiannis, M. Sassano, and A. Astolfi. Dynamic scaling and observer design with application to adaptive control. *Automatica*, 45(12):2883–2889, 2009. doi:10.1016/j.automatica.2009.09.013.

N. Kazantzis and C. Kravaris. Nonlinear observer design using lyapunov's auxiliary theorem. *Systems & Control Letters*, 34(5):241–247, 1998. doi:10.1016/S0167-6911(98)00017-6.

H. K. Khalil. High-gain observers in nonlinear feedback control. In H. Nijmeijer and T. Fossen, editors, *New Directions in nonlinear observer design*, Lecture Notes in Control and Information Sciences, 1999. doi:10.1007/BFb0109930.

H. K. Khalil. *Nonlinear Systems*. Prentice-Hall, 2002.

C. Kravaris, V. Sotiropoulos, C. Georgiou, N. Kazantzis, M. Xiao, and A. J. Krener. Nonlinear observer design for state and disturbance estimation. *Systems & Control Letters*, 56(11-12):730–735, 2007. doi:10.1016/j.sysconle.2007.05.001.

G. Kreisselmeier. Adaptive observers with exponential rate of convergence. *IEEE Transactions on Automatic Control*, 22(1):2–8, 1977. doi:10.1109/TAC.1977.1101401.

A. Krener and A. Isidori. Linearization by output injection and nonlinear observers. *Systems & Control Letters*, 3(1):47–52, 1983. doi:10.1016/0167-6911(83)90037-3.

A. J. Krener and M. Xiao. Nonlinear observer design in the siegel domain. *SIAM J. Control Optim.*, 41(3):932–953, 2002. doi:10.1137/S0363012900375330.

A. J. Krener and M. Xiao. Erratum: Nonlinear observer design in the siegel domain. *SIAM J. Control Optim.*, 43(1):377–378, 2004. doi:10.1137/S0363012903435114.

P. Krishnamurthy and F. Khorrami. Dynamic high-gain scaling: State and output feedback with application to systems with iss appended dynamics driven by all states. *IEEE Transactions on Automatic Control*, 49(12):2219–2239, 2004. doi:10.1109/TAC.2004.839235.

M. Krstić. On using least-squares updates without regressor filtering in identification and adaptive control of nonlinear systems. *Automatica*, 45:731–735, 2009. doi:10.1016/j.automatica.2008.09.024.

M. Krstić, I. Kanellakopoulos, and P. Kokotović. *Nonlinear and Adaptive Control Design*. John Wiley & Sons, Inc., 1995.

A. Lage, E. Nakagawa, R. Time, E. Vefring, and R. Rommetveit. Full-scale experimental study for improved understanding of transient phenomena in underbalanced drilling operations. In *SPE/IADC Drilling Conference*, 1999. doi:10.2118/52829-MS.

A. C. Lage and R. W. Time. Mechanistic model for upward two-phase flow in annuli. In *SPE Annual Technical Conference and Exhibition, 1-4 October*, 2000. doi:10.2118/63127-MS.

A. C. Lage, K. K. Fjelde, and R. W. Time. Underbalanced drilling dynamics: Two-phase flow modeling and experiments. *SPE Journal*, 8:61–70, 2003. doi:10.2118/83607-PA.

A. C. V. M. Lage. *Two-Phase Flow Models and Experiments for Low-Head and Underbalanced Drilling*. PhD thesis, Stavanger University College, 2000.

H. Lei, J. Wei, and W. Lin. A global observer for autonomous systems with bounded trajectories. *International Journal of Robust and Nonlinear Control*, 17:1088 – 1105, 2007. doi:10.1002/rnc.1161.

L. Ljung. *System identification: theory for the user, 2nd ed.* Prentice-Hall, Inc., 1999.

H. P. Lohne, J. E. Gravdal, E. W. Dvergsnes, G. Nygaard, and E. H. Vefring. Automatic calibration of real-time computer models in intelligent drilling control systems - results from a north sea field trial. In *International Petroleum Technology Conference*, 2008. doi:10.2523/12707-MS.

A. Loría. Global tracking control of one degree of freedom euler-lagrange systems without velocity measurements. *European Journal of Control*, 2(2):144–51, 1996.

A. Loría. Explicit convergence rates for mrac-type systems. *Automatica*, 40(8): 1465–1468, 2004. doi:10.1016/j.automatica.2004.04.004.

A. Loría. From feedback to cascade-interconnected systems: Breaking the loop. In *Proc. 47th IEEE Conf. Decision and Control CDC 2008*, pages 4109–4114, 2008. doi:10.1109/CDC.2008.4738647.

A. Loria and E. Panteley. *A separation principle for a class of Euler-Lagrange systems*, chapter 2, pages 229–247. Springer, 1999. doi:10.1007/BFb0109929.

A. Loría, E. Panteley, D. Popović, and A. R. Teel. δ-persistency of excitation: A

necessary and sufficient condition for uniform attractivity. In *Proceedings of the 41st IEEE Conference on Decision and Control*, volume 3, pages 3506 – 3511, 2002. doi:10.1109/CDC.2002.1184418.

A. Loría, E. Panteley, D. Popović, and A. R. Teel. A nested matrosov theorem and persistency of excitation for uniform convergence in stable nonautonomous systems. *IEEE Transactions on Automatic Control*, 50(2):183–198, 2005. doi:10.1109/TAC.2004.841939.

G. Luders and K. Narendra. An adaptive observer and identifier for a linear system. *IEEE Transactions on Automatic Control*, 18(5):496–499, 1973. doi:10.1109/TAC.1973.1100369.

D. G. Luenberger. Observing the state of a linear system. *IEEE Transactions on Military Electronics*, 8(2):74–80, 1964. doi:10.1109/TME.1964.4323124.

R. Maglione, G. Gallino, G. Robotti, R. Romagnoli, and R. Rommetveit. A drilling well as viscometer: Studying the effects of well pressure and temperature on the rheology of the drilling fluids. In *European Petroleum Conference*, 1996. doi:10.2118/36885-MS.

K. P. Malloy, C. R. Stone, J. George H. Medley, D. Hannegan, O. Coker, D. Reitsma, H. Santos, J. Kinder, J. Eck-Olsen, J. McCaskill, J. May, S. Services, K. Smith, and P. Sonneman. Managed-pressure drilling: What it is and what it is not. In *IADC/SPE Managed Pressure Drilling and Underbalanced Operations Conference & Exhibition*, 2009. doi:10.2118/122281-MS.

N. D. Manring. *Hydraulic Control Systems*. John Wiley & Sons, Inc., 2005.

R. Marino and P. Tomei. Global adaptive observers for nonlinear systems via filtered transformations. *IEEE Transactions on Automatic Control*, 37(8):1239–1245, 1992. doi:10.1109/9.151117.

R. Marino and P. Tomei. Adaptive observers with arbitrary exponential rate of convergence for nonlinear systems. *IEEE Transactions on Automatic Control*, 40 (7):1300–1304, 1995. doi:10.1109/9.400471.

R. Marino and P. Tomei. *Nonlinear control design: geometric, adaptive and robust*. Prentice Hall International (UK) Ltd., 1996.

R. Marino, G. L. Santosuosso, and P. Tomei. Robust adaptive observers for nonlinear systems with bounded disturbances. *IEEE Transactions on Automatic Control*, 46(6):967–972, 2001. doi:10.1109/9.928609.

H. Merritt. *Hydraulic Control Systems*. John Wiley & Sons, 1967.

J. A. Moreno. Approximate observer error linearization by dissipativity methods. In *Control and Observer Design for Nonlinear Finite and Infinite Dimensional Systems*. Springer Berlin / Heidelberg, 2005.

K. S. Narendra and A. M. Annaswamy. *Stable Adaptive Systems*. Prentice Hall, 1989.

S. Nicosia and P. Tomei. Robot control by using only joint position measurements. *IEEE Transactions on Automatic Control*, 35(9):1058–1061, 1990. doi:10.1109/9.58537.

R. Nybø, K. S. Bjørkevoll, R. Rommetveit, P. Skalle, and M. Herbert. Improved and robust drilling simulators using past real-time measurements and artificial intelligence. In *SPE Eurepec/EAGE Annual Conference and Exhibition*, 2008. doi:10.2118/113776-MS.

G. Nygaard and G. Nævdal. Nonlinear model predictive control scheme for stabilizing annulus pressure during oil well drilling. *Journal of Process Control*, 16: 719–732, 2006. doi:10.1016/j.jprocont.2006.01.002.

G. Nygaard, L. Imsland, and E. A. Johannessen. Using nmpc based on a low-order model for control pressure druing oil well drilling. In *8th International Symposium on Dynamics and Control of Process Systems,June 6-8*, 2007a.

G. H. Nygaard, E. Johannessen, J. E. Gravdal, and F. Iversen. Automatic coordinated control of pump rates and choke valve for compensating pressure fluctuations during surge and swab operations. In *IADC/SPE Managed Pressure Drilling and Underbalanced Operations Conference and Exhibition*, 2007b. doi:10.2118/108344-MS.

R. Ortega, A. Loría, P. J. Nicklasson, and H. Sira-Ramirez. *Passivity-based Control of Euler-Lagrange Systems*. Springer, 1998.

B. Paden and R. Panja. Globally asymptotically stable pd+ controller for robot manipulators. *International Journal of Control*, 47(6):1697–1712, 1988. doi:10.1080/00207178808906130.

E. Panteley, A. Loría, and A. Teel. Relaxed persistency of excitation for uniform asymptotic stability. *IEEE Transactions on Automatic Control*, 46(12):1874–1886, 2001. doi:10.1109/9.975471.

J. Petersen, R. Rommetveit, and B. A. Tarr. Kick with lost circulation simulator, a tool for design of complex well control situations. In *SPE Asia Pacific Oil and Gas Conference and Exhibition*, 1998. doi:10.2118/49956-MS.

J. Petersen, K. S. Bjørkevoll, and K. Lekvam. Computing the danger of hydrate

formation using a modified dynamic kick simulator. In *SPE/IADC Drilling Conference*, 2001. doi:10.2118/67749-MS.

J. Petersen, K. S. Bjørkevoll, and R. Rommetveit. Dynamic pre-modeling of mpd operations enabled optimal procedures and operations. In *IADC/SPE Asia Pacific Drilling Technology Conference and Exhibition, 25-27 August 2008, Jakarta, Indonesia*, 2008a. doi:10.2118/115291-MS.

J. Petersen, R. Rommetveit, K. S. Bjørkevoll, and J. Frøyen. A general dynamic model for single and multi-phase flow operations during drilling, completion, well control and intervention. In *IADC/SPE Asia Pacific Drilling Technology Conference and Exhibition*, 2008b. doi:10.2118/114688-MS.

L. Praly. Asymptotic stabilization via output feedback for lower triangular systems with output dependent incremental rate. *IEEE Transactions on Automatic Control*, 48(6):1103–1108, 2003. doi:10.1109/TAC.2003.812819.

B. Rehm, J. Schubert, A. Haghshenas, A. S. Paknejad, and J. Hughes, editors. *Managed Pressure Drilling*. Gulf Publishing Company, 2008.

K. Reif, F. Sonnemann, and R. Unbehauen. An ekf-based nonlinear observer with a prescribed degree of stability. *Automatica*, 34(9):1119–23, 1998. doi:10.1016/S0005-1098(98)00053-3.

R. Rommetveit and E. Vefring. Comparison of results from an advanced gas kick simulator with surface and downhole data from full scale gas kick experiments in an inclined well. In *SPE Annual Technical Conference and Exhibition*, 1991. doi:10.2118/22558-MS.

N. Sadegh and R. Horowitz. Stability and robustness analysis of a class of adaptive controllers for robotic manipulators. *The International Journal of Robotics Research*, 9:74–92, 1990. doi:10.1177/027836499000900305.

J.-J. E. Slotine and W. Li. On the adaptive control of robot manipulators. *The International Journal of Robotics Research*, 6:49–59, 1987. doi:10.1177/027836498700600303.

M. W. Spong, S. Hutchinson, and M. Vidyasagar. *Robot Modeling and Control*. John Wiley & Sons, 2006.

Ø. N. Stamnes, J. Zhou, G.-O. Kaasa, and O. M. Aamo. Adaptive observer design for the bottomhole pressure of a managed pressure drilling system. In *IEEE Conference on Decision and Control*, 2008. doi:10.1109/CDC.2008.4738845.

Ø. N. Stamnes, J. Zhou, O. M. Aamo, and G.-O. Kaasa. Adaptive observer design for nonlinear systems with parameteric uncertainties in unmea-

sured state dynamics. In *IEEE Conference on Decision and Control*, 2009. doi:10.1109/CDC.2009.5400944.

Ø. N. Stamnes, O. M. Aamo, and G.-O. Kaasa. Redesign of adaptive observers for improved parameter identification in nonlinear systems. *Automatica*, 47:403–410, 2010a. doi:10.1016/j.automatica.2010.11.005.

Ø. N. Stamnes, O. M. Aamo, and G.-O. Kaasa. Redesigned adaptive observers with tunable convergence rate. In *IFAC Symposium on Nonlinear Control Systems*, 2010b.

Ø. N. Stamnes, O. M. Aamo, and G.-O. Kaasa. Adaptive redesign of nonlinear observers. *IEEE Transactions on Automatic Control (accepted)*, 2011a.

Ø. N. Stamnes, O. M. Aamo, and G.-O. Kaasa. A constructive speed observer design for general euler-lagrange systems (accepted). *Automatica*, 2011b.

Ø. N. Stamnes, O. M. Aamo, and G.-O. Kaasa. Global output feedback tracking control of euler-lagrange systems (accepted). *IFAC World Congress*, 2011c.

Ø. N. Stamnes, G.-O. Kaasa, and O. M. Aamo. Adaptive estimation of downhole pressure for managed pressure drilling operations. *Submitted to IEEE Multi-Conference on Systems and Control*, 2011d.

F. Thau. Observing the state of nonlinear dynamic systems". *International Journal of Control*, 17:471–479, 1973.

A. Tornambe. Use of asymptotic observers having high-gains in the state and parameter estimation. In *Proc. 28th IEEE Conference on Decision and Control*, pages 1791–1794 vol.2, 1989. doi:10.1109/CDC.1989.70462.

E. J. van Riet, D. Reitsma, and B. Vandecraen. Development and testing of a fully automated system to accurately control downhole pressure during drilling operations. In *SPE/IADC Middle East Drilling Technology Conference & Exhibition*, 2003. doi:10.2118/85310-MS.

F. White. *Fluid Mechanics*. McGraw-Hill, 1994.

A. Xu and Q. Zhang. Nonlinear system fault diagnosis based on adaptive estimation. *Automatica*, 40(7):1181–93, 2004. doi:0.1016/j.automatica.2004.02.018.

Y. Xu, M. Iwase, and K. Furuta. Time optimal swing-up control of single pendulum. *Journal of Dynamic Systems, Measurement and Control*, 123(3):518–527, 2001. doi:10.1115/1.1383027.

F. Zhang, D. M. Dawson, M. S. de Queiroz, and W. E. Dixon. Global adaptive

output feedback tracking control of robot manipulators. *IEEE Transactions on Automatic Control*, 45(6):1203–1208, 2000. doi:10.1109/9.863607.

Q. Zhang. Adaptive observer for multiple-input-multiple-output (mimo) linear time-varying systems. *IEEE Transactions on Automatic Control*, 47(3):525–529, 2002. doi:10.1109/9.989154.

Q. Zhang. Revisiting different adaptive observers through a unified formulation. In *Proc. 2005 European Control Conf. and 44th IEEE Conf. on Decision and Control*, pages 3067–3072, 2005. doi:10.1109/CDC.2005.1582632.